Drew University

College of Liberal Arts

Kinetic and Computational Analysis of phosphorothioate and phosphorodithioate substitutions in metal ion catalyzed cleavage of RNA models.

A Thesis in Biochemistry and Molecular Biology

by

Saif Yasin

Submitting in Partial Fulfillment

of the Requirements

for the Degree of

Bachelor in Arts

With Specialized Honors in Biochemistry and Molecular Biology

April 2017

Dedication

To my family, who are always willing to help every step of the way. And to my grandfather, Ziauddin Ahmed Khan, whose curiosity for information and love of museums inspired me to pursue science. I was honored to defend my thesis on the day we celebrate his memory.

-S. Yasin

Abstract

Metal ion catalysis is critical to phosphodiester cleavage; therefore, determining their underlying catalytic mechanisms is essential for understanding phosphodiesterase function. This study utilized kinetic and computational methods to quantify the catalytic significance of metal ion interactions with non-bridging oxygen moieties using thio-substitutions, which should diminish inner sphere coordination. Experimentally, Ca^{2+} catalyzed cleavage of 5-uridine, 3'-guanosine dinucleotide model (UpG), and its phosphorothioate and phosphorodithioate analogs indicated that R_P and S_P enantiomers display minimal thio-effects (k_O/k_S) of 2.7 and 2.5, respectively, compared to the dithioate model defect of 37. These results suggest direct interactions with the non-bridging oxygen moieties, but that a single thiosubstitution can be compensated for. Despite catalytic defects, binding did not exhibit defects. Furthermore, the lack of catalysis provided by $Co(NH_3)_6^{3+}$, an outer sphere model, highly supports our hypothesis of inner sphere coordination. Density Functional Theory computations on an RNA model suggest inner sphere coordination would exhibit both binding and catalytic defects upon thio-substitutions. While monothioate substitutions suggest minimal structure defects, dithioate substituted RNA models exhibited energetic defects, worsened hydrogen bonding stabilization, and hindered electrostatic interactions. Therefore, we propose that initial metal ion binding relies on outer sphere coordination, while catalysis involves direct interactions with non-bridging oxygen atoms through inner sphere coordination. Further analysis is necessary to improve the validity of our model system, to characterize the role of the solvation shell to catalysis and to investigate the role of outer sphere coordination in binding. Overall, thio-substitutions are found to serves as a useful model, highlighting the importance of direct coordination to the remarkable rate enhancement provided by metal ions in phosphodiester transesterification.

TABLE OF CONTENTS

LIST OF FIGURES

CHAPTER 1

CHAPTER 2

CHAPTER 3

CHAPTER 4

LIST OF TABLES

CHAPTER 2

CHAPTER 3

Acknowledgements

I believe that this work perfectly describes how Drew has not only transformed me into the student I am today, but also the person I embody. For this reason, I have many people to thank. First, my family who were excited to listen and support me in my endeavors. Second, my friends, in particular, Julie Alex and Zoe Coates Fuentes, for the connections that made arduous schoolwork more bearable. Third, Jal Trivedi, the roommate who always listened and critiqued every statement about phosphodiester bond cleavage, even at 3 am. Fourth, Kyle Messina, for mentoring me, and Arline Tarazona for collecting data critical to the conclusions we made. Fifth, the Drew University Chemistry Department, in particular Dr. Mary-Ann Pearsall and Dr. Sandra Keyser, for their continued involvement in my academic growth. Sixth, my readers, Dr. Ryan Hinrichs and Dr. Minjoon Kouh, whose comments helped push my work forward. They deserve a special thanks for reading so much writing. And, finally, Dr. Cassano, who has advised me for the past four years in an enumerable number of ways and for countless hours. Thank you for the mentorship and opportunities you have afforded me as they truly changed the student I am and fostered my curiosity for research that I aim to continue.

-S. Yasin

CHAPTER 1: BACKGROUND

1.1. Motivation

The Cassano laboratory uses small molecule models to elucidate the mechanism of metal ion catalyzed phosphodiester cleavage. This particular study furthers this goal through the investigation of Ca^{2+} catalyzed cleavage of RNA models. Previous literature has highlighted the ability of metal ions to offer exquisite rate enhancements for this transesterification reaction; however, the mechanism of catalysis is still heavily debated. Three catalytic modes have been proposed as possible interactions utilized by metal ions including (1) activation of oxygen nucleophiles, (2) electrophilic stabilization of non-bridging oxygen atoms, and (3) stabilization of leaving group departure (Zhang et al., 2016) (Figure 1). Through the use of thio-substitutions we aim to probe the role of electrophilic stabilization of non-bridging oxygen moieties in catalysis (Binding Mode 2). Experimental and computational studies presented here highlight the critical nature of these inner sphere electrostatic interactions in metal ion catalysis of phosphodiester cleavage.

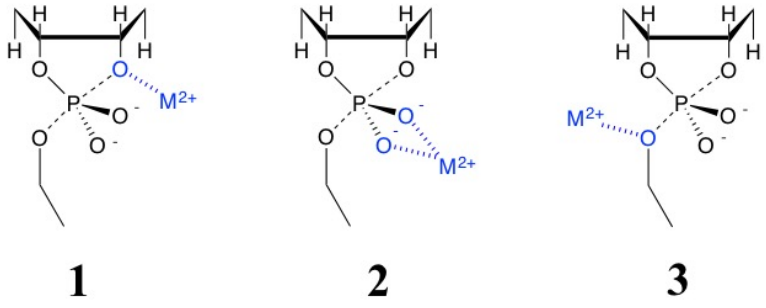

Figure 1. Modes of Metal Ion Catalysis. Three catalytic modes exist that may involve both direct and indirect interactions. (1) Activation of the 2' Oxygen Nucleophile (2) Electrophilic stabilization of non-bridging oxygen atoms (3) Stabilization of leaving group departure (Figure adapted from Harris et al. (2010)).

1.2. Relevance of Enzyme Catalysis

Fundamentals of Enzyme Catalysis

The chemical reactions necessary for life require catalysis in order to proceed at appropriate rates under physiological conditions (Cooper, 2000). All cell processes, including macromolecular synthesis (Elliott & McLaughlin, 1978), cellular signaling (Sun & Tonks, 1994), reproduction (Sivak, 1972), and metabolism (Alves et al., 2002) utilize enzyme catalysts for the remarkable rate enhancements and specificities they show. Therefore, understanding enzymes is necessary to better understand biological function.

It is generally believed that the driving force behind enzyme catalysis is the reduction of a reaction's activation energy barrier (Schramm, 1998). In order to do so enzymes bind and stabilize a high energy transition state (Figure 2) (Pauling, 1946; Pauling, 1948; Silverman, 2000). Studies have investigated how these interactions with transition state species afford enzymes their remarkable specificities and rate enhancements, as these qualities in particular make them extremely useful in biological and industrial settings. First, enzymes seem to have exquisite selectivity for the molecules they bind to in catalysis (Michal & Schomburg, 2012). Oftentimes this binding strength is investigated using the dissociation constant, K_D, with low values suggesting favorable binding at equilibrium. Enzymes have particularly low K_D values with ranges of 10^{-3}-10^{-6} M for their substrates and ranges of 10^{-14}-10^{-23} M for the transition states they stabilize (Schramm, 1998). Furthermore, enzymes also catalyze specific reactions, differentiating between various favorable side reactions that may occur (Michal & Schomburg, 2012).

Enzymes can catalyze their respective reactions with rate enhancements of up to 10^{10}-10^{15}-fold, suggesting that these proteins can allow reactions that would occur in hundreds or millions of years in uncatalyzed conditions to happen within seconds (Radzicka & Wolfenden, 1995). Because enzymes perform such a magnificent chemical feats, there are several applications in organic synthesis (Mortison & Sherman, 2010), energy production (Ma et al., 2016), bioremediation (Wilfred Chen 1999), and human health (Kroemer & Pouyssegur, 2008), which would find these molecular machines widely useful.

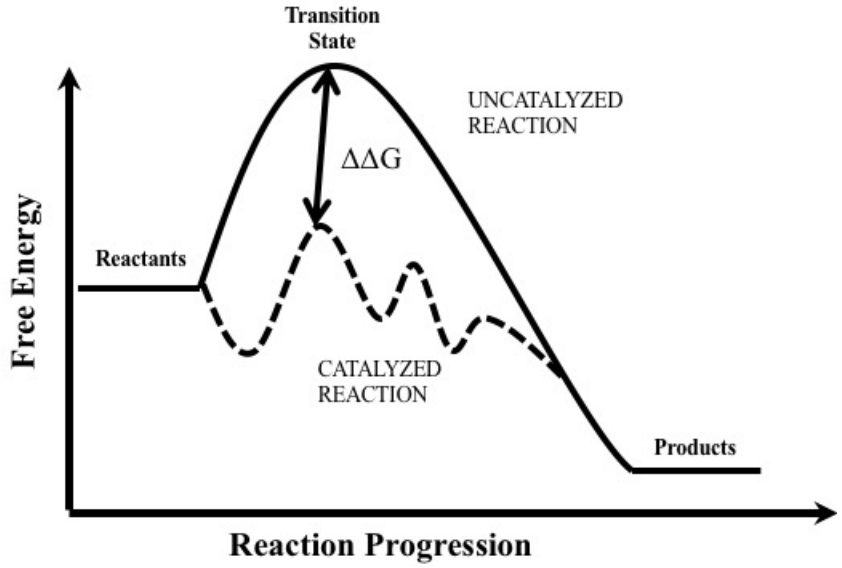

Figure 2. General Reaction Coordinate Diagram for an uncatalyzed and enzyme-catalyzed reaction coordinate. Enzyme catalysis is often implicated in a mechanistic change, which is shown above. The ΔΔG, the change in the energy of activation, is a quantity of energy used to quantify the effectiveness of a particular catalyst.

Models for Mechanistic Insight

In order to harness the chemical functionality of enzymes for industrial and medical applications, it is necessary to garner insight on the mechanism of catalysis. Because transition state stabilization is a dominant paradigm for catalysis, this process generally begins with an understanding of transition state structure. However, the transition state, with a lifetime of 10^{-13} seconds, the timescale for one bond vibration, is difficult to study as there are few spectroscopic methods available to measure its properties (Schramm, 1998). Therefore, several techniques, including X-ray crystallography (Schramm, 2006), computational modeling (Topf et al., 2002), and site directed mutagenesis (Wilkinson et al., 1983), have been adapted to garner information on how specific protein enzymes contribute to catalysis. Unfortunately, each of these methods have their own specific limitations in garnering mechanistic insight. In many cases the combination of several techniques has highlighted the subtleties of transition state structure/stabilization, which highlight the difficulty of studying protein enzymes (Pudney et al., 2007).

In order to simplify analysis and make mechanistic conclusions, many researchers have relied on small molecule model systems (Kool & Waters, 2007). While being limited for direct biological conclusions, these systems allow researchers to better isolate the importance of individual catalytic strategies, which may be difficult to discern when studying the entire system (Rawlings et al., 2006). Therefore, the goal of our lab is to adopt the use of these model systems to study a class of enzymes known as phosphodiesterases and nucleases.

1.3. Enzyme Catalysis in Phosphoryl Transfer Reactions

Phosphoryl Transfer in Biology

Phosphodiesterases and nucleases catalyze phosphodiester cleavage, which is among a class of reactions known as phosphoryl transfer. These reactions involve P-O bond cleavage within phosphate esters, a process ubiquitously present in biological reactions involved in energy production, cellular signaling, DNA replication, and gene expression (Kamerlin et al., 2013). These phosphoryl groups and reactions are so widely useful to biological systems because they afford the opportunity for dynamic regulation of processes through the use of enzymes as the group maintains both kinetic stability and thermodynamic instability (Westheimer, 1987).

Reactions with phosphodiesters are particularly interesting because they are responsible for the inherent stability of genetic material which preserves the integrity of cellular information (Westheimer, 1987). Their inherent stability, while important, is compromised by the use of enzymes like nucleases and phosphodiesterases, which catalyze phosphodiester cleavage for processes like DNA damage repair and mRNA splicing (Pinjari et al., 2009). Because of the inherent kinetic stability of the phosphodiester bond these enzymes must allow for remarkable rate enhancement for the reaction to happen at biologically relevant timescales. The half life of RNA, our diester model of interest (see below), in aqueous conditions at pH 7 and 25 ^{o}C, is 110 years (Schroeder et al., 2006). This is compared to the 0.5 millisecond half-life of RNA within a RNAase active site, which offers 6.9 x 10^{12} fold rate enhancement (Thompson et al.,

1995). Unfortunately, the mechanism allowing for these catalytic rate enhancements still remains unclear.

Studying this mechanism can better educate the design of small cleaving molecules as artificial nucleases (Bonfá et al., 2003; Feng et al., 2006), which can have therapeutic applications for disease as gene therapies (Murtola & Strömberg, 2008). In addition, it could help design potential strategies to control processes that rely on phosphoryl transfer. For example, viruses utilize the cyclic dinucleotide molecule cGAMP to stimulate an uncontrolled spread of immune response; therefore, molecules could be designed to hydrolyze this phosphodiester in order to mediate the response (Bridgeman et al., 2015; Gentili et al., 2015). In addition, a mechanistic understanding of cGAMP's hydrolysis can aid in the design of nonhydrolyzable analogs as vaccine adjuvants and cancer therapeutics (Li et al., 2014). Thus, understanding the mechanism of cleavage/hydrolysis can elucidate how these enzymes function to promote such remarkable rate enhancements and open the door for the rational design of useful catalysts.

Aqueous Phosphodiester Cleavage

While enzymes could alter mechanisms in order to catalyze their respective reactions, studying the uncatalyzed reaction can suggest important interactions that could be stabilized by an enzyme active site (Jencks, 1969). Therefore, studying aqueous phosphoryl transfer can help elucidate potential mechanisms phosphodiesterases employ to accelerate cleavage (Lönnberg, 2011; Mikkola et al., 1999). Several studies have focused on the reactions of phosphoryl functional groups, particularly the nucleophilic

displacement of phosphomonoesters (Khan & Kirby, 1970; Kirby & Jencks, 1965), phosphodiesters (Kirby & Varvoglis, 1968), and phosphotriesters (Kirby & Younas, 1970) (Figure 3). Phosphomonoesters are found to be particularly reactive due to electrostatic repulsion toward the leaving group on account of the large distribution of negative charge. Phosphotriesters are similarly reactive; however, this is on account of their susceptibility to nucleophilic attack. Overall, the phosphodiester is particularly unreactive in comparison to these other phosphoester moieties making its enzymatic and non-enzymatic mechanisms of particular interest. The uncatalyzed reaction coordinate for these reactions are particularly well characterized by both experimental and computational models. Linear free energy relationships (LFER) and kinetic isotope effects (KIE) have been critical techniques to garnering this insight (Chen et al., 2014; Harris et al., 2010; Huang & York, 2014; Oivanen et al., 1998).

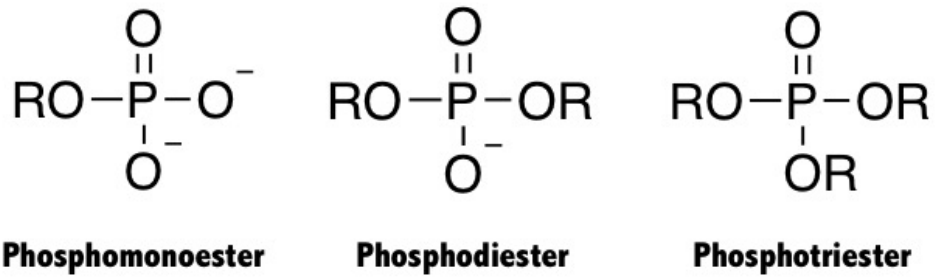

Figure 3. Variety of Phosphoesters. These phosphoryl functional groups exists in three forms and mainly differ in their charge. These differences cause variations in the rate of hydrolysis. Phosphomonoesters and phosphotriesters are particularly reactive, due to heavy repulsion toward the leaving group and limited repulsion against nucleophiles respectively. In comparison, phosphodiesters exhibit enhanced stability.

Linear free energy relationships aim to use chemical modifications on leaving groups and nucleophiles to probe transition state structure (Lassila et al., 2011; Oivanen

et al., 1998). These experiments give Brønsted coefficients, which take into account the effect of either leaving group or nucleophile reactivity, pK_a, on the reaction rate (Bronsted, 1928). The magnitude of these coefficients in comparison to others can give insight into the charge distribution within a transition state, and is useful to differentiate between associative, highly advanced bond formation, and dissociative, highly advanced bond fission, transition states (Rosta et al., 2008). Results with uncatalyzed models can be compared to those catalyzed by phosphodiesterases in order to better assess how enzyme catalysis is affecting the progression of nucleophile bond formation and leaving group bond cleavage. While this technique can help discern between potential reaction coordinate pathways and catalytic contributions (Jencks & Jencks, 1977), its results can be complicated due to effects of solvation and chemical structure on reaction equilibria (Lassila et al., 2011).

Another technique, kinetic isotope effects, is widely used for mechanistic studies to assess the degree of bond formation and in some cases protonation in the transition state (Chen et al., 2014; Zhang et al., 2016). These studies involve the comparison of reaction rates between those of unaltered substrates to those with isotopic substitutions. Effects on the rate occur because heavier isotopes have lower zero point vibrational energies, which could alter the reaction coordinate activation energy barrier (Figure 4) (Harris & Cassano, 2008). These differences can be measured and would highlight the differences in bond stiffness between the reactant and transition state through comparing rate constants ($KIE=k_{light}/k_{heavy}$) (Hengge, 2002). Stiffer bonding environments prefer heavier isotopes. Therefore, if we consider a heavy atom isotopic substitution, decreased

stiffness in transition state bonding would lead to a normal (above 1) KIE, while increased stiffness in transition state bonding would lead to an inverse (below 1) KIE (Chen et al., 2014). Several mechanistic conclusions have been made using this technique (Harris et al., 2010); however, because isotopic substitutions change all vibrational modes of the atom there are cases where kinetic conclusions are ambiguous and require computational comparisons (Chen et al., 2014). Despite limitations both LFER and KIE methods have allowed researchers to garner detailed mechanistic information about uncatalyzed phosphoryl transfer.

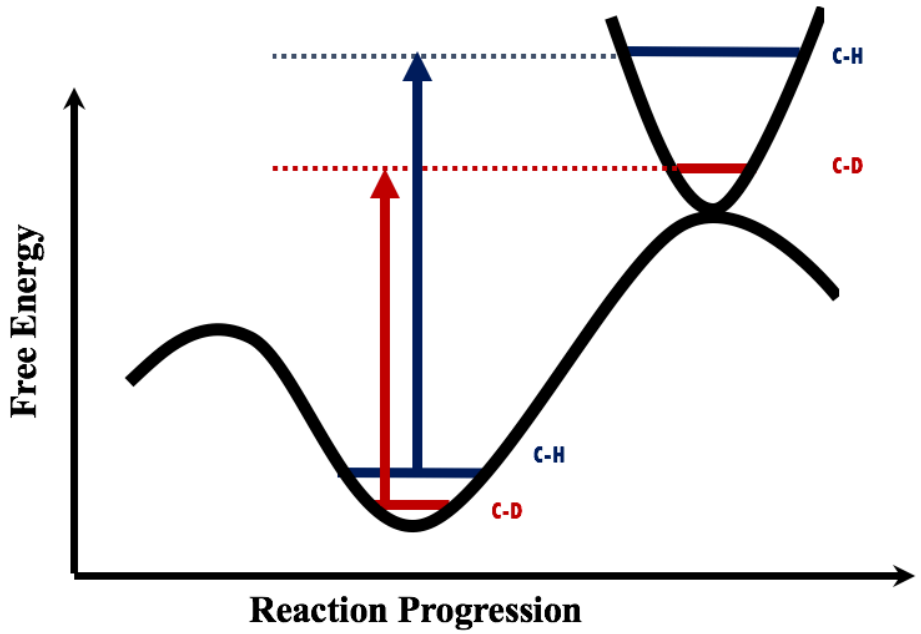

Figure 4. KIE Analysis Reaction Coordinate. Representation of the effect of deuterium (H-1 to D-2) isotopic substitution in place of hydrogen on activation energy. Heavy atom isotopic substitutions reduce vibrational frequencies, which reduce reactant zero point energies in the reactant and transition state. Effects on the rate constant, which allow for KIE calculations, are based on the change in stiffness upon transformation to the transition state. In this case an inverse isotope effect is shown, with a tight transition state.

Several mechanistic studies have allowed for detailed insight into the mechanism of RNA cleavage by 2'-O-transphosphorylation, our phosphoryl transfer model system. This particular phosphodiester is less stable than its DNA counterpart, due to the presence of a 2'-OH, which acts to promote intramolecular cleavage as a nucleophile (Wang & Kool, 1995). RNA cleavage is initiated by the nucleophilic attack of the hydroxyl at the phosphoryl center, which proceeds through a phosphorane intermediate (Brown & Todd, 1955) (Figure 5). The degradation of this phosphorane results in the loss of an alkyl leaving group. The general mechanism is thought to be stepwise, with a stable phosphorane, or concerted, a phosphorane with a limited life time (Lönnberg et al., 2004).

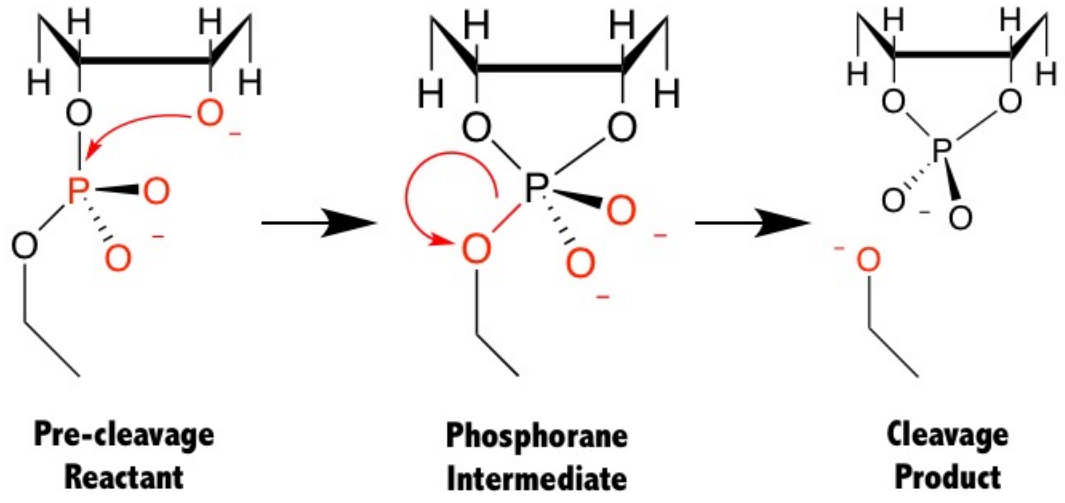

Figure 5. Basic Mechanistic Scheme for Phosphodiester Transesterification. 2'OH nucleophile can be deprotonated in a pre-equilibrium step or attack while protonated depending on chemical conditions. Similarly, the negatively charge leaving group may leave as an oxyanion or as an alcohol depending on chemical environment. The stability for the phosphorane is determinant of whether the mechanism is stepwise or concerted. The reaction mechanism is extremely slow, with a half life of 110 years (Schroeder et al., 2006), due to the unfavorable repulsion of charge and development of charge indicated by red atoms.

The RNA transesterification reaction mechanism is highly pH dependent, as it has been found to have acid and base catalyzed mechanisms (Oivanen et al., 1998). Below a pH of 2, the hydronium catalyzed mechanism dominates, which involves a protonated, stable phosphorane intermediate that undergoes psuedorotation (Oivanen et al., 1998). Therefore, this mechanism is stepwise and may involve an isomerization side reaction with cleavage of the P-O(3') rather than the P-O(5') (Figure 6) (Oivanen et al., 1998).

On the other hand, the predominant reaction at a basic pH range above 7 involves the production of 2',3'-cyclic phosphate and 5'-linked nucleosides (Jarvinen et al., 1991) (Figure 7). This reaction is found to begin with rapid deprotonation of the 2'-OH, yielding an activated nucleophile. LFER data with reactive leaving groups like aryl ester show Bronsted coefficients for the leaving group at -0.59 suggesting less advanced bond fission, which implies a weakly advanced transition state that correlates with a concerted mechanism (Davis et al., 1988). However, LFER results with alkyl leaving groups have significantly higher Bronsted coefficients at -1.28 highlighting greater bond fission in comparison to aryl esters (Kosonen et al., 1997; Lönnberg et al., 2004). These results suggest that the phosphorane with an alkyl leaving group is longer lived, suggesting a stepwise mechanism for alkaline catalyzed 2'-O-transphosphorylation (Lönnberg et al., 2004). KIE results with ^{18}O substitutions in the leaving group corroborate this mechanistic picture. Results for alkyl esters indicate normal KIE (1.034) (Harris et al., 2010), while aryl esters have KIE closer to unity (1.006) (Hengge et al., 2000). Therefore, the results suggest a later transition state, with relatively more advanced bond cleavage, for alkyl leaving groups in comparison to aryl models. This highlights a stepwise

mechanism for alkaline phosphodiester cleavage of DNA and RNA (Figure 7) (Harris et al., 2010).

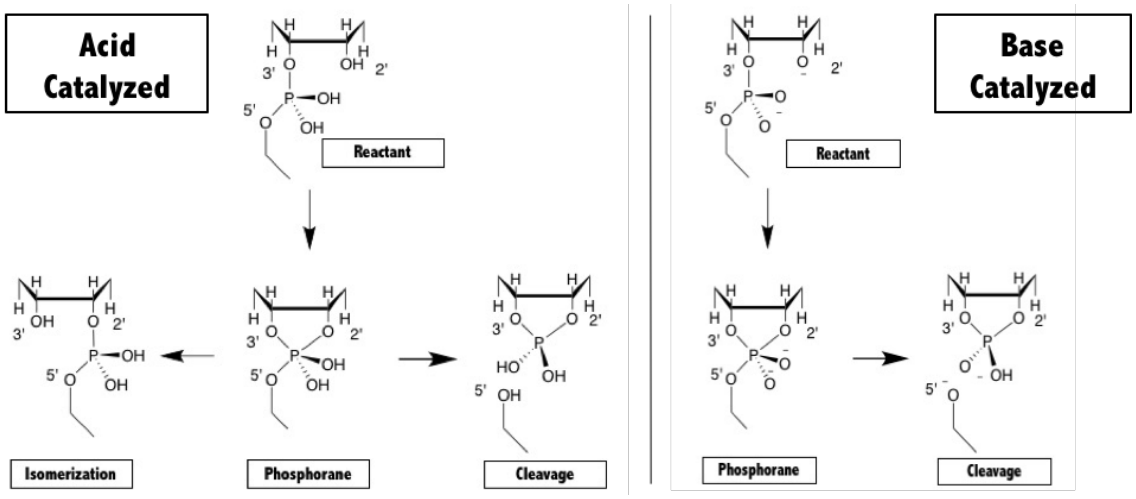

Figure 6. Reactions Present under Acid/Based Catalyzed Mechanism of RNA Transesterification. Under acidic conditions a long lived phosphorane is stable, which may undergo a pseudorotation between apical and equatorial positions leading to the possible isomerization in addition to cleavage (Westheimer, 1968). Base catalysis involves a highly charged unstable phosphorane that only promotes cleavage. The half-life of the phosphorane is dependent on the reactivity of the leaving group.

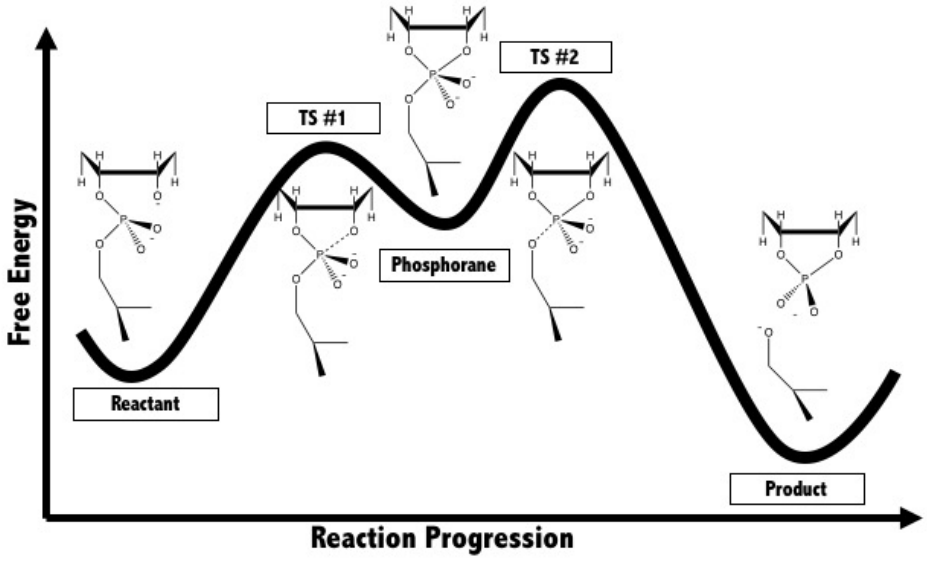

Figure 7. Reaction Coordinate for Alkaline Catalyzed Phosphodiester transesterification. The reaction involves a stepwise mechanism with the formation of a phosphorane, and is rate-limited by its degradation as the leaving group is cleaved.

It is critical to note that several aspects of the uncatalyzed mechanism described above involve unfavorable chemical arrangements. Therefore, three potential interactions would be particularly useful as catalytic strategies:

1. Leaving Group Departure Stabilization: The cleavage of the alkyl leaving group is the rate determining step (Harris et al., 2010), and rates are highly dependent on leaving group reactivity (Kirby & Younas, 1970). Enzyme catalysis could stabilize the growing negative charge on these high pK_a leaving groups, facilitating bond cleavage.
2. Electrostatic Stabilization: The non-bridging oxygen moieties have been implicated in repelling nucleophiles giving phosphodiester bonds their particular stability (Westheimer, 1987). Enzymes could stabilize the negative charge on unstable phosphoranes to facilitate their formation. Increased phosphorane formation would would increase the opportunity for leaving group bond cleavage.
3. Nucleophilic Activation: LFER studies have shown that reaction rates have high sensitivity to the nucleophile (Khan & Kirby, 1970). For example, at neutral pH the addition of fluorine atoms near the nucleophile, which increase the rate of deprotonation of the 2'-OH, corresponds with an increase in the cleavage reaction rate (Ye et al., 2007). Enzyme catalysis involving the deprotonation of nucleophiles would enhance catalysis by increasing phosphorane formation.

Estimations suggest that 1 and 3 can accelerate the reaction by a factor of up to 10^6-fold, while 2 is estimated to offer rate enhancement of up to 10^5-fold (Emilsson et al., 2003).

Therefore, these serve as potential modes of catalysis. Study of the enzymatic mechanism will help differentiate between each mode's relative importance.

Ribonucleases

Several protein and RNA catalysts exist that facilitate the RNA cleavage reaction described above. Many have been the focus of mechanistic research for the design of biomimetic artificial nucleases (Breslow, 1982). RNase A (Raines, 1998) is a prime example of a protein enzyme; however, recent work has focused on catalytic RNA molecules such as the hammerhead (Pley et al., 1994), hairpin (Rupert & Ferré-D'Amaré, 2001), hepatitis delta virus (Nakano et al., 2000), glmS (Klein & Ferré-D'Amaré, 2006), and Varkud satellite (Lilley, 2004) enzymes. Interestingly, studying the RNA cleavage reaction in particular allows for the unique comparison of catalysis by protein and RNA enzymes for the same function, which has currently suggested similar, but decreased activity by RNA catalysts (Doudna & Lorsch, 2005; Narlikar & Herschlag, 1997). Furthermore, several of these enzymes rely on metal ions as active site cofactors for proper catalysis (Kamerlin et al., 2013; Lassila et al., 2011; Wilcox, 1996). For example, all ribozymes rely on metal ions for either catalysis or structural stability (Piccirilli et al., 1993). Additionally, RNA cleavage reactions are particularly interesting to study because they can exhibit non-enzymatic catalysis by metal ions and small molecules, which allow for the design of simple model systems (Lönnberg, 2011). Therefore, studying this class of reactions can help elucidate the role metal ions play in catalysis of phosphoryl transfer.

1.4. Metal Ion Catalysis

Metalloenzymes

Several experimental techniques, including site-directed mutagenesis, kinetic studies, and x-ray crystallography, have been critical in allowing for an evaluation of the role metal ions play in the function of metalloenzymes. Many of these studies involved enzymes that catalyze phosphoryl transfer, including restriction endonucleases (Galburt & Stoddard, 2002), DNA/RNA polymerases (Beese & Steitz, 1991; Castro et al., 2007), phosphodiesterases (Huai et al., 2003), and ribozymes including ribonuclease P (Beebe et al., 1996) and the tetrahymena ribozyme (Piccirilli et al., 1993). The removal of an enzyme's metal ion, and in some a cases a specific metal ion, has been implicated in a reduction or even the depletion of enzymatic activity. For example, in the case of the hammerhead ribozyme, the rate of phosphate hydrolysis occurs 10,000 fold faster when 10 mM Mg^{+2} ions are present (Scott, 1999). Site directed mutagenesis studies, which compare enzymatic activity after a mutation of a residue that is thought to bind a metal ion, highlight the critical nature of metal ions. I-PpoI, a homing endonuclease which cleaves DNA, relies on an asparagine bound magnesium metal ion for activity (Mannino et al., 1999). When this particular residue is mutated to an alanine, the magnesium (II) metal ion cannot coordinate to the protein and subsequently reduces the enzyme's activity by 15,384-fold (Mannino et al., 1999). These results highlight that the metal ion is critical to the function of metalloenzymes that catalyze phosphodiester hydrolysis.

It is important to recognize that metal ions can play several different roles within an enzyme active site. Molecular dynamic simulations of the HDV ribozyme active site

suggests that Mg^{2+} acts as either a Lewis acid or a Bronsted base to facilitate nucleophilic activation and promote catalysis (Chen et al., 2013). Some studies even highlight the possibility that indirect outer sphere coordination may be a possible mechanism for metal ion catalysis, as in the case of the acyl transferase ribozyme (Suga et al., 1998). Therefore, mechanistic studies are required to isolate the chemical role of metal ions. However, studies on protein and RNA enzymes offer limited flexibility on the chemical modifications required to confirm specific mechanisms, which makes the use of small model systems necessary for these conclusions.

Metal Ions with Model Systems

Given the structural complexities of eliminating metal ion binding sites in enzymes, model systems can be particularly useful to simplify analysis. These rely on smaller substrates and catalysts, which are less structurally sensitive to chemical modifications from the reaction environment (Lönnberg, 2011). In particular, the study of RNA 2'O-transphosphorylation (see above) is particularly useful because it can be catalyzed non-enzymatically by divalent ions (Breslow & Huang, 1991; Ikenaga & Inoue, 1974) and organometallic compounds (Lönnberg, 2011; Zastrow & Pecoraro, 2013). Therefore, simple model catalysts can be substituted for more complex protein and RNA catalysts, and can allow researchers to specifically investigate metal ion interactions with transition state structures. Methods like KIE and LFER can be used to investigate these simple catalysts to garner information about the various catalytic interactions that may exist, so the role of metal ions in phosphoryl transfer can be isolated (Zhang et al., 2016).

Based on a study of the uncatalyzed RNA transesterification reaction, three catalytic modes have been proposed as interactions utilized by metal ions including (1) activation of oxygen nucleophiles (Figure 8A), (2) electrophilic stabilization of non-bridging oxygen atoms (Figure 8B), and (3) stabilization of leaving group departure (Figure 8C) (Zhang et al., 2016). These catalytic modes in conjunction with studies of the uncatalyzed mechanism suggest several mechanistic possibilities for metal ion interactions.

First, several researchers have focused on enzymatic activation of oxygen nucleophiles as a mode of rate enhancement, which have been found to be present within the Group I Intron and the HDV ribozyme (Anderson et al., 2006). Metal ions can potentially directly deprotonate the 2'OH to activate the intramolecular nucleophilic attack of RNA or can coordinate a base, water or more likely hydroxide, to engender a general (buffer catalyzed) or specific (hydroxide catalyzed) mechanism of catalysis (Figure 8D) (Korhonen et al., 2013).

Second, as it has been found that the departure of the leaving group is a rate limiting step of RNA transesterification due to the high pK_a of alkyl leaving groups. Interactions that stabilize leaving group oxygen moieties may be necessary (Harris et al., 2010). The crystal structure of the 3'-5' endonuclease active site show metal ions directly stabilizing the leaving group (Beese & Steitz, 1991). Leaving group stabilization has also been proposed to occur through a general acid mechanism (Figure 8E) (Korhonen et al., 2013). This mechanism would stabilize the growing negative charge through protonation to promote leaving group departure.

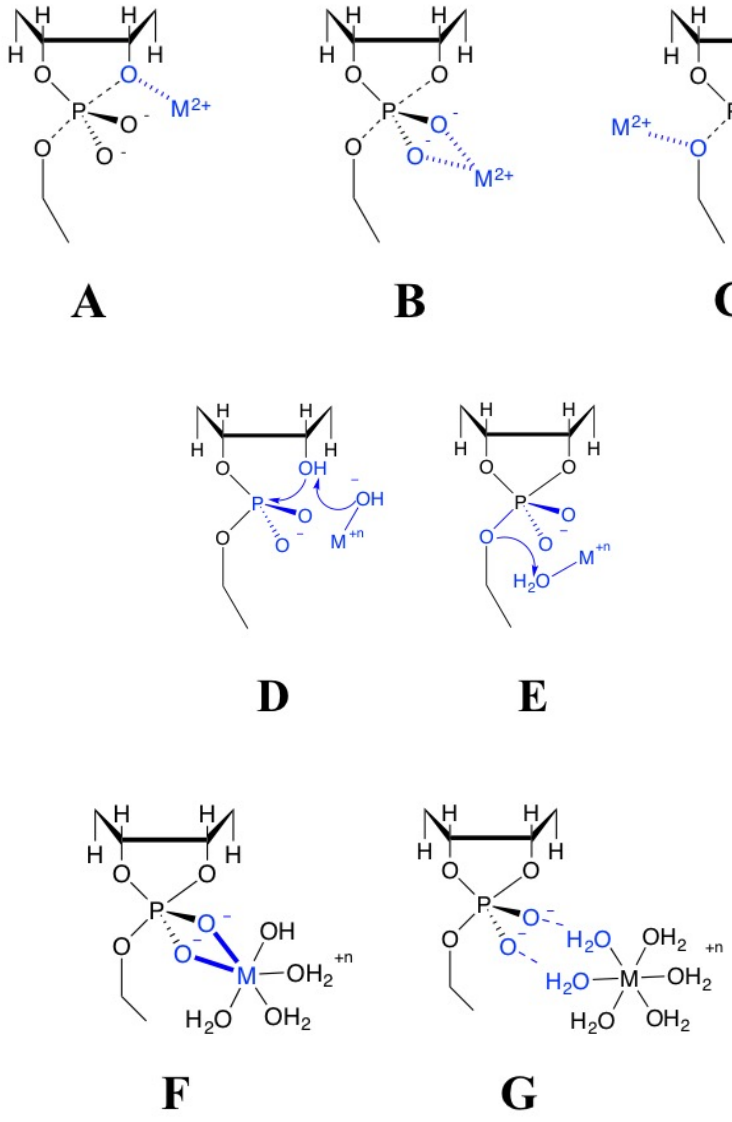

Figure 8. Modes and Mechanisms of Metal Ion Catalysis. Three catalytic modes exist that may involve both direct and indirect interactions. (A) Activation of Oxygen Nucleophile (B) Electrophilic stabilization of non-bridging oxygen atoms (C) Stabilization for leaving group departure. (D/E) Proposed General Acid/Base Mechanism with increased local concentration of metal ion. (D) General Base nucleophilic activation of 2'-Hydroxyl moiety (E) General Acid stabilization of RNA 5'-alkyl leaving group. (F/G) Proposed mechanism of Lewis Acid Stabilization of non-bridging Oxygen Atoms of the dianionic phosphorane intermediate. (F) Direct Inner sphere mechanism of interaction that requires the loss of two solvent interactions to accommodate proposed bidentate binding (G) Outer sphere mechanism of electrophilic stabilization mediate the solvent medium through electrostatics or hydrogen bonding.

Third, the negative charge present on both non-bridging oxygen atoms of the phosphorane intermediate require stabilization through electrophilic catalysis. Several x-ray crystal structures, including that of an endonuclease (Beese & Steitz, 1991) as well as a spliceosome (Stahley & Strobel, 2005), suggest metal ion interactions with non-bridging oxygen moieties. These interactions would stabilize the negative charge as the metal ion serves as a Lewis acid to offer electrostatic stabilization (Korhonen et al., 2013). Metal ion binding can occur through direct inner sphere coordination (Figure 8F) or solvent mediated outer sphere coordination (Figure 8G) (Corona-Martínez et al., 2012). Overall, various possibilities exist. Their relevance to metal ion catalysis can be assessed through the use of kinetic and computational studies.

In order to conduct these mechanistic studies, researchers rely on several different types of phosphodiester compounds that can allow for simpler experimental analyses. Examples include monophosphate dinucleotides (Breslow & Huang, 1991; Oivanen et al., 1998; Zhang et al., 2016), short oligonucleotides (Kuusela et al., 1995), and simple aryl and alkyl esters of nucleotides (Kosonen et al., 1997; Lönnberg et al., 2004). Kinetic studies using these systems in the presence of metal ions and organometallic complexes can offer a depth of information about ion-diester interactions.

In order to make valuable catalytic and mechanistic conclusions from experimentation it is necessary to determine the number of metal ions that are involved in the interaction. For example, the number of metal ions offering direct catalysis in homing endonuclease active sites can vary widely between 1 and 3 (Galburt & Stoddard, 2002). While x-ray crystallography can be useful to investigate the number of ions within

enzyme active sites, the same is not true for smaller model systems. A study by Kirk et al. (2010) examined the dependence of second-order rate constants for hydroxide attack (k_{OH}) on [M^{+n}]. Their thymidine-5'-p-nitrophenyl phosphate (T5PNP) DNA model at 50^{o}C indicated different kinetic mechanisms for Mg^{2+} and Ca^{2+} assisted cleavage (Kirk et al., 2010). Mg^{2+}utilizes a mononuclear single ion mechanism, whereas Ca^{2+}relies on parallel single and double ion mechanisms (Kirk et al., 2010). The double ion mechanism of Ca^{2+} helps explain the two ions' similar catalytic ability, despite their difference in Lewis acidity, which would suggest Mg^{2+} as the more favorable catalyst (Kirk et al., 2010). Similar experimental methods were adopted to study the RNA model system utilized in this study (see below), which also offered insight into binding strength through K_D determination. Therefore, these aspects of the study help elucidate binding modes and allow for comparisons to x-ray crystallography studies, which have already suggested a double metal ion mechanism of catalysis within several different active sites (Beese & Steitz, 1991; Galburt & Stoddard, 2002).

In addition to highlighting the rate's dependence on the number of metal ions, several studies have focused on the relative difference in rate enhancements of different metal ions. This is particularly motivated by the desire to design more efficient catalysts to optimize artificial nucleases for applications in gene therapies. For example, the use of lanthanides, Eu^{3+}, Tb^{3+}, and Yb^{3+}, show efficient catalysis for the cyclization/cleavage of the model 1-p-nitrophenyl phosphate ester (Breslow & Huang, 1991). Transition metals have also shown excellent catalysis, as in the case of Pb^{2+} (Breslow & Huang, 1991). However, in order to understand biological catalysis, many of these studies have also

looked into biologically relevant metal ions like Zn^{2+}, Mg^{2+}, Fe^{3+}, Fe^{2+}, and Ca^{2+} (Lönnberg, 2011). Zn^{2+} was found to be a particularly efficient catalyst for the cyclization/cleavage of 1-p-nitrophenyl phosphate ester. On the other hand Mg^{2+} yielded moderate catalysis and Ca^{2+} offered close to no catalysis. However, in a study of the cleavage of adenylyl(3'-5')adenosine (ApA) Mg^{2+} and Ca^{2+} were found to exhibit higher catalytic rate enhancement than their larger alkaline earth counterparts Sr^{2+} and Ba^{2+} (Yashiro et al., 2002). Therefore, several trends, including some that follow periodic trends, exist for levels of rate enhancement, and require mechanistic information to elucidate.

Several studies have utilized KIE and LFER experiments in order to gauge mechanistic information, because it is necessary to understand the effects metal ions may have on transition state structure. An early LFER study by Herschlag and Jencks (1986) found the that the addition of both Mg^{2+} and Ca^{2+} cause extremely minimal effects on both the nucleophilic and leaving group Brønsted coefficients in monoester hydrolysis. Therefore, these results suggest that the metal ions are not altering the transition state structure of catalysis, which argues against the hypothesis that metal ions act as Lewis acids to promote electrophilic catalysis (Herschlag & Jencks, 1987). However, these particular experiments used monoester models. While monoesters can act as diester transitions state models because of the chemical similarity to the dianionic phosphorane (Corona-Martínez et al., 2012), the relative instability of monoesters and dramatically different transition state suggest that metal ions may play a larger role in the diester cleavage reaction coordinate. The catalytic rates of these metal ions suggest very little

rate enhancement relative to diester compounds (Herschlag & Jencks, 1987). Furthermore, studies with an RNA model, 2-hydroxypropyl-4-nitrophenyl phosphate (HpPNP), suggest this. A KIE study with a dinuclear organometallic zinc complex finds larger leaving group isotope effects and small nucleophile isotope effects, which suggests a later transition state with advanced leaving group bond fission (Humphry et al., 2008). In addition, despite the reactive aryl leaving group, which would suggest a concerted mechanism, isotope effects suggest the presence of a stable phosphorane (Humphry et al., 2008). Therefore, this study serves as a key example of how complexes can affect transition state structure.

Several studies have suggested that the major mechanism used by metal ions is the general acid/base mechanism of catalysis (Korhonen et al., 2013). LFER studies of an RNA diester with an alkyl leaving group find that in the presence of Zn^{2+} the leaving group Brønsted coefficient decreases in magnitude, which suggests lower charge on the leaving group because it departs as an alcohol (Mikkola et al., 1999). These results suggest leaving group stabilization is promoted by a general acid mechanism of catalysis (Mikkola et al., 1999). Density functional theory computations similarly suggest a metal ion coordinated water involved in the rate limiting cleavage of the phosphorane intermediate in the proposed hammerhead ribozyme cleavage mechanism (Torres et al., 2003). Additionally, studies have also highlighted the importance of the general base mechanism to activate nucleophilic attack. The rate constant for Zn^{2+} catalysis is found to pH dependent, which suggests either a general or specific base mechanism due to the dependence on hydroxide concentration (Ikenaga & Inoue, 1974; Zhang et al., 2016).

Additionally, kinetic experiments in DMSO, which allow for the separation of effects by general and specific base catalysis, depict that metal ions generally rely on specific base catalysis, with some unique metal ions, Mg^{2+} and Na^{+}, also promoting cleavage through general base catalysis (Corona-Martínez et al., 2012).

Based on these studies it is clear that metal ions can utilize several catalytic strategies, such as Zn^{2+} exhibiting both general acid and base mechanisms (Ikenaga & Inoue, 1974; Mikkola et al., 1999; Zhang et al., 2016). Therefore, it is also critical to investigate the role electrophilic stabilization plays in the cleavage of phosphodiesters. In studies of acid/base mechanisms it has been proposed that the electrophilicity of metal ions can stabilize general acid/base transition state structures (Corona-Martínez et al., 2012). X-ray structures have suggested the possibility that these interactions are specifically occurring with non-bridging oxygen atoms in the active sites of nucleases and ribozymes (Beese & Steitz, 1991; Stahley & Strobel, 2005). Computational studies have also suggested that these interactions are particularly favorable and may be critical to catalysis in some cases. Density functional theory models of Mg^{2+} ions and di-metal bridge complexes depict favorable direct interactions with the non-bridging oxygen atoms of both biological phosphates and phosphoranes (Mayaan et al., 2004). Gas phase calculations of methyl(ethylene)phosphorane show the formation of a greatly stabilized Mg^{2+} complexes with a large favorable change in free energy (-388.86 kcal/mol) as it binds the phosphate ligand (Mayaan et al., 2004). In addition, the analysis of a Zn^{2+} dinuclear complex binding to HpPNP shows several favorable binding modes that rely on interactions with non-bridging oxygen atoms of the phosphoryl moiety, which suggest

that these interactions are critical to understanding the catalysis by these active zinc ion complexes (Gao et al., 2011). Additionally, experimental work on binuclear zinc ion complexes have shown an absence of a primary isotope effect when D_2O was substituted for H_2O, which suggests that the complex may not involve a proton transfer (Yang et al., 2005). These results indicate that general acid-base catalysis may not be driving rate enhancement, but electrostatic stabilizations at the non-bridging positions (Yang et al., 2005).

Interestingly, several studies contradict the work described above, suggesting that interactions via electrophilic catalysis, specifically in the non-bridging position may not be as relevant to catalysis as compared to those directly involved in the reaction coordinate (e.g. leaving group stabilization and nucleophilic activation). Work done using a mononuclear zinc complex with oligonucleotides aimed to differentiate between electrophilic catalysis and general base catalysis (Korhonen et al., 2013). The study found that the scissile phosphodiester bonds are cleaved more rapidly; however, electrophilic catalysis is not expected to predict such a result because of the limited difference in electron density among different phosphates, which would suggest a more spread binding distribution (Kuusela et al., 1995). These results suggest that for cases like RNA, where leaving group departure is rate limiting, it seems that electrophilic catalysis may be less important than general base (Korhonen et al., 2013). This is further supported by ^{18}O isotope effects of non-bridging oxygen atoms, which show that the addition of metal ions, Zn^{2+} and Mg^{2+}, have insignificant effects on the KIE results: suggesting that the non-bridging oxygen bonding environment remains unchanged throughout metal ion binding

(Jones et al., 1991; Zhang et al., 2016). However, there are limitations to both these studies because of the potential of multiple contributions leading to observed effects, causing a diminished focus on the role of non-bridging oxygen atoms. In addition, computational models that were used to aid the interpretation of experimental KIE studies suggested that current experimental values support a dinuclear binding mode that involves interactions with the non-bridging oxygen atoms (Chen et al., 2015). Overall, this review of the literature highlights the current debate and minimal understanding about the role of these oxygen atoms in catalysis with several contradicting claims. Therefore, this highlights the necessity of more specific model system that addresses this question.

1.5. Experimental Techniques to Probe Role of Electrophilic Catalysis

Several model systems exist to probe transition state structure; however, many are limited in studying the direct contributions of non-bridging oxygen atom stabilization. LFERs and KIEs are limited by the various potential chemical effects that may confound analysis and limit conclusions (Lassila et al., 2011). Other techniques exist that can help assess the mechanism of electrostatic stabilization, to differentiate between inner sphere and outer sphere coordination, and its total relevance to catalysis. It has been found that the deconvolution of Raman spectroscopic signals (Christian et al., 2010; Christian et al., 2011) and analysis of shifts in ^{31}P-NMR peaks (Suzumura et al., 2002) can probe the effects metal ions have on P-O bond vibrations to assess interactions with non-bridging positions. While both these spectroscopic techniques offer great insight into binding it seems that there is limited information about catalysis, which therefore suggests the need

to rely on investigating the kinetic effects of different chemical perturbations. One method, relied upon in this study, is thio-substitutions (Oivanen et al., 1998), the replacement of oxygen for sulfur to interfere with direct metal ion contact sites, which has been commonly used in enzyme systems to assess the relative importance of inner sphere coordination (Hougland et al., 2005). This strategy is reviewed in detail at the beginning of Chapter 2.

1.6. Background on Computational Work

Use of Computational Chemistry

Experimental methods, while extremely useful in garnering mechanistic information, are often limited in giving a complete mechanistic picture (Lassila et al., 2011). Multiple mechanistic models can generally fit to kinetic data; therefore, kinetics can suggest particular pathways, but cannot generally yield a singular unambiguous model (Florián et al., 1998). Computational methods have recently become popular in assisting in the interpretation of experimental information because it offers the ability to isolate the importance of specific electronic and structural interactions. Computations allow for an analysis of proteins and molecules at the atomistic level with insight on bond orders, molecular orbitals, energies, entropies, and even charge (Warshel, 2003). Overall, these computational models are thought to help elucidate advances in transition state theory and their application to enzymes (Garcia-Viloca et al., 2004).

In our studies computational methods allow us to better isolate the electronic and energetic impact of thio-substitutions on metal ion binding to phosphodiesters and the transesterification reaction coordinate. In order to utilize these methods on our system the

following section will introduce a background to computational chemistry; however, for greater depth one should refer to texts by Foresman (1996) and Jensen (2016).

Computational Methods and Models

The overall goal of computational methods is to garner insight into electronic structure by calculating the lowest energy distribution of electrons and nuclei within a region of space. Essentially, these computations treat molecules as a series of negatively and positively charged particles and aim to attain the most stable distribution through the use of several different theories to model molecules (Jensen, 2016). Quantum methods offer complexity in their molecular analysis by assessing the potential energy surface of molecules and related molecular properties through approximating solutions to Schrödinger's equation (Equation 1) (Foresman & Frisch, 1996). This time-independent equation involves the use of the Hamiltonian operator, $\hat{H}$, on the wave function, $\psi(r)$, to obtain the total energy of the system (E). Through treating electrons more specifically, energy calculations can be based on several electrostatic interactions including attractive interactions between electrons and local nuclei, as well as repulsive interactions between electron pairs and nuclei pairs. However, the wavefunctions, which are linear combinations of atomic orbitals, of a multi-electron system quickly become complicated, which increase the computational resources required by electronic structure methods (Jensen, 2016). Despite the difficulty and length of these calculations, these quantum methods allow for more sophisticated electronic structure determinations, which is why several catalytic studies utilize these methods for energetic evaluations of active site species (Warshel, 2003). Therefore, our study will rely on solely quantum mechanical

models, specifically density functional theory for its robustness in comparison with experimental methods (Grimme et al., 2007).

$$\hat{H}\psi(r) = E\psi(r) \textbf{ (1)}$$

Density Functional Theory

Density functional theory (DFT) is highly relied upon in electronic structure calculations of biological phosphates (Chen et al., 2015; Kluge & Weston, 2005; Mayaan et al., 2004). The wide use of DFT is particularly due to its computational speed, because of the inherent assumption that a molecule's electron density corresponds directly to its energy (Jensen, 2016). Because DFT treats electrons collectively rather than individually the computational resources required are reduced, while still offering relative accuracy as it considers electronic correlations (Foresman & Frisch, 1996).

In calculating total electronic energy DFT considers four different energetic terms (Jensen, 2016). First, the kinetic energy of electrons, which quantify their energy of motion. Second, their potential energy, which is dependent on their electrostatic interactions with the nucleus. Third, their repulsion with other correlated electrons in the vicinity. Fourth, a term unique to DFT, any other interactions that may exist: the exchange correlation. While the former three values are based on charge distribution within a molecule, the exchange term involves both interactions between electrons with correlating and differing spins. Different functionals within DFT have been developed to model this term (Jensen, 2016). The accuracy of a functional in considering specific parameters of the exchange term determines the computational cost of the model. A common functional for work on phosphodiesters and biological phosphates (Chen et al.,

2015; Kluge & Weston, 2005; Liu et al., 2006) is the Becke, three-parameter, Lee-Yang-Parr exchange correlation functional (B3LYP) (Becke, 1993). However, recent work on phosphodiester hydrolysis have suggested other functionals as more experimentally relevant models (Ribeiro et al., 2010). Among these is the TPSSTPSS functional, which has more flexible spatial limits to better account for weaker interactions like hydrogen bonding (Tao et al., 2003). This functional has been applied to several metal ion catalyzed reactions (Gao et al., 2011), and has served as a better model for Ca^{2+} ions in our current study. Therefore, TPSSTPSS DFT calculations offer the potential to study Ca^{2+} catalyzed phosphodiester cleavage to correlate to kinetic results and help further highlight models that can adequately study Ca^{2+} for applications to larger QM/MM studies.

Solvation

In addition to adequately describing electrons within molecules, biological systems offer an additional complication because of the aqueous environment, which plays critical enthalpic, entropic, and electronic roles in reaction systems (Jensen, 2016). Gas phase models treat the system within a dielectric close to zero, which overestimate any electrostatic interactions for solvated systems. Therefore, better models have adapted the use of explicit and implicit solvent models (Jensen, 2016). Explicit solvent models involve including all water molecules in the system, which could reach an enumerable number of molecules that increase the computational cost of the system (Foresman & Frisch, 1996). Therefore, the use of implicit models, such as the polarizable continuum model (PCM), are opted for in order to limit computational cost. In PCM, computations

model the dielectric of the solvent and create a cavity within the medium for the solute. Despite the relative ease of calculations provided by PCM, recent studies by Dhaouadi et al. (2009) found that the use of implicit solvent alone has limited accuracy when looking specifically to infra-red frequencies of vibration for dimethyl phosphate, a small model system, that has been heavily characterized. Therefore, the use of implicit solvent as well as explicit water molecules as a model of the primary hydration sphere has been found to improve accuracy; therefore, this has been adopted for our purposes.

1.7. Cassano Lab Model System

Our lab has utilized computational studies to further investigate kinetic results that are discussed below to more confidently make mechanistic conclusions. Similar to the literature reviewed above, the Cassano lab relies upon a small molecule model system, the RNA dinucleoside uridylyl-3'-guanosine (5'-UpG-3', UpG), which has been used in several other phosphodiester mechanistic studies (Zhang et al., 2016). Additionally, this model allows for comparisons to other dinucleoside models as base identity does not significantly alter rates of hydrolysis as shown by a study at neutral pH and 50^{o}C (Yashiro et al., 2002). The choice of RNA is a particular useful model system for three particular reasons. First, RNA allows for kinetic trials in more accessible timescales as it is more chemically labile than its DNA counterpart. Second, the transesterification can undergo non-enzymatic catalysis by metal ions to isolate their role. Third, metal ions are found to selectively cleave the phosphodiester bond as opposed to other possibilities such as N-glycoside cleavage (Yashiro et al., 2002). Therefore, this

system will allow us to selectively study the role of metal ion catalysis in phosphodiester cleavage.

Several metal ions have been utilized in previous studies, such as Mg^{2+}, Zn^{2+}, Co^{3+}, and lanthanide ions; however, limited work has been done using Ca^{2+}, the focus of our particular study. Ca^{2+}has not generally been shown to offer dramatic catalysis, as it does not assist in the cyclization/cleavage of 3',5'-uridyluridine at neutral pH (Breslow, 1982; Breslow & Huang, 1991). However, recent work has suggested use of Ca^{2+} by DNAzymes to offer relatively high catalysis in comparison to other popularly studied ions (Zhou et al., 2017). Ca^{2+} has also been shown as a cofactor in phosphatidylinositol cleavage, an analogous reaction, in protein enzymes (Bai et al., 2010). Furthermore, the choice of Ca^{2+}specifically offers the unique opportunity to conduct reactions at alkaline conditions due to its relative solubility compared to other commonly studied ions. While $Mg(OH)_2$ and $Zn(OH)_2$ have solubility constants (K_{sp}) of 6×10^{-10} and 3×10^{-16}, $Ca(OH)_2$ is significantly higher at 6.5×10^{-6} (Harris, 2010). The opportunity to conduct kinetic trials at alkaline conditions allow for faster reaction rates due to the relatively more activated nucleophile, which are first order with respect to hydroxide concentrations (Ikenaga & Inoue, 1974). In addition, alkaline conditions isolate the cleavage reaction. At neutral and acidic pH both isomerization (Oivanen et al., 1998) and desulfurization (Ora et al., 1998) reactions occur, which would complicate kinetic analysis. Therefore, this particular system allows us to isolate calcium assisted cleavage from these side reactions and has been a recent major focus of the Cassano lab.

Prior work by Kyle Messina in the Cassano lab highlights several aspects of this model system that allows for application for our particular use. First, kinetic trials at various concentrations of calcium chloride suggest that the hydrolysis rate constant has a saturable first order dependence on [Ca^{2+}] (Messina, 2013). Second, the reaction is characterized as first order with respect to hydroxide similar to other results in the literature (Zhang et al., 2016), which highlight the role of specific base catalysis in this reaction mechanism (Messina, 2013). Therefore, these results allow for further steps to be taken for mechanistic conclusions with the mononuclear metal ion, beginning with an analysis of the role of the general acid-base mechanism to Ca^{2+} assisted catalysis.

1.8. Current Study

The goal of the current study is to evaluate the effects of thio-substitutions on Ca^{2+} catalysis within our dinucleoside model system. Results should help probe the role Ca^{2+} plays as a Lewis acid that would stabilize non-bridging oxygen moieties through inner sphere coordination. These conclusions will be made through utilizing both experimental and computational methods.

Kinetic Studies

Kinetic experiments will isolate the role of non-bridging oxygen atoms to Ca^{2+} catalysis of UpG cleavage. First, the use of solvent deuterium isotope effects will help identify the role of proton transfer to catalysis. Reactions run slower in D_2O would suggest a general acid/base mechanism; however, previous work in the Cassano lab suggest against this possibility (Messina, 2013). Second, we will evaluate the difference between the pseudo first order rate constants of various UpG dinucleotide models (Figure

9). The use of thio-substituted dinucleotides should allow for an investigation of the role of inner sphere coordination to catalysis. Ca^{2+} is a hard metal ion that is expected to discriminate against sulfur moieties, while binding to oxygen moieties. Therefore, substitutions for sulfur in the non-bridging position will help identify the role those positions play in the metal ion's mechanism of catalysis. Based on the expectation that the inner sphere mechanism is the dominant catalytic mechanism, it is expected that thio-substitutions cause dramatic catalytic and binding defects (Figure 10). Prior results within the Cassano lab using monothioate models suggested limited inner sphere coordination because of the modest catalytic defects and limited effects on binding observed. However, it was hypothesized that the monothioate model may be limited due to the potential for monodentate binding with the remaining oxygen moiety (Figure 11). Therefore, in this study the use of a dithioate model is evaluated, which is expected to hinder Ca^{2+} ability to bind the nucleotide and catalyze its cleavage, suggesting inner sphere coordination as a prominent mechanism.

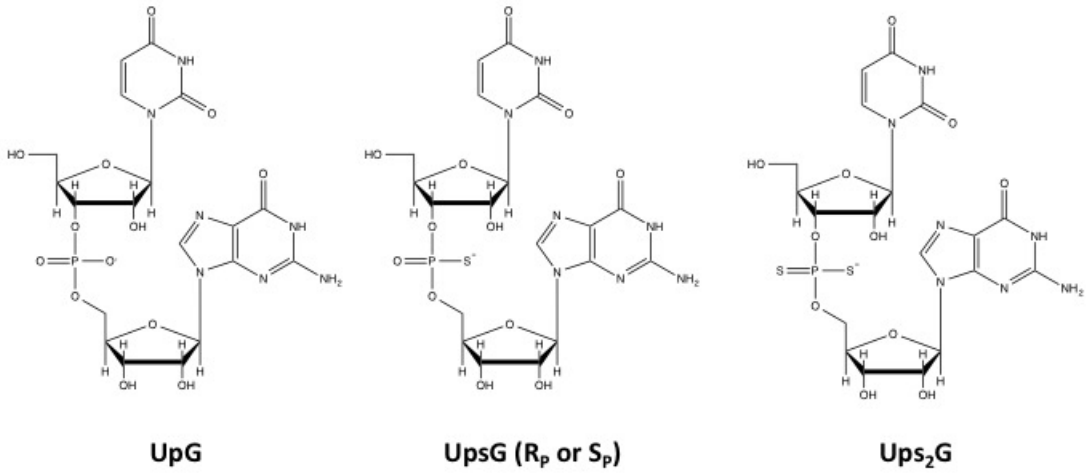

Figure 9. Various 3'-UpG-5' Dinucleotide Models. In order to assess to relative importance of non-bridging oxygen atoms to metal ion electrophilic stabilization the

cleavage of UpsG and Ups_2G was compared to UpG. UpsG exist as an R_p and S_p diastereomer, which must be separated by high pressure liquid chromatography for kinetic trials.

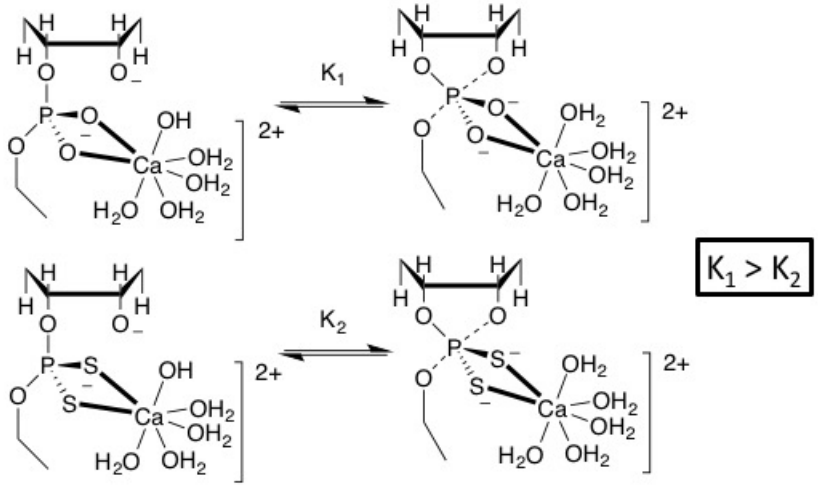

Figure 10. Hypothesized kinetic results for dithio-substitution of non-bridging oxygen atoms. The formation of the phosphorane and is subsequent cleavage is expected to decrease upon thio-substitution due to the interference of inner sphere coordination. The equilibrium constant of phosphorane formation is expected to decrease upon the dithio-substitution (K_2) as compared to the diester equilibrium constant (K_1), which would suggest decreased cleavage.

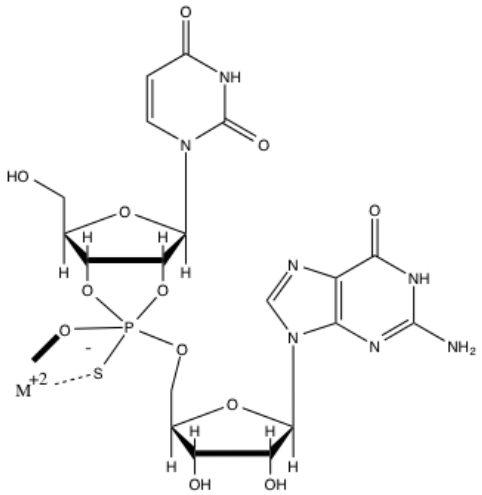

Figure 11. Hypothesized Binding Mode to Monothioate Dinucleotides. Prior kinetic results show minimal catalytic defects for monothioate substituted models, which suggest some amount of binding is occurring. Monodentate binding is suggested and confirmation can be achieved through the use of computational modeling.

Furthermore, kinetics studies are done comparing Ca^{2+} to other metal ions to more completely evaluate the possibility of inner sphere coordination. First, Ca^{2+} is compared to Mg^{2+}, a harder metal ion in its periodic group; therefore, the two metal ions share similar reactivity. If inner sphere coordination were to be a dominant catalytic paradigm, it is expected that the harder Mg^{2+} would have more dramatic thio-effects (Figure 12). Second, $Ca^{2+}$is compared to $Co(NH_3)_6^{3+}$, a kinetically inert transition metal ion complex that serves as a popular model for outer sphere coordination. $Co(NH_3)_6^{3+}$is expected to be a less effective catalyst and should exhibit minimal thio-effects as it is unable to coordinate with non-bridging oxygen moieties (Figure 13). This same result is expected when comparing Ca^{2+} to tetramethyl ammonium (I), which serves as a control for possible Na^{+} catalysis. Third, Na^{+} catalysis is assessed, which should be similar to tetramethyl ammonium (I) with minimal catalysis to confirm its use as a control species to maintain ionic strength. Overall, these metal ion comparisons should corroborate Ca^{2+} thio-substitution experiments to suggest the critical importance of inner sphere coordination to metal ion catalysis of phosphodiester cleavage.

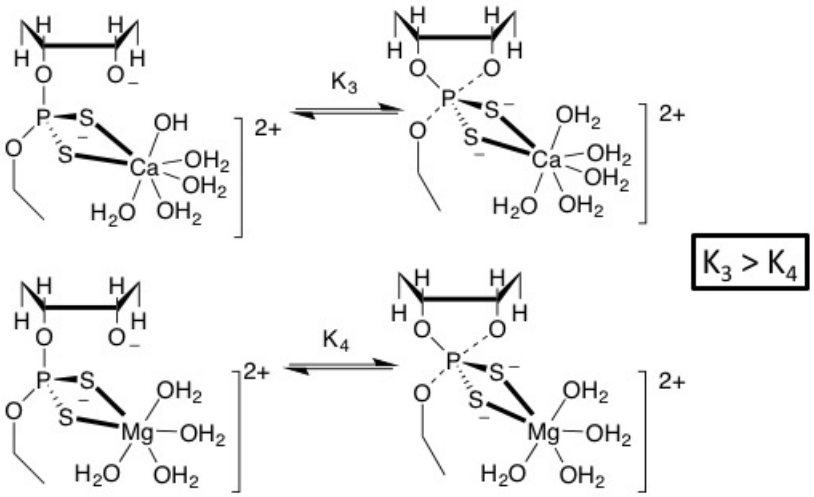

Figure 12. Hypothesized kinetic results for comparisons to Mg^{2+}. Ca^{+2} and Mg^{2+} have similar cleavage rate with in the literature; however, if the inner sphere mechanism is prominent Mg^{2+} should exhibit a larger catalytic defect as it is a harder metal ion. Therefore, the formation of the phosphorane and its subsequent cleavage for the dithio-model should decrease for Mg^{2+}, as depicted by a lower equilibrium constant.

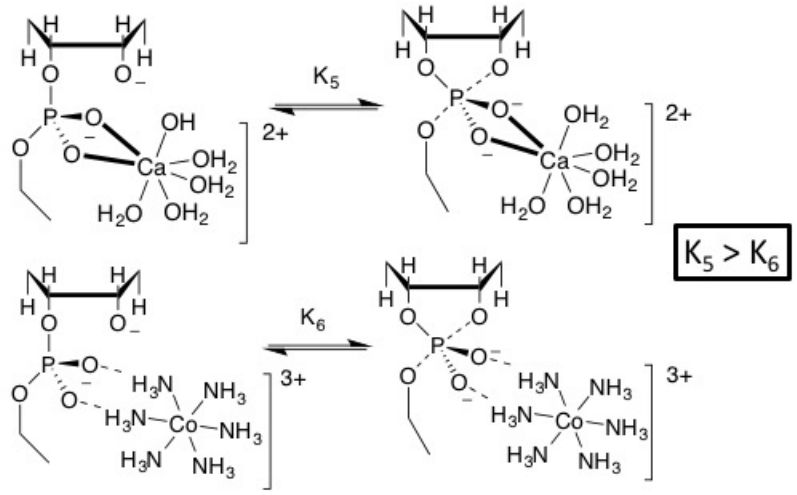

Figure 13. Hypothesized kinetic results for comparisons to $Co(NH_3)^{3+}$. $Co(NH_3)^{3+}$ should exhibit lower phosphorane formation as it lacks the ability to stabilize phosphorane formation through inner sphere coordination as shown by the equilibrium.

Computational Studies

In order to further understand kinetic results as well as garner a more complete picture of the effects of thio-substitutions on metal ion binding to various reaction coordinate species, a computational model was developed. Previous computational work has investigated metal ion binding to phosphoryl functionalities as well as investigated the effect of thio-substitutions on phosphoryl model systems. However, few studies have investigated the effect of thio-substitutions on metal ion binding to the phosphoryl model systems. Our goal was to utilize a model of base catalyzed RNA phosphodiester cleavage to compare the effects of thio-substitutions on uncatalyzed as well as Mg^{2+} and Ca^{2+} catalyzed reactions (Figure 14). Specifically, Density Functional Theory was used to evaluate the effects of thio-substitutions on inner sphere coordination through analyzing the bond orders, structures, molecular orbitals, and energies of reactant, phosphorane, and product species. It is expected that results suggest the metal ions exhibit monodentate binding to monothioate models and have diminished coordination toward sulfur non-bridging atoms.

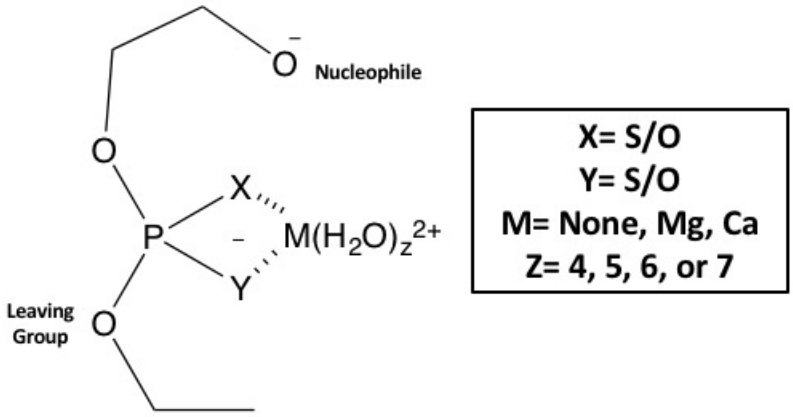

Figure 14. Computational Model. In order to simplify computational calculations a basic diester model was used with an ethoxide leaving group. In order to assess the effects of thio-substitutions for experimental comparisons the non-bridging positions were substituted for sulfur atomsin certain calculations. Calculations were run with no ion, Mg^{2+}, and Ca^{2+}. In addition, to assess the relative energies of ligand substitutions reactant complexes we optimized with various size primary hydration sphere shells. Above depicts our reactant model; however, calculation were also completed for phosphorane and product structures.

Overall, the goal of the study is to utilize both kinetic and computational methods to assess thio-substitutions as a model to make mechanistic conclusions. Chapter 2 will highlight the kinetic defect present in our thio-substituted model. Chapter 3 will elucidate the energetic and electronic defects seen computationally that may explain experimental trends. Overall, these studies will shed light on the relative importance of inner sphere coordination and Lewis acid interactions to metal ion catalysis of RNA phosphodiester cleavage.

CHAPTER 2: KINETIC ANALYSIS

2.1. Introduction

Several different kinetic manipulations, such as solvent kinetic isotope effects and thio-substitutions, are utilized to suggest the mechanism of Ca^{2+} catalyzed phosphodiester cleavage. Each method offers the opportunity to highlight specific interactions and narrow down catalytic possibilities.

Solvent Deuterium Isotope Effects

In order to properly investigate the role of electrophilic catalysis (Figure 15) it is important to assess the contributions of more commonly relied upon mechanisms, such as general acid/base catalysis (Figure 15). A common experimental technique that detects the presence of general acid-base catalysis involves the use of solvent isotope effects to determine whether a proton transfer is rate limiting or rate controlling (Yang et al., 2005). Similar to heavy atom isotope effects, this involves the comparison of aqueous rate constant of Ca^{2+} assisted phosphodiester transesterification to that in a deuterium oxide (D_2O) solvent (SDIE= k_{H2O}/k_{D2O}). Deuterium, the heavier isotope, prefers stiffer bonding environment; therefore, transition states involving O-D bond breaking will be high in energy compared to O-H bond breaking events (Quinn & Sutton, 1991; Schowen, 1972). Therefore, the presence of a normal isotope effect greater than 1 ($k_{H2O}>k_{D2O}$) would suggest a rate limiting proton transfer, which would support the possibility of a general acid-base mechanism (Yang et al., 2005).

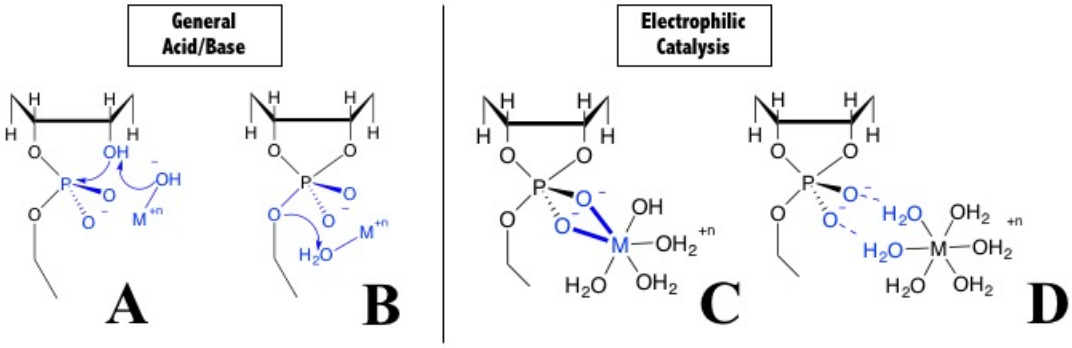

Figure 15. Mechanistic Possibilities. The goal of our kinetics studies is to elucidate the role of electrophilic catalysis. However, first SDIEs are used to assess the relevance of general base catalysis (A) and general acid catalysis (B). Next thio-substitutions will be utilized to differentiate between inner sphere (C) and outer sphere binding (D).

Thio-Substitutions

In order to specifically assess the role of electrophilic catalysis, studies often rely upon thio-substitutions of oxygen moieties. Based on the theory of interactions between Lewis acids and bases, the expectation is that hard anions will interact more favorably with hard cations. Therefore, studies using thio-substitutions assume that small ions with direct inner sphere interactions in positions that are substituted will be interrupted by the soft sulfur. If this interaction is catalytically important, the substitution should cause defects in the enzyme or metal ion's ability to catalyze the reaction, which can be measured through chemical kinetics (Herschlag et al., 1991). Cleavage of phosphodiester compounds can be significantly impaired due to thio-substitutions, particularly in the non-bridging position. A Ca^{2+}-dependent phosphatidylinositol-specific phospholipase C from *Streptomyces antibioticus* had 300,000,000-fold catalytic defect due to an Sp non-bridging oxygen thio-substitution, which highlight Ca^{2+}'s sensitivity to thio-substitutions

(Bai et al., 2010). These dramatic and measurable kinetic effects make these studies useful for mechanistic insight.

This theory has been particularly useful in the study of ribozymes using an assay known as a "metal ion specificity switch". In this experiment a particular oxygen atom is replaced with a sulfur. If the oxygen atom was catalytically relevant, then a Mg^{2+} dependent ribozyme should experience catalytic defects. However, in order to confirm the effect was due to disruption in metal ion interactions and not structural alterations, a softer, more "thiophilic", ion is replaced for Mg^{2+}. A gain in activity would suggest that the replaced oxygen atom directly interacted with the metal ion. Several examples exist for studies of the hammerhead ribozymes with phosphorothioate models, where cleavage only occurs after Mn^{2+} and Cd^{2+} are present (Scott, 1999; Suzumura et al., 2002). Overall the use of thio-rescue experiments have shown examples ranging from limited rescue of activity to complete rescue, which highlights various issues, including sterics, at play upon these substitutions in biological systems (Lönnberg et al., 2007). These sulfur substitutions can have dramatic effects on hydrogen bonding, metal ion binding, solvation, and van der Waals interactions simultaneously (Lönnberg et al., 2007). Due to the various factors present in these larger systems, it is difficult to unambiguously discriminate between inner and outer sphere interactions (Hougland et al., 2005).

Therefore, the use of thio-substitutions, in smaller model systems, a less common use of thio-substitutions, can prove useful in assessing the role of non-bridging oxygen atom interactions in metal ion catalysis as well as the subtleties within the thio-substitution technique as they could apply to ribozymes. Current work on thio-

substitutions in small molecule model systems have aimed to gauge how the sulfur atom impacts the stability of metal ion complexes. The relative stability of complexes with phosphoryl moieties compared to their thioate counterparts is shown to be dependent on the specific metal ion studied. In comparing complexes of adenosine 5'-O-thiomonophosphate ($AMPS^{2-}$) and its parent nucleotide adenosine 5'-O-monophosphate (AMP^{2-}), several metal ions are able to bind with sulfur atoms. Zn^{2+} and Cd^{2+} exhibit high binding affinities for the complex despite the substitution in the non-bridging position (Sigel et al., 1997). Mg^{2+} and Ca^{2+} served as example complexes exhibiting limited thio-defects, with only approximately a 1.1-fold defect in binding for both ions (Sigel et al., 1997). Similar to these results on a monoester model, it seems that these effects on binding are present in comparing a uridylyl-(5'-3')-[5']-uridylate ($pUpU^{3-}$) diester model with its monothioate model ($pUpsU^{3-}$), where binding primarily occurs at the terminal phosphate (Knobloch et al., 2008). Findings suggest that both Mg^{2+} and Pb^{2+} do not exhibit major binding defects upon thio-substitutions, but both seem to weakly coordinate with the sulfur atom with no chelation by Mg^{2+} and minimal chelation by Pb^{2+} (Knobloch et al., 2008). Pb^{2+} in this case serves as a comparison to Ca^{2+} as they are known to share similar coordination properties (Knobloch et al., 2008; Martin, 1986). In these cases, it seems that monothioate substitutions have limited binding affects; however, the remaining oxygen atom may allow for compensatory interactions that make binding monothioate bonds stable, which suggests the need for dithioate models for a more conclusive analysis of thio-defects. Additionally, while binding can offer great insight into reactivity trends, kinetic trials are the most useful for mechanistic insight.

Dithioate models are particularly useful for testing our current hypothesis, as the dual substitution should cause dramatic effects on catalysis. Currently minimal work has been done using dithioate diester models, which can most probably be attributed to the difficulty in obtaining these models synthetically or commercially. Work done using alkyl and aryl uridine phosphorodithioates find that the uncatalyzed mechanism is unaffected by these substitutions, which suggest that direct comparisons may be possible when analyzing thio-effects on metal ion catalysis (Ora & Hanski, 2011). This trend continues in reactions of a 3',3'-phosphorodithioate linkage, which exhibit negligible thio-effects in uncatalyzed phosphodiester cleavage (Lönnberg et al., 2007). It is hypothesized that while the polarizable sulfurs stabilize the phosphorane, the dithioate's poorer solvation may eliminate any visible thio-effects. Therefore, it is necessary to study whether metal ion interactions exhibit different trends upon thio-substitution to probe both the role of electronics and solvation.

Our work utilizes a dithioate model of UpG, a 5'-3' dinucleotide, where both non-bridging oxygen atoms are substituted with sulfur. Thio-effects of Ca^{2+} assisted cleavage and hydroxide assisted cleavage were compared, as well as the kinetic rate dependence of dithioate cleavage on $CaCl_2$ concentrations to obtain binding parameters. It is hypothesized that the dithioate substitution should cause binding and catalytic defects, and show thio-effects well above that of hydroxide catalysis.

Comparisons to Metal Ions

Unfortunately thio-effects are limited in their ability to unambiguously differentiate between inner and outer sphere coordination (Hougland et al., 2005). In many cases comparisons to other metal ions can prove to be useful (Corona-Martínez et al., 2012). Our studies utilize comparisons with $Co(NH_3)_6^{3+}$, Mg^{2+}, Na^{+}.

$Co(NH_3)_6^{3+}$, with its slow ligand exchange rate of 10^{-10} s^{-1} prevents substitution of the primary shell of amine ligands, which preclude the complex from interacting with the phosphodiester via inner sphere coordination (Basolo & Pearson, 1988). Therefore, the catalytic rate enhancements provided by this complex can serve as a model to assess the importance outer sphere coordination. It is particularly useful in studies of Mg^{2+} dependent enzymes as it maintains a similar size and geometry to the fully hydrated hexacoordinate magnesium ion (Corona-Martínez et al., 2012). Work on the mechanism of metal ion catalysis in the acyl-transferase ribozyme find minimal catalytic defects due to a substitution of Mg^{2+} to $Co(NH_3)_6^{3+}$, which suggests the possibility of $Mg(H_2O)_6^{2+}$ being the catalytically active species rather than direct coordination by Mg^{2+}. However, in many cases this substitution is actually detrimental to catalysis. For example, $Co(NH_3)_6^{3+}$ is found to inhibit the activity of the hepatitis delta virus ribozyme because of the weak catalytic activity of outer sphere coordination (Das & Piccirilli, 2005).

Interestingly, in smaller model systems minimal work has been done comparing the catalysis of ions like Mg^{2+} and Ca^{2+} to the inert outer sphere complex. A study using an HpPNP RNA model found that Ca^{2+} and Mg^{2+} catalyzed specific base reactions were 16 and 100-fold faster that those with $Co(NH_3)_6^{3+}$ present (Corona-Martínez et al., 2012).

Additionally, $Co(NH_3)_6^{3+}$ is found to bind the transition state weakly, which suggests against complex formation through outer sphere coordination. These results suggest that ion pairing is responsible for any of the complex's catalytic behavior (Corona-Martínez et al., 2012). Therefore, in our particular study Ca^{2+} catalysis is compared to $Co(NH_3)_6^{3+}$ catalysis to assess the role of outer sphere coordination in RNA dinucleotide cleavage at alkaline pH (Figure 16). If the outer sphere mechanism was relevant to catalysis then $Co(NH_3)_6^{3+}$ would cause greater rate enhancements due its greater charge. However, based on prior experiments it is expected that outer sphere coordination plays a minimal role in catalysis. The cobalt complex should offer poor rate enhancement. Additionally, we investigated $Co(NH_3)_6^{3+}$ binding through kinetic trials at varying concentrations, as it is not expected to show weak binding. Finally, cobalt hexamine (III) trials are run with monothioate and dithioate models to confirm the hypothesis that thio-substitutions do not disrupt outer sphere coordination as well as highlight the role of hydrogen bonding in outer sphere electrophilic catalysis.

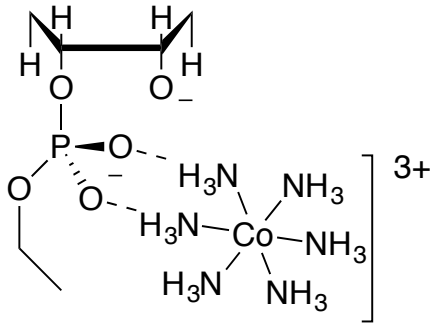

Figure 16. Proposed Mechanism of Outer Sphere Interaction by Cobalt Hexamine (III). The outer sphere mechanism may rely on electrostatic stabilization and hydrogen bonding; however, it can directly coordination with the phosphodiester bond.

In addition, similar to the work of Corona-Martínez et al. (2012), Mg^{2+}, a hard metal ion, is used to probe the relevance of Lewis acid-base interactions. Several kinetic studies have looked into catalytic rate enhancement by Mg^{2+} because of its biological relevance (Beebe et al., 1996; Cate et al., 1997). While Mg^{2+} is not as catalytically active as lanthanides or transition metals (Breslow & Huang, 1991), in many cases including an RNA model, HpPNP, Mg^{2+} is found to be a better catalyst than Ca^{2+} (Breslow & Huang, 1991; Corona-Martínez et al., 2012). However, in some case, like differences in binding of AMP^{2-} and $AMPS^{2-}$, Ca^{2+} and Mg^{2+} share similar reactivity (Sigel et al., 1997). In addition, Mg^{2+} has been shown to be exhibit kinetic thio-effects in ribozyme systems similar to calcium; however, to date no study has compared the degree of these effects (Hougland et al., 2005). In our kinetic trials it is expected that Mg^{2+} is more catalytically active as the better Lewis acid, while also exhibiting larger thio-effects.

2.2. Methods

High Pressure Liquid Chromatography Analysis

In order to purify samples and analyze kinetics experiments, a separation technique known as High Pressure Liquid Chromatography (HPLC) was used to separate products and reactants in reaction mixtures for kinetic quantification (Harris, 2010). Similar to various other types of chromatography HPLC maintains a mobile phase, liquid solution, and a stationary phase, which is present within a column.

Our particular setup utilizes a nonpolar C18 column, which attracts hydrophobic molecules, as the stationary phase with a polar aqueous mobile phase. Elution is highly dependent on the molecule's rate of adsorption and desorption to the stationary phase.

Nonpolar substances will more favorably adsorb to the column and elute at later times. Furthermore, the polarity of the mobile phase can impact molecular interactions with the high pressure solvent. Acetonitrile is used to increase the nonpolar properties of the aqueous solvent system: decreasing the retention time of all elutants. Using this chromatography system our guanine leaving group product would exhibit shorter retentions times than our relatively non-polar bulky dinucleotide reactants for all our models.

UpG and UpSG-R_p aliquots were analyzed by Agilent 1100 Series HPLC through an Xbridge C18 3.5 micron 4.6X150 mm column stationary phase and a 2% acetonitrile, 0.1 M ammonium acetate aqueous mobile phase solution flowing isocratically. UpsG-S_p aliquots were analyzed with a 4% Acetonitrile, 0.1 M Ammonium Acetate aqueous mobile phase solution. $Co(NH_3)_6Cl_3$ reactions required 2% Acetonitrile isocratic flow, due to interference of UV-Vis absorbance signal inherent to the metal ion complex. Ups_2G reactions were analyzed through a Bondclone C18 300X3.9 mm 10 micron column stationary phase. The aqueous mobile phase used for purification was isocratic with 5 minutes of 5% acetonitrile (Solution A), which was followed by a gradient increase in 95% acetonitrile (Solution B) to a 50:50 ratio in 20 minutes.

Products and reactants were differentiated based on elution times of standard samples of UpG, UpsG (Sp/Rp), Ups_2G and guanosine (Figure 17). Peaks were individually integrated for kinetic analysis for all reaction times in various reaction conditions.

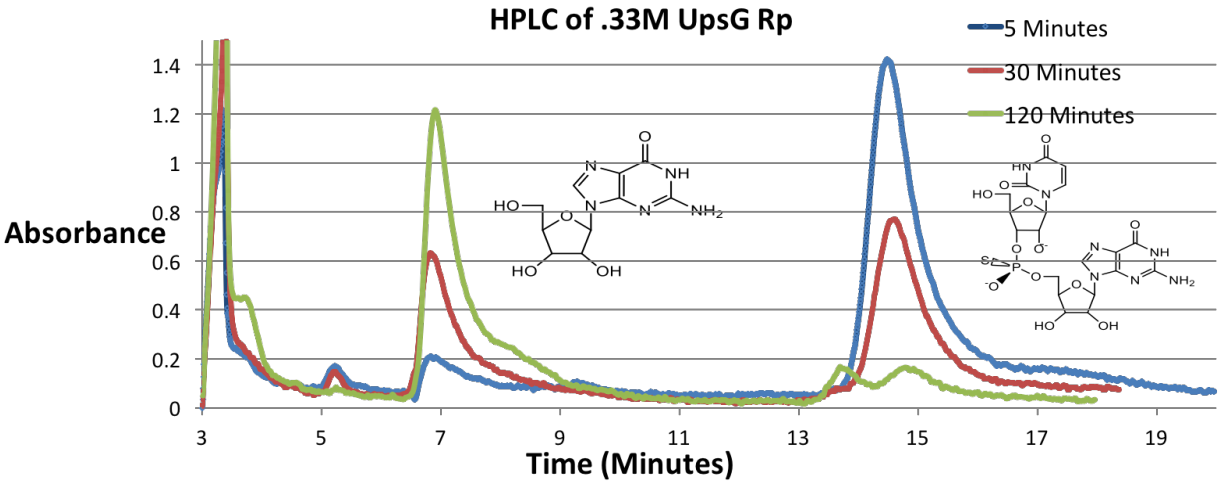

Figure 17. HPLC Data of a neutralized 0.33M Ca^{+2} trial. Aliquots from 5 minute (blue), 30 minutes (red) and 120 minutes (green) are shown. UpsG Rp reactant's retention time is about 15 minutes and G product peak has a retention time of about 7 minutes. As the reaction proceeds, the amount of reactant decreases and the amount of product increases. The peak area is proportional to the concentration of compound. Figure adapted from Kyle Messina (2013).

Dinucleotide Sample Preparation

UpG (Dharmacon) stock solutions were deprotected as per Dharmacon instructions. Solutions were resuspended and then concentrations were determined through measurements of UV-Vis absorbance at 260 nm using a Beckmann 630 DU spectrophotometer and calculation via Beer's law using a molar absorptivity of 20000 M^{-1} cm^{-1} (Ambion Oligo eta calculator). 5 nmol aliquots were dried down using Speed Vac SC110 and stored at -20ºC prior to kinetic trials. UpsG (Dharmacon) stock was deprotected in the same manner as UpG; however, enantiomers were then separated through reversed phase chromatography using Agilent 1100 Series HPLC with a Phenomenex C18 300X390 mm 10 micron column stationary phase and a 4% acetonitrile, 0.1M ammonium acetate aqueous mobile phase solution. UpsG Rp and Sp

enantiomer solutions were dried similarly to UpG and resuspended in 1 mL of Millipore filtered water five times to remove any residual ammonium acetate salt. Resuspended solutions were spun down in a Desktop Microcentrifuge Eppendorf 5424 at 15,000RPM for 15 minutes, and UpsG supernatant was collected for both the Rp and Sp enantiomers. Concentrations were determined similarly to UpG, using a molar absorptivity of 21500 M^{-1} cm^{-1} at 260 nm (Ambion Oligo eta calculator). Aliquots of 2 or 3 nmol were dried down and stored at -20ºC before reactions. The dithioate model, Ups_2G (AM Biotechnologies), was purified from crude product mixture through reversed phase chromatography with a Bondclone C18 300X3.9 mm 10 micron column stationary phase. The aqueous mobile phase used for purification was isocratic with 5 minutes of 5% acetonitrile (Solution A), which was followed by a gradient increase in 95% acetonitrile (Solultion B) to a 50:50 ratio in 20 minutes. Ups_2G solutions were desalted as described for UpsG samples. Concentrations were determined similarly to prior samples, using a molar absorptivity of 23000 M^{-1} cm^{-1} at 260 nm, calculated based on assumed effect of sulfur on molar absorptivity based on change in molar absorptivity between UpG and UpSG. Aliquots of 3 or 4 nmol were dried down using Speed Vac SC110 and stored at -20ºC before reactions. Dinucleotide samples were used in subsequent kinetic assays.

Kinetic Assays

Reactions with varying Ca^{2+}, Mg^{2+}, $Co(NH_3)_6^{3+}$ concentrations were run with dinucleotide samples of interest and were began using a 500-µL initiation mixture kept at a constant ionic strength of 1 M maintained by NaCl, and in some cases 1 M tetramethyl ammonium chloride. Initiation mixtures were generally pH 11.5 with 50mM CAPS

Buffer (Sigma Aldrich), except for comparisons to Mg^{+2}, which used 50 mM EPPS at a pH of 8.75 due to its relative insolubility at alkaline conditions. All reactions were run at 37ºC aside from comparisons to Mg^{+2}, which was run at 50ºC. After reactions were initiated at elevated pH conditions, aliquots were quenched at specified time points by 50 µL 87.5 mM EPPS or HEPES free acid (Sigma Aldrich) to pH 7-8 and stored at -20ºC until HPLC analysis. All reaction mixture pH's were determined through mock reactions prior to kinetic analysis of chromatograph data.

Kinetic Analysis

Peaks were manually integrated at 260 nm and normalized using extinction coefficient for each compound. The extinction coefficient for G was 13,200 M^{-1} cm^{-1} (NIST Chemistry Webbook), 20,000 M^{-1} cm^{-1} for UpG (Ambion Oligo eta calculator), 21500 M^{-1} cm^{-1} for UpsG R_p and S_p (Ambion Oligo calculator), 23000 M^{-1} cm^{-1}, which was estimated based on the difference between known UpG and UpsG values. Normalized concentrations gave the fraction of reactant remaining for UpG, UpsG, and Ups_2G reactions using Equation 2.

$$fDinucleotide = \frac{[Dinucleotide]}{[Dinucleotide] + [Guanosine]} \qquad \textbf{(2)}$$

Where [Dinucleotide] represents reactant concentrations for various model systems and [Guanosine] represents the cleavage product. Calculations of fraction reactant remaining were fit to a single exponential decay function using Kaleidagraph™ to give rate constants to compare between reaction conditions. Thio-effects were calculated via Equation 3.

$$ThioE = \frac{k_o}{k_s} \quad \textbf{(3)}$$

2.3. Results

Solvent Deuterium Isotope Effects

Comparisons of reaction run in H_2O and D_2O both under alkaline conditions at 37°C with 0.33 $CaCl_2$ show an inverse SDIE with a larger rate constant, for reactions run in a D_2O solvent (Figure 18). Results showed a slightly inverse solvent deuterium isotope effects (SDIE) with a value of 0.694 (Table 1). These inverse isotope effects suggest that a proton transfer is not involved in the rate limiting step, which suggests that the general acid-base mechanism is not responsible for Ca^{2+} assisted catalysis. This particular result was also corroborated in un-buffered conditions (Messina, 2013).

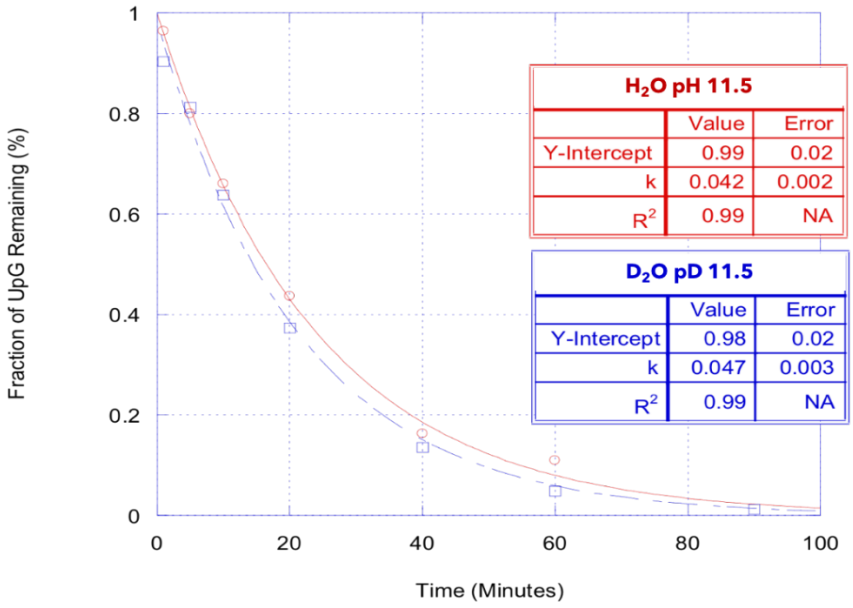

Figure 18. Solvent Deuterium Isotope Effect Result. Fraction of UpG remaining against time elapsed for single trial containing 0.33M Ca^{+2}, CAPS Buffer (pH 11.5) and either H_2O(red) or D_2O(blue). Data is fit to an exponential curve. When comparing the H_2O to the D_2O trials an inverse SDIE is observed.

Table 1: UpG Solvent Deuterium Isotope Effects with pH maintained by CAPS buffer			
	$k_{H_2O}(min^{-1})$	$k_{D_2O}(min^{-1})$	SDIE
Average	0.047	0.068	0.694
Std Error	0.005	0.005	0.016

Kinetic Assays of Thio-Substituted Models

In assessing the difference between thio-models, reactions of 0.33 M $CaCl_2$ for all model systems showed that the addition of sulfur caused a decrease in the rate constant. The calculation of thio-effects through a comparison of each thio-model to UpG showed a substantional decrease in catalysis for the dithioate model (Thio-Effect=18.6), which is markedly larger than that of the monothioates (Thio Effect=1.7 and 2.6 for Rp and Sp, respectively) (Messina, 2013) (Figure 19). Results suggest that the dithioate substitution is synergistic and causes a dramatic decrease in catalysis. Furthermore, these results are specific to Ca^{2+} catalyzed cleavage as its seems that reactions catalyzed by NaOH at a pH of 13 with the dithioate have minimal thio-defects (Thio Effect=3.8) in comparison to the 18.6-fold thio-defect in the presence of Ca^{2+} (Figure 19). Additionally, NaOH catalyzed cleavage showed similar small thio-effects for phosphoromonothioate models (Thio Effect=1.7 and 2.6 for Rp and Sp, respectively), which are equivalent to those present for Ca^{2+} (Figure 19) (Cassano, Unpublished Results). Therefore, these results suggest that thio-substitutions have minimal effects on the stability of the dinucleotide models. Additionally, these results suggest that monothioate models do not disturb catalysis;

however, the dithioate substitutions cause observable catalytic defects, suggesting the importance of electrophilic catalysis with the non-bridging oxygen moieties. Furthermore, it is proposed that these results highlight the importance of inner sphere coordination as it is expected that outer sphere mechanisms would not exhibit large defects in catalysis.

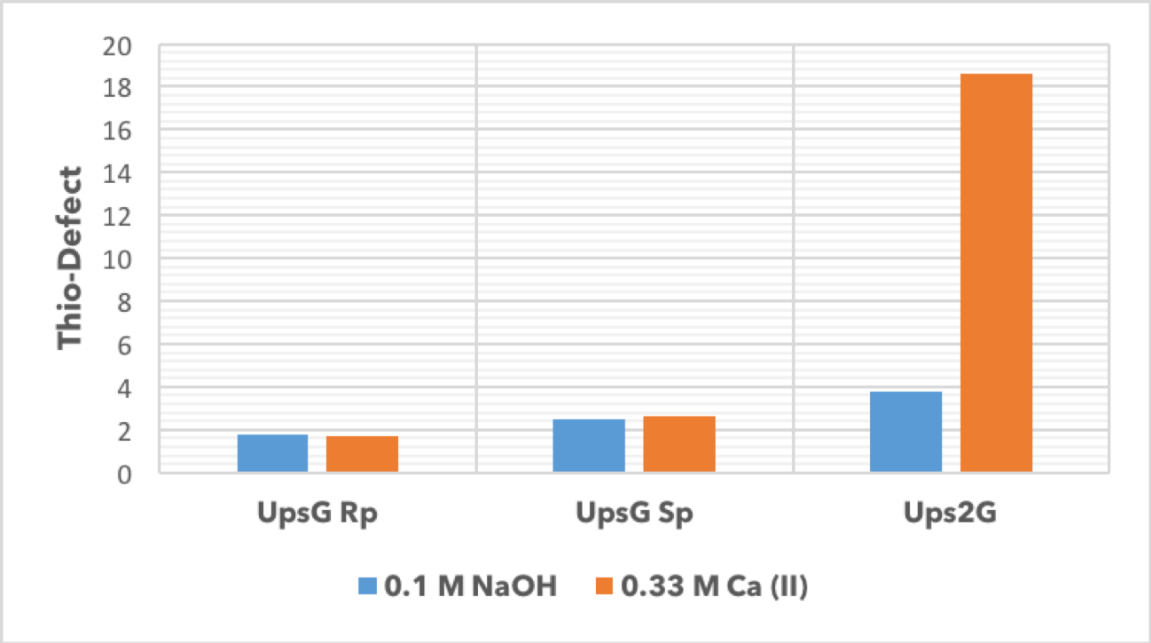

Figure 19. Thio-Defects for Phosphoromonothioate and Phosphorodithioate Models of UpG. Reactions of UpG, UpsG S_p, UpsG R_p, and Ups_2G were run under conditions with 0.1 M NaOH and 0.33 M $CaCl_2$. Minimal defects are seen in the case of NaOH for all model system as well as Ca^{2+} with the monothioates. A larger defect is present for Ca^{2+} catalyzed cleavage of the diester. Monothioate data in $CaCl_2$ courtesy of Messina (2013) and in NaOH courtesy of Cassano (Unpulished).

To further support conclusions on the relative catalytic importance of binding non-bridging oxygen atoms, the dissociation constant (K_D) of Ca^{2+} with each model was calculated through reactions at varying Ca^{2+} concentrations. k_{obs} values obtained from exponential decay fits were plotted against concentration and fit to a rectangular hyperbola (Equation 4).

$$k_{obs} = \frac{k_{max}*[Ca^{+2}]}{K_D+[Ca^{+2}]} + k_0 \textbf{ (4)}$$

k_0 represents rate constants at 0 M $CaCl_2$, k_{max} represents rate constants at saturation, and K_D represents the dissociation constant of the Ca^{+2}*Phosphodiester Model complex. Therefore, this fit allows for comparisons of binding across different phosphodiester models. These reactions, work by Kyle Messina and Arline Tarazona, suggest trends similar to comparisons against hydroxide catalyzed reactions. The general trend was that at constant concentration of $CaCl_2$ the trend in k_{obs} was UpG > UpsG (Sp) > UpsG (Rp) >Ups_2G (Figure 20). Thio-substitutions decrease cleavage rates. These rate trends lead to similar trends in k_{Ca}, which highlight that thio-substitions limit the calcium metal ion's catalytic potential. When k_0, k_{Ca}, and K_D terms of UpG reactions were compared to those of the thio-models for thio-effects of each term, several key observations were made (Figure 21). First, k_0, the rate constant without Ca^{2+} exhibits minimal thio-defects, which suggest defects greater than five-fold cannot attributed to dinucleotide stability. Second, defects in k_{Ca}, while minimal for monothioate models, reached a 37-fold defect for the dithioate model, thereby, suggesting impaired catalysis, most likely through defects in coordination and electrophilic catalysis to the non-bridging oxygen moieties. The substitution of the softer sulfur would worsen possible Lewis acid-base interactions with the hard calcium metal ion. This defect is more pronounced than previously found in our studies of thio-models. Third, no significant differences exist between the K_D values of models, suggesting similar rates of dissociation. All changes in K_D were within experimental error, thereby, suggesting minimal differences across all conditions.

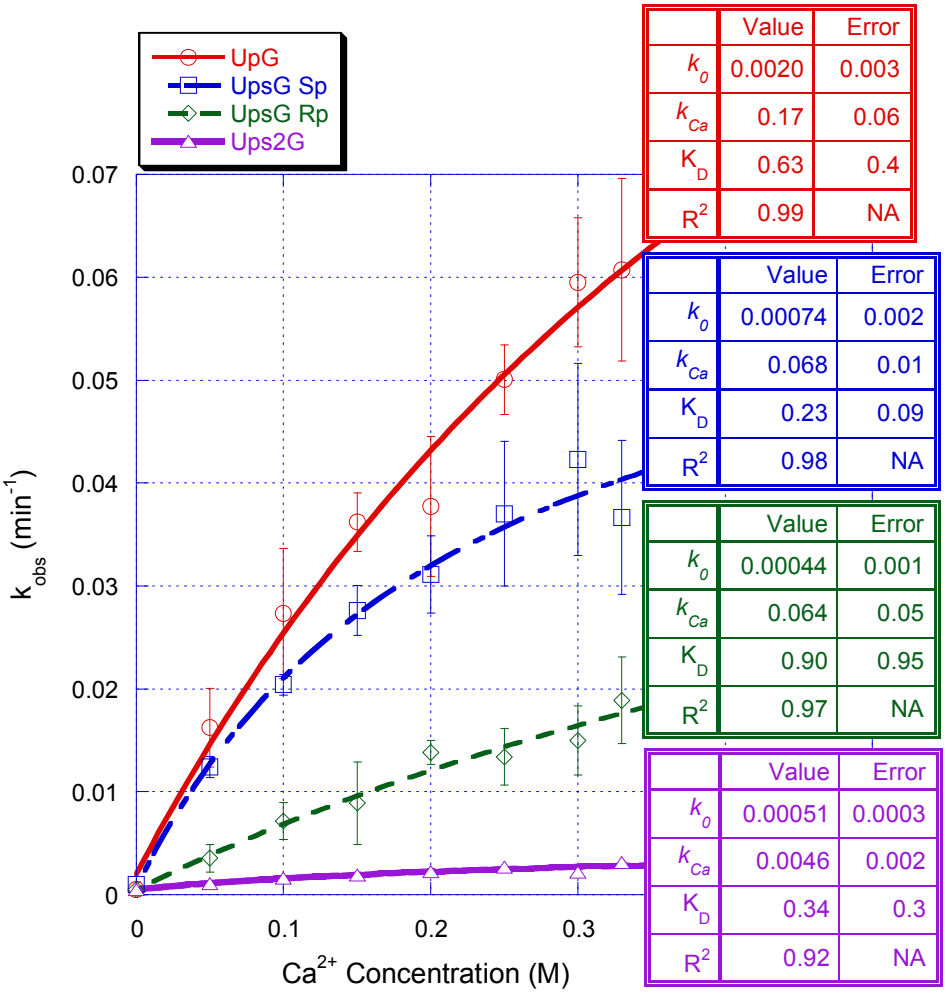

Figure 20. Concentration dependence of Ca^{+2} catalyzed cleavage of UpG (red circles), UpsG S_P (blue squares), UpsG R_P (green diamonds), and Ups2G (purple triangles). The data are modeled by a rectangular hyperbola fit where k_0 is the observed rate constant at 0 M Ca^{+2}; k_{Ca} is the observed rate constant for saturating Ca^{+2}; and K_D is the binding constant between Ca^{+2} and the given dinucleotide. All reactions were performed at 37°C, pH 11.5 and ionic strength 1.0 (controlled with NaCl).

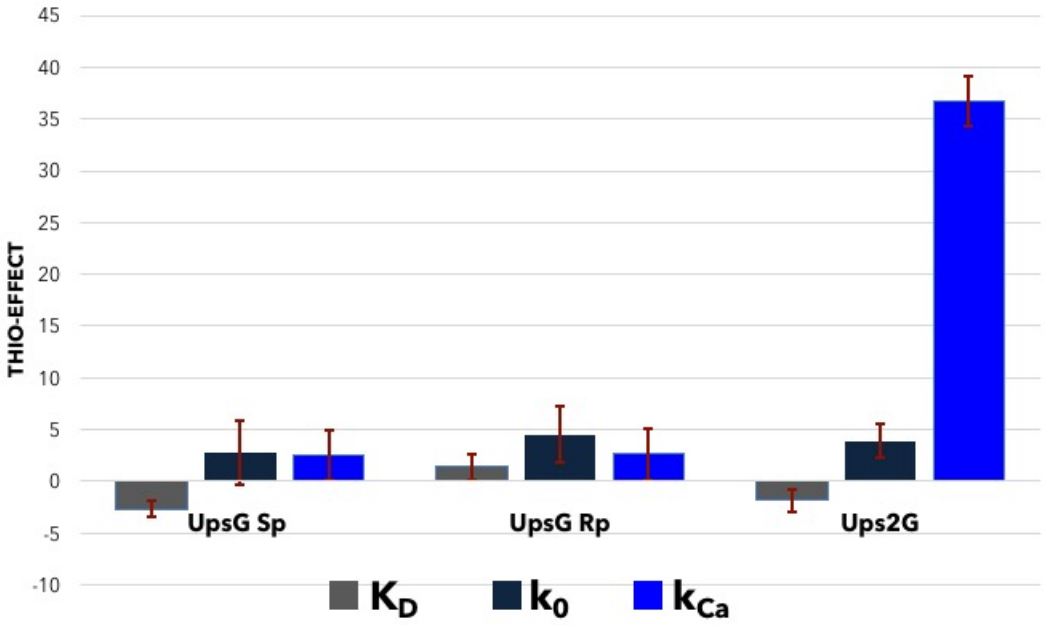

Figure 21. Thio-effects on K_D (gray), k_0 (dark blue), and k_{Ca} (light blue) for both S_P and R_P UpsG and Ups2G. All values are taken from the curve fits in Figure 8. Thio-effects for the rate constants are calculated from Eq. 3 in the methods. However, for K_D the effect was calculated by $K_D(S)/K_D(O)$. Negative values for the Thio-effect indicate the sulfur substitution engendered an enhancement in the parameter rather than a deleterious effect. Red error bars indicated the relative standard error for each thio-effect.

Kinetics Comparisons to Other Metal Ions

Comparisons of Ca^{2+} and $Co(NH_3)_6^{3+}$ highlighted the minimal catalytic role of outer sphere coordination. Preliminary catalytic studies comparing rates of UpG phosphodiester cleavage at 1 M ionic strength with 0.16 M $Co(NH_3)_6^{3+}$, 0.16 M Ca^{2+}, and 1 M Na^+, as a control, show minimal catalysis by the cobalt metal ion complex with lower rate constants (Figure 22). Fold catalysis, which was calculated by comparison of rate constants to that of the sodium negative control, showed 33-fold catalysis for Ca^{2+}, but only 2.5-fold catalysis for $Co(NH_3)_6^{3+}$, suggesting that outer sphere catalysis is weak in providing transition state stabilization (Table 2).

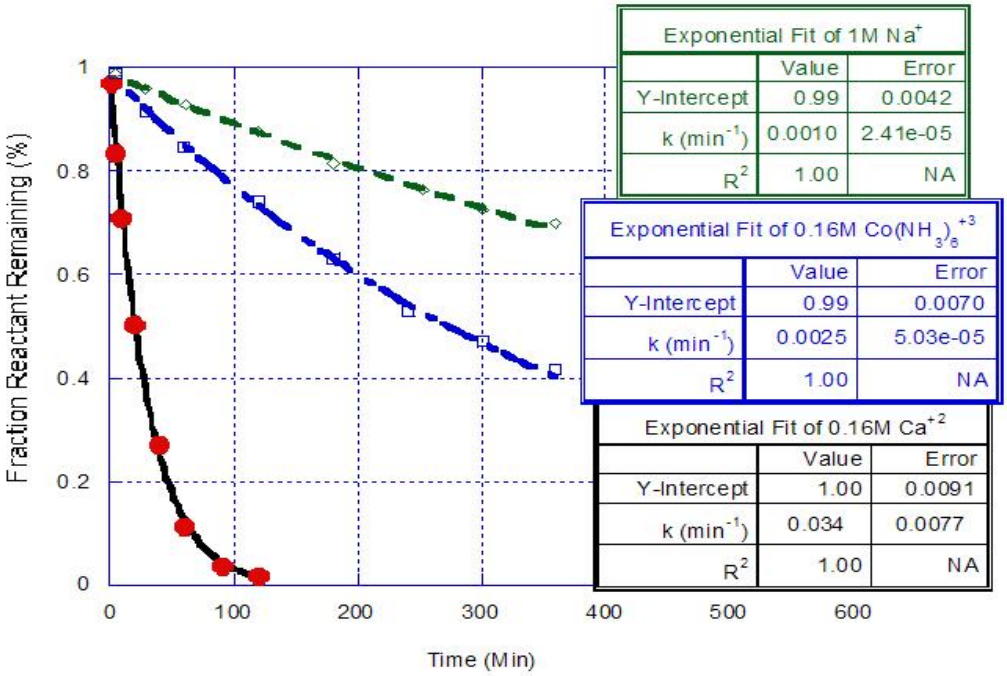

Figure 22. Exponential fit for fraction of UpG remaining against time elapsed for 0.15 M Ca^{+2} (red circles, black line), 0.16M $Co(NH_3)_6^{+3}$ (blue squares) or 1.0 M Na^{+} (green diamonds) trials at pH 11.5 and 37°C. Ca^{+2} (34X) had better catalytic effects than $Co(NH_3)_6^{+3}$ (3X), which likely suggesting that outer sphere coordination is minimally important to catalysis.

Table 2: Rate Enhancement Comparison between Ca^{+2} and $Co(NH_3)_6^{+3}$ at pH 11.5 and 1 M Ionic Strength

Metal Ion	k (min^{-1})	Fold Catalysis (UpG Model)	ΔΔG (kJ/mol)
0.16 M Ca^{+2}	3.6E-2	33-Fold	9.66
0.16 M $Co(NH_3)_6^{+3}$	2.7E-3	2.5-Fold	2.30
1M Na^{+}	1.1E-3	-	-

Similar to studies done with Ca^{2+}, kinetic trials with varying concentrations of $Co(NH_3)_6^{3+}$ were use to determine the K_D of binding to UpG. The general trend shows increased k_{obs} upon an increase in concentration of $Co(NH_3)_6^{3+}$ (Figure 23). However, these increases when plotted still show a poor fit to a rectangular hyperbola fit as evidenced by negative values of k_0 and k_{Ca} with large error values. These results suggest the rectangular hyperbola is not sufficient to model the interaction between cobalt hexamine and UpG. A linear dependence is more likely, which suggests that significant saturation is not observed at these concentrations. The interaction is likely simple ion pairing.

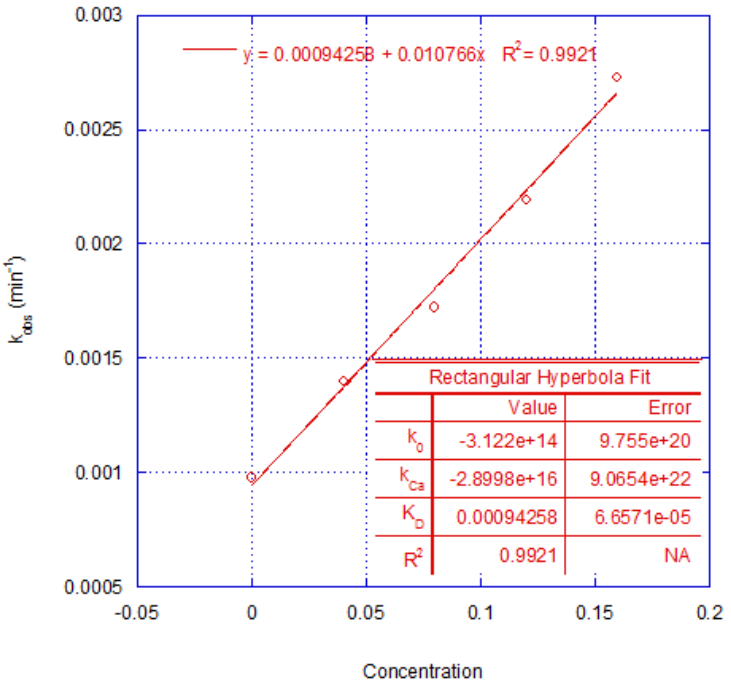

Figure 23. Concentration dependence of $Co(NH_3)_6^{+3}$ catalyzed cleavage of UpG. Rectangular Hyperbola Model (fiton bottom right) poorly fits data suggesting a linear dependence (fit on top left), which argue against the formation of a complex with the UpG substrate.

While it is clear that $Co(NH_3)_6^{3+}$ cannot form a stable complex with UpG at an ionic strength of 1 M, some amount of catalysis (2.5-fold) is occurring. This may be through electrostatics or hydrogen bonding. In order to assess the role of hydrogen bonding, reactions of $Co(NH_3)_6^{3+}$ are run with thio-models, which should disrupt these interactions as sulfur is a worse hydrogen bond acceptor in comparison to oxygen. At pH 11.5, kinetic comparisons were made between $Co(NH_3)^{3+}$ and Ca^{2+} for UpG, UpsG Rp, and Ups_2G. Results show that thio-effects for cobalt hexamine minimal in all cases, which suggest against a large role for hydrogen bonding (Table 3). These results suggest the presence of additional interactions within Ca^{2+} catalysis that are hindered by thio-substitutions.

In addition, the use of a tetramethyl ammonium (I), $N(CH_3)_4^+$, control allowed for the comparison of Ca^{2+} to Na^+. Na^+'s lower charge leads to limited thio-defects highlighting the key role of electrostatics to catalysis (Table 5). However, the results highlight the fact that Na^+ offers greater catalysis in comparison to $N(CH_3)_4^+$, which calls into question its use as a control. However, the limited reaction progression for $N(CH_3)_4^+$ calls for the need to take longer reaction time points to obtain trustworthy kinetic values.

Table 3: ThioEffect Comparison between Ca^{2+} and $Co(NH_3)_6^{3+}$ for UpG, UpsG R_p, and Ups_2G

Metal Ion	k_o (min^{-1})	k_s (min^{-1})	Thio Effect	k_{s2} (min^{-1})	DiThio Effect
0.16 M Ca^{+2}	3.6E-2	1.4E-2	2.7	9.4E-4	37.2
0.16 M $Co(NH_3)_6^{+3}$	2.7E-3	2.2E-3	1.2	9.1E-4	3.0
1 M Na^+	1.1E-3	1.2E-3	0.9	4.4E-4	2.5
1 M $N(CH_3)_4^+$	2.1E-5	-	-	9.9E-5	0.2

Ca^{2+} was also found to offer better catalysis than Mg^{2+} at pH 8.4 and 47°C (Figure 24). The fact that the harder ion offers less rate enhancement would suggest that Lewis acid-base catalysis may not be the sole factor involved. Thio-substitutions should highlight the role of Lewis acidity as it has been determined that they disrupt coordination. Monothioate substitutions suggest slightly higher thio-effects with Mg^{2+}; however, the thio-effects for both monothioate and dithioate models are thought to be minimally different between Ca^{2+} and Mg^{2+} (Table 4). This results directly contradicts our hypothesis that Mg^{2+} ions should exhibit great thio-defects due to differences in Lewis acidity. Therefore, it is likely that the the pH change impacts the size of the thio-defect present, which would suggest that the relative importance of electrophilic catalysis may vary across different pH conditions.

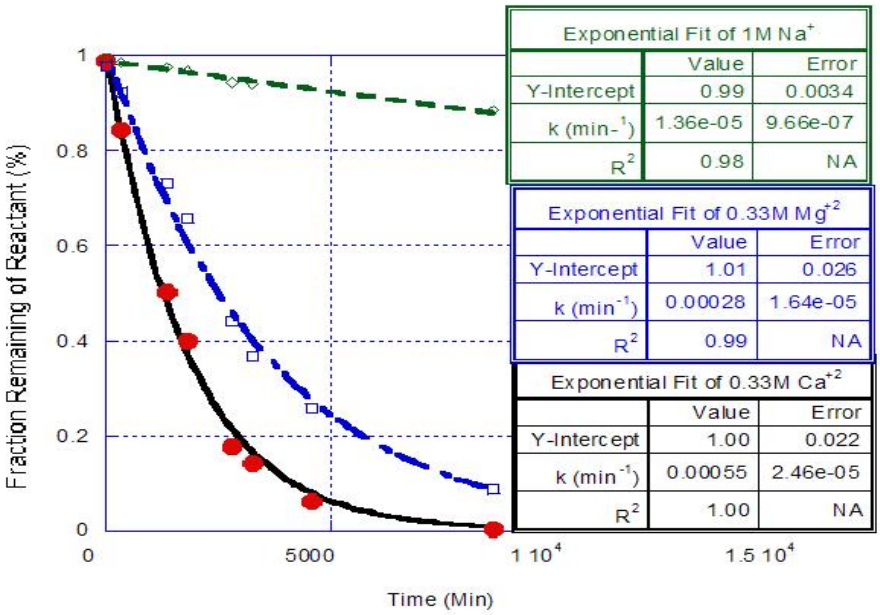

Figure 24. Exponential fit for fraction of UpG remaining against time elapsed for 0.33 M Ca^{+2} (red circles, black line), 0.33M Mg^{+2} (blue squares) or 1.0 M Na^{+} (green diamonds) trials at pH 8.4 and 47°C. Ca^{+2} (39X) had better catalytic effects than Mg^{+2} (20X). Both exhibit small thio-effects, with Mg^{+2} slightly larger in magnitude.

Table 4: ThioEffect Comparsion between Ca^{2+} and Mg^{2+} for UpG, UpsG R_p, and Ups_2G

Metal Ion	k_o (min^{-1})	k_s (min^{-1})	Thio Effect	k_{s2} (min^{-1})	DiThio Effect
Ca^{+2}	5.0E-4	2.1E-4	2.4	1.2E-4	4.2
Mg^{+2}	2.7E-4	8.7E-5	3.1	5.9E-5	4.6
Na^{+}	1.6E-5	2.2E-5	0.7	2.1E-5	0.8

2.4. Discussion

Slightly Inverse Solvent Deuterium Isotope Effects Suggest Against General Acid Base Mechanism of Catalysis

The lack of a normal isotope effect agrees with the literature results for Ca^{2+} catalysis of 2-hydroxypropyl 4-nitrophenyl phosphate (HPNP) RNA model, which have an SDIE value of 0.47 in the presence of 1-3 mM hydroxide (Corona-Martínez et al., 2012). In addition, the lack of a normal isotope effect, while surprising, has also been found for a dinuclear Zn^{2+} organometallic complex with a uracil aryl ester (Yang et al., 2005). Therefore, these results suggest against general acid-base and suggest toward a mechanism of electrophilic catalysis potentially through binding non-bridging oxygen atoms (Yang et al., 2005). However, its seems that different metal ion studies show contradicting results. For example, the Zn^{2+} metal ion gave a large SDIE of 13.2 for the cleavage of UpG, thereby suggesting the general acid-base mechanism (Zhang et al., 2016). This was also seen in LFER studies, which highlighted both general acid and general base catalysis by Zn^{2+} for alkyl phosphodiesters (Mikkola et al., 1999). It is

surprising that similar model systems give such dramatically different results; however, findings have also suggested that different metal ions may exhibit drastically different mechanisms (Corona-Martínez et al., 2012; Korhonen et al., 2013). For HPNP cleavage, Mg^{2+} is found to rely on both specific and general base (SDIE=1.23) catalysis, while Ca^{2+} only relies on the specific base mechanism (Corona-Martínez et al., 2012). Rationale for this difference is currently unknown, but it is possible that these trends can be related to effects of solvent coordination (Corona-Martínez et al., 2012). In addition, compared to other KIE studies, SDIE experiments have several caveats. First, the use of different solvents requires corrections to the pH; therefore, any discrepancies in this conversion can cause dramatic effects on rates (Quinn & Sutton, 1991). Second, the use of D_2O will involve a global exchange of all ionizable groups (Quinn & Sutton, 1991). Therefore, different protons, such as the formation of hydrogen bonds with the solvent can limit the ability to isolate particular reaction steps (Quinn & Sutton, 1991). Unfortunately, these experiments do not allow for isolated conclusions about protonation. Despite these limitations, current data does not provide evidence for general acid-base as a major mechanism of Ca^{2+} catalysis, which highlights the need to understand the importance of stabilizing non-bridging oxygen atoms of the phosphoryl.

Kinetics with monothioate and dithioate substituted models suggest inner sphere coordination

Thio-substitution results highlight the importance of non-bridging oxygen atoms to catalysis, which is not particularly surprising as calcium-dependent enzymes have shown non-bridging thio-defects (Zhou et al., 2017). However, a calcium dependent

phospholipase C actually saw a much larger defect at the order of 10^8-fold, which suggests our experimental value maybe insignificant (Bai et al., 2010). However, due to residues present within the enzyme active site, these defects may be more pronounced than in aquous metal ion models, which suggests that these modest defects can highlight worse coordination. While catalysis seems to decrease upon a dithioate substitution, the same trend is not evident in terms of binding. The thio-effects of K_D values, the equilibrium constant of the dissociation of the Ca^{2+}-substrate complex, are minimal and not significantly different across the various thio-models. Therefore, it is suspected that all UpG metal ion complexes are relatively equal in terms of stability, which is not necessarily surprising as this was suggested in studies of Ca^{2+} binding to AMP^{2-} (Sigel et al., 1997). This similar binding can be related to entropic release of water molecules into bulk solvent, which would favor binding despite any differences in coordination. Another possibility is that metal ion binding can occur primarily through outer sphere coordination, which would likely show minimal thio-defects, similar to $Co(NH_3)_6^{3+}$. In addition, the accuracy of K_D measurements are limited because measurements were not made at saturating conditions due to constraints in maintaining 1 M ionic strength. The similarity could also be a coincidental equivalence due to effects on solvation and electrostatics that cannot be isolated and may oppose each other. Despite these possibilities current results suggests that dithioate substitutions have minimal effects on complex stability, but cause a decrease in coordination and catalysis (Figure 25). Therefore suggesting that the catalytic mechanism involves electrophilic catalysis at the

non-bridging oxygen atoms of the phosphoryl, likely through direct inner sphere coordination that may be monodentate or bidentate.

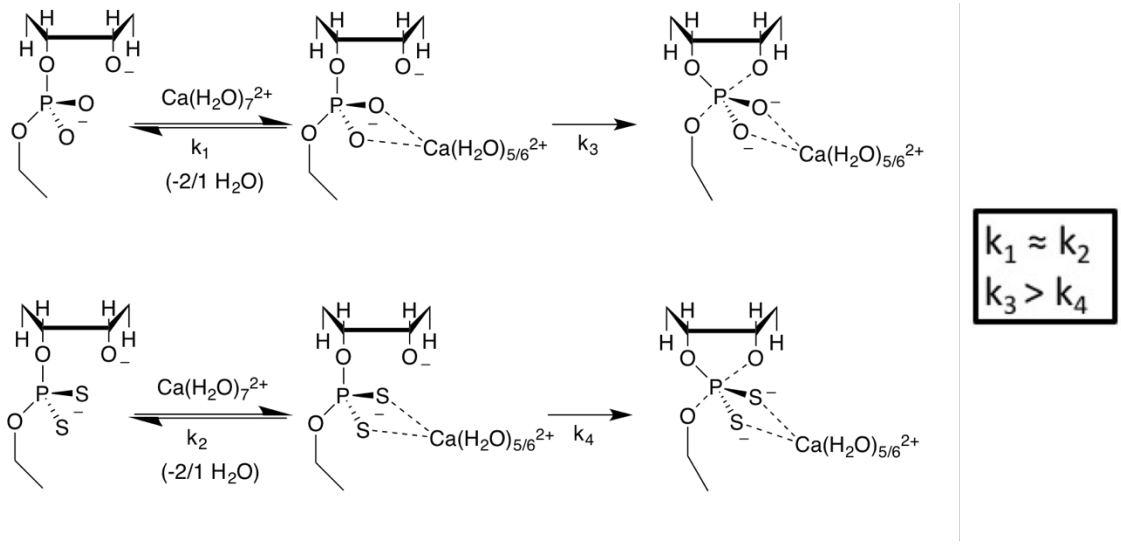

Figure 25. Proposed Mechanism Explaining Thio-Effects. Measurements of K_D suggest similar stabilities of both complex which suggest equivalent rate contants in the first step involving metal ion binding (k_1 and k_2). Values of k_{Ca} suggest decreased cleavage with a dithioate substitution (k_4). This suggests that while complex formation may exist, the stabilization of the non-bridging oxygen atoms through electrophilic catalysis that would allow for limited repulsion between 2'-nucleophile is decrease due to thio-substitions. Therefore, leading to larger cleavage rate constants for the diester (k_3). Due to limited monothioate defects, kinetics cannot unambiguously differentiate between possibilities of monodentate and bidentate binding.

Comparisons to various metal ions further support the contribution of inner sphere coordination to catalysis

In the case of our outer sphere model, results indicate that the rate constant for Ca^{2+} is 13-fold higher than that of $Co(NH_3)_6^{3+}$, which agrees with results using an HpPNP model system with a 16-fold difference (Corona-Martínez et al., 2012). Therefore, these results suggest minimal catalysis for outer sphere coordination, which suggests Ca^{2+} is less likely to rely on this mechanism. Minimal $Co(NH_3)_6^{3+}$ catalysis is most probably due

to electrostatic interactions and hydrogen bonding, which likely offers minimal rate enhancement in the mechanism utilized by Ca^{2+}.

Furthermore, $Co(NH_3)_6^{3+}$ thio-effects were found to be minimal in both the monothioate model and the dithioate. The larger defect in Ca^{2+} as compared to the outer sphere model suggest that the dithioate substitution is a proper model to assess inner sphere catalysis. The minimal defect is more probably due to disruption of hydrogen bonding, which has been found to be critical to phosphorane stabilization (Mayaan et al., 2004). However, in order to further investigate this claim, we utilized our computational work of an outer sphere $Mg(H_2O)_6^{2+}$, which has been generally accepted to be of similar size to $Co(NH_3)_6^{3+}$. Therefore, the complex of $Mg(H_2O)_6^{2+}$ with our phosphodiester model (See Chapter 3) can allow for assessment of the electrostatic interactions that exist. Through the use of Coulomb law (Equation 5), one can calculate the energy involved in the electrostatic interaction of the outer sphere interaction (Figure 26).

$$\Delta E = \frac{kq_1q_2}{\varepsilon r} \textbf{(5)}$$

Where k is Coloumb's constant ($9.0x10^9$ Nm^2C^{-2}), q_1 and q_2 are multiples of $1.6x10^{-19}$ C to account for the charge of each species, ε is the dielectric of water (78.54 @ 25 ^oC, the temperature of the calculation), and r is the distance calculated by Gaussian between the two charged species. The calculation suggests an electrostatic interaction of 11.6 kJ/mol, but when corrected for the difference from Na^+ (assuming consistent r) to make comparisons with the experimental $\Delta\Delta G$ the electrostatic interaction is suggested to offer 7.7 kJ/mol of stabilization. This is larger that the 2.3 kJ/mol $\Delta\Delta G$ determined experimentally. Therefore, it is likely hydrogen bonding does not offer major energetic

contributions to catalysis, as electrostatics account for all potential stabilization. This comparison must be taken with caution due to assumptions of size similarity, but computational thio-defects are also found to be less dramatic with outer sphere models, which highlights the minimal role hydrogen bonding would play in outer sphere coordination. Overall, binding is likely reliant on Coulombic forces.

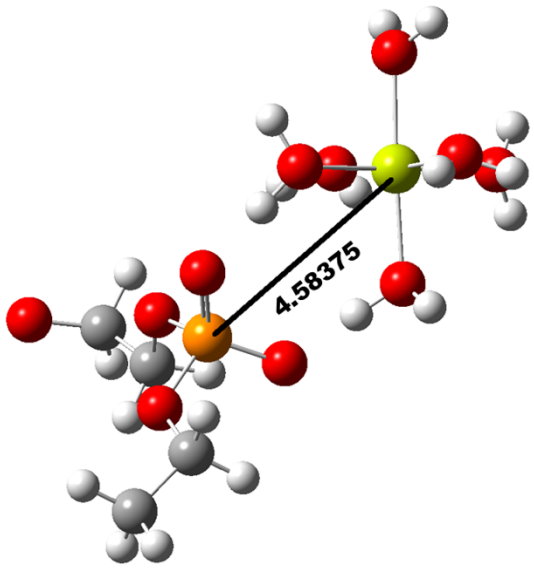

Figure 26. TPSSTPSS 6-311G++(d,p) optimized structure of $Mg(H_2O)_6^{2+}$ complex with diester model. Indicated bond length highlights the r used for electrostatic potential calculation.

Further analysis was conducted to investigate the correlation between binding and catalysis. $Co(NH_3)_6^{3+}$ is found to minimally bind with no saturation at accessible concentrations. $Co(NH_3)_6^{3+}$ was found to also poorly bind to a HpPNP model transition state structure, suggesting that in both cases any stabilization is primarily through ion pairing (Corona-Martínez et al., 2012). Ca^{2+} is found to form a stable complex that saturates, which definitively argues against outer sphere coordination as a major catalytic

mode. In addition, the fact that comparisons to Na^{+} showed dramatically higher catalysis, it is clear that electrostatics are critical to this catalytic mode. Inner sphere coordination would allow for closer electrostatic interactions that would increase the contribution of these ionic bonding interactions to catalysis.

Work with the hard Mg^{2+} suggests Ca^{2+} is catalytically more active. The fact that the harder ion offers lower rate enhancements would suggest that Lewis acid-base catalysis may not be the sole factor involved in this comparison. A possibility is that Mg^{2+} and Ca^{2+} may utilize different mechanisms of catalysis. Corona-Martínez et al. (2012) found that this is the case with the HpPNP RNA model for which Mg^{2+} uniquely utilized general base catalysis, whereas Ca^{2+} cannot. These differences are thought to be explained by effects from solvation that are currently mistunderstood (Corona-Martínez et al., 2012). In our case solvation can be used to potentially explain these unexpected kinetic results as Mg^{2+} utilizes a hexacoordinate hydration sphere while Ca^{2+} is heptacoordinate. The hexacoordinate hydration sphere is suggested to make inner sphere coordination more difficult. First, the Mg^{2+} ion is harder with a larger charge density, which would create strong solvent interactions that are more difficult to break. Second, the Mg^{2+} has a smaller primary hydration shell to compensate for loss of two water molecules upon bidendate binding. Therefore, the process of inner sphere coordination may not be as thermodynamically favorable or available for Mg^{2+}. Computational models of Mg^{2+} have found outer sphere coordination to be a favored distribution, while Ca^{2+} favors inner sphere when coordinating to dimethyl phosphate, a simple diester model (Petrov et al., 2005). Other models suggest an opposite trend (Corona-Martínez et al.,

2012). Overall, the catalytic difference could possibly be due to a reliance on weaker outer sphere interactions for Mg^{2+}; however, fold catalysis is larger than $Co(NH_3)_6^{3+}$ so this interaction must be relatively strong in comparison to the inert complex. More likely is the fact that inner sphere coordination is not as thermodynamically favored; therefore, the stabilized inner sphere coordinated complex is formed less commonly, which decreases catalysis. For this reason it is proposed that major differences in thio-defects are not seen.

However, it is also surprising that in both cases, Ca^{2+} and Mg^{2+} exhibited smaller defects in the pH 8 conditions as compared to that of Ca^{2+} in pH 11.5. There are several possible explanations of this kinetic trend. First, at the lower pH of 8, it is likely that the rate limiting step of the reaction may change. Previous work has suggested that the pK_a of the 2'-OH of each RNA dinucleotide model is around 13 (Cassano, Unpublished Results). It is possible that at the lower pH the activation of the 2' nucleophile will require general base catalysis by the metal ion. If this were the case, then electrophilic catalysis is less directly relevant to catalysis, which would explain lower thio-effects. Second, more nuetral conditions may lead to an increase in protonation of non-bridging oxygen atoms, which would diminish the need for metal ion coordination. Overall, prior work with 3',3'-phosphorodithioate diester corroborate minimal thio-effects in less basic conditions as their reactions were run in the pH 5-6 range with a Zn^{2+} catalyst (Lönnberg et al., 2007). This suggests that the role of the metal ion is dramatically dependent on the environment it is presented with. The residues within an enzyme activate would control

this environment, which highlights the possibility that different active sites may be utilizing metal ions differently.

Currently, limited studies have been done investigating the relationship of thio-defects and pH, which suggests the need to investigate possible trends that may exist. Ca^{2+}'s relative solubility in both acidic and basic conditions make it an optimal metal ion for that type of study. Therefore, the Mg^{2+} model suggest solvation may play a larger role in catalysis and highlights a potential pH dependence for thio-defects.

Overall, metal ion comparison results highlight the importance of inner sphere coordination and highlights the importance of solvation structures to catalysis in our model of alkaline cleavage.

2.5. Kinetic Conclusions

Experimental results highlight the importance of inner sphere coordination of phosphoryl non-bridging oxygen atoms as a mode of electrophilic catalysis. Therefore, we can suggest the following conclusions

1. Ca^{+2}- catalyzed cleavage of RNA and its non-bridging thio-analogs proceeds by a saturable, single metal ion model.
2. Lack of large SDIE argues against general acid/base catalytic mechanisms.
3. Ca^{+2} binding is not substantially affected by sulfur substitutions, suggesting binding occurs by electrostatic interactions only and possibly through the primary hydration sphere.
4. Weak catalysis by Na^{+} in comparison to Ca^{2+} highlight the electrostatic dependence of catalysis. It also suggests that Na^{+}, our control, offers a basal level of catalysis.

5. $[Co(NH_3)_6]^{+3}$ provides very little catalysis, and minimal thio-effects with phosphoromonothioates and phosphorodithioates. Therefore, outer sphere electrostatics cannot solely explain catalysis, as it may rely on an inner sphere mechanism.
6. Phosphoromonothioate substitutions engenders small thio-effects (~3 fold) for Ca^{+2} and Mg^{+2} catalyzed reactions. Therefore, monodentate and bidentate modes of binding cannot currently be differentiated.
7. Phosphorodithioate substitutions yields a synergistic catalytic defect (~40 fold) relative to the S_P and R_P phosphoromonothioates in basic condition, but less dramatic defects at lower pH systems (~4 fold). Thio-effects may be pH dependent.
8. Results at alkaline conditions suggest that catalysis occurs through stabilizing the phosphorane intermediate using electrophilic catalysis. Specifically, this likely involves inner-sphere coordination. Disrupting the interaction with one non-bridging sulfur atom can be compensated by the remaining non-bridging oxygen atom.

CHAPTER 3: COMPUTATIONAL STUDIES

3.1. Introduction

In addition to experimental thio-substitutions, the effects of these chemical modifications can also be investigated computationally for mechanistic insight. Surprisingly, thio-substituted computational models are limited within the literature despite its use as an experimental technique. Therefore, our study aims to help bridge this gap. Previous work has modeled thio-substitutions of cyclic phosphate esters and phosphate diesters, and these computational models were consistent experimental results (Liu et al., 2006; Liu et al., 2005a). In general, sulfur substitutions in the non-bridging position are found to have minimal impact on the transesterification of phosphate models. While sulfur can better hold negative charge, its larger size leads to weaker solvent interactions, which limit the potential for any visible effects on the rate (Liu et al 2006). Liu et al. (2006) highlight this minimal difference when investigating reverse ethylene phosphate methanolysis, a mimic of our transesterification reaction. Calculations of transition state structure suggests barrier changes of -0.8 kJ/mol and 1.3 kJ/mol for monothioate and dithioate substitutions respectively. Therefore, in uncatalyzed transesterification, thio-substitutions are found to cause minimal effects, which correspond with our experimental data with relatively consistent k_0 data, in the presence of 0 M Ca^{2+}. Therefore, investigations of computational phosphodiester-metal ion models may prove to offer similar accuracy to help with mechanistic interpretations of experimental results.

Currently, there are minimal studies investigating the effects of thio-substitutions in metal ion binding to phosphoryl functional groups. Despite this gap in the literature there have been computational studies that investigate metal ion coordination. These studies can offer information about the types of interactions present, structural modifications caused by the metal ion, the value of explicit solvent interactions to catalysis, any mechanistic/transition state alterations caused by the catalyst, etc. Mayaan et al. (2004) calculated structures of Mg^{2+} ions and di-metal bridges coordinated to phosphodiester model system. A common model, dimethyl phosphate exhibited tight binding to Mg^{2+}. Upon substitution of one water for DMP, the metal-ligand bond decreases from 2.111 Å to 2.005 Å (Mayaan et al., 2004). The phosphate ligand is found to exhibit a bond length increase of 0.036 Å due to the new charge transfer interactions possible in the presence of a metal ion. Further, the metal ion solvation shell was shown to exhibit hydrogen bonding interactions that are difficult to visualize in experimental settings. An example is the unstable methyl(ethylene)phosphorane, where Mg^{2+} induces hydrogen bonding using its solvation shell (Mayaan et al., 2004). Overall, metal ion binding causes significant structural changes upon coordination to offer stabilization. Therefore, it is likely that sulfur substitutions may impede tight binding, decreasing the thermochemical drive to form an inner sphere complex.

Currently, a single study exists in investigating the effect of thio-substitutions on formation of these metal ion-phosphoryl complexes. Using a dimethyl phosphate model system, metal ion binding to the model and its thioate analogs are assessed. Monothioate substitutions are found to change the mode of metal ion binding. The P-O_{nbo}-M bond

angle increases upon monothioate substitutions, suggesting that the metal ion is no longer bisecting the O_{nbo}-P-O_{nbo}. In addition, this highlights the preference metal ions have in interacting with oxygen moieties over sulfur (Dhaouadi et al., 2009). This trend is consistent with hard/soft coordination models and would corroborate our monothioate experimental observations. Therefore, the importance of thio-substitutions in inhibiting metal ion interactions is highlighted as a possibility.

Unfortunately, this study solely focuses on ground state structures. Currently, minimal theoretical examinations have looked into modeling metal ion mediated hydrolysis due to the computational cost of these systems. Recent work using Zn^{2+} models highlight inner sphere interactions that directly stabilize leaving group oxygen atoms (Gao et al., 2011; Torres et al., 2003). These catalytic models can highlight relevant interactions critical to catalysis. Therefore, in our particular study, computational chemistry will be used to aid in the interpretation of experimental thio-substitution studies as well as better define the reaction coordinate (Figure 27). Our goal is to add to prior work that has investigated metal ion binding as well as work that quantified the energetic effects upon thio-substitutions, in order make overall catalytic conclusions. Therefore, our study adds to literature reviewed above by surveying reactant, phosphorane, and product structures for all possible non-bridging thio-models with both Mg^{2+} and Ca^{2+} binding, including aspects of energy, structure, and electronics. Overall it will offer information about changes in coordination for comparison to kinetic results.

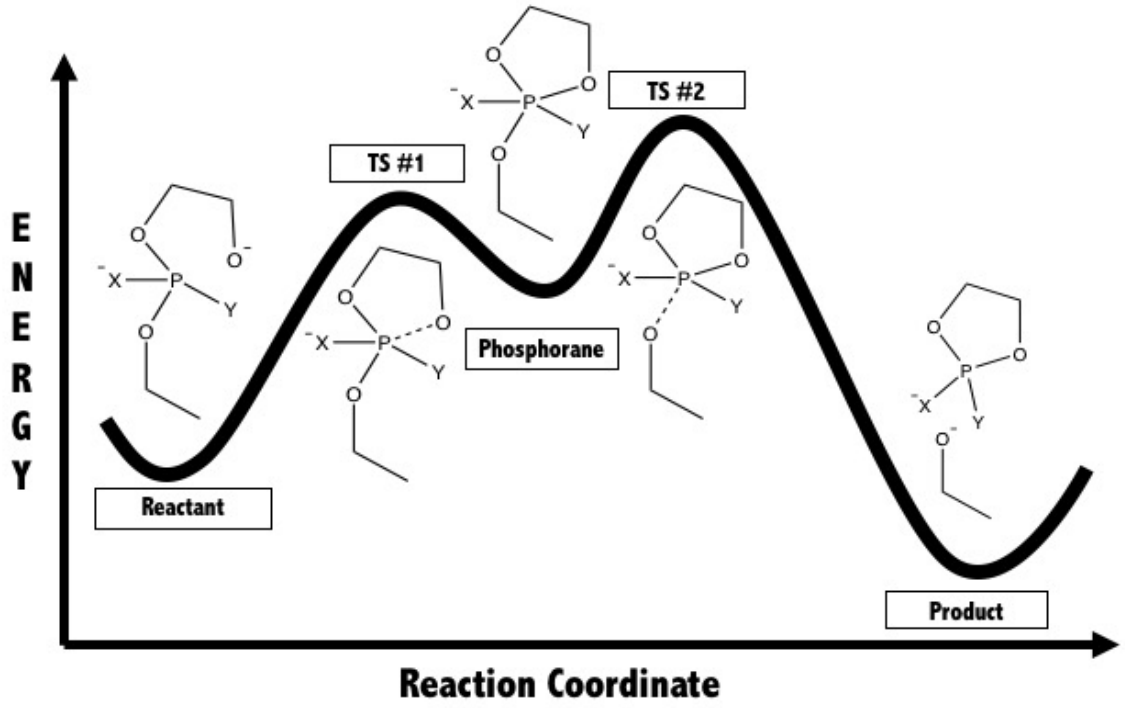

Figure 27. Reaction Coordination Species Structures Calculated for Computations. For all five reaction coordinate species that were four models, where X and Y, being the non-bridging positions, can be oxygen or sulfur atoms, for the diester, monothioate (Rp/Sp), and dithioate. In addition, each calculation was run in the presence of calcium (II), magnesium (II), and an uncoordinated control.

3.2. Methods

Input Structures

Input structures for all electronic structure calculations were generated via GaussView 5™ (Dennington et al., 2009). In order to minimize computational cost a simple phosphodiester model (Figure 28) was used. Based on Liu et al. (2006) all calculations were conducted for diester, monothioate (Rp and Sp), and dithioate models. Additionally, metal ion binding of Mg^{2+} and Ca^{2+}, were investigated. Based on prior computations by Mayaan et al. (2004) on Mg^{2+} binding to biological phosphates, initial structures for uncoordinated and Mg^{2+} coordinated structures were calculated with the

hybrid Becke three-parameter exchange functional (Becke, 1993) and the Lee Yang, Parr correlation functional (B3LYP) (Lee et al., 1988).

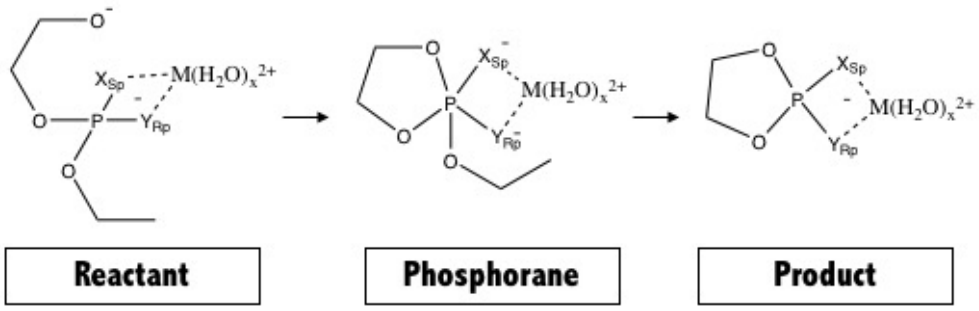

Figure 28. Computational RNA Diester Models. This basic structure of ethyl (2-oxidoethyl) phosphate (Et-2-O-Et^{-2}) is used for all reactant, product and phosphorane input structures. Negatively charged oxygen is the nucleophile, whereas the ethoxide acts as a leaving group. X and Y specifically represent the non-bridging oxygen and sulfur moieties that are manipulated in the study. M, is the coordinated species, which can include Mg^{2+} and Ca^{2+}, with various primary solvation shells.

Solvent Phase Structure Calculations

Calculations were performed with the GAUSSIAN 09 software package (M. J. Frisch, 2009) using Kohn-Sham density functional theory. To obtain Ca^{2+} coordinated species, all structures were optimized with the Tao-Perdew-Staroverov-Scuseria (TPSS) (Tao et al., 2003) density functional based on work conducted on monozinc complexes (Fan & Gao, 2007). Recent work suggested that this particular functional offers unmatched accuracy compared to popular methods such as B3LYP (Staroverov et al., 2003). All geometry optimizations were conducted using the 6-311G++(d,p) basis set as it is optimal for DFT functionals (Helgaker et al., 2000), with stability conditions verified for the restricted closed shell Kohn-Sham functional determinants (Bauernschmitt & Ahlrichs, 1996; Seeger & Pople, 1977). Further calculations gave insight into the electronics of

these optimized structures. Frequency calculations were conducted at the same level of theory and basis set to gain vibrational information on stationary points within the reaction coordinate. Energy and bond order calculations were subsequently refined further with the TPSSTPSS functional and a 6-311G++(3df,2pd) basis set to maximize accuracy of converged electronic energy values (Curtiss et al., 1991).

All calculations were conducted using the polarizable continuum method (PCM) solvent to model the dielectric of water (Amovilli et al., 1998). The solvent cavity topology was specified under the constraints of the United Atom Topological Model (Takano & Houk, 2005), which has been found to best mimic experimental phosphodiester transesterification results (Chen et al., 2014).

Optimization calculations were used to obtain the geometric structures of metal ion coordinated and non-coordinated species. Frequency calculations were necessary to obtain thermodynamic quantities on bond forces at specific positions along the potential energy surface, and helped confirm minima structures. Overall, these structural and energetic insights suggest disrupted interactions upon thio-substitutions.

Analysis of Thermodynamic Quantities

Following methods of Mayaan et al (2004) all structural results were broken down to their thermodynamic quantities. Several components are used in conjunction for complete energetic analysis as shown in Equation 6-9 below.

$$G = H - TS \quad (\mathbf{6})$$

$$G = (E + RT) - TS \quad \mathbf{(7)}$$

$$G = ((E_0 + E_{vib} + E_{rot} + E_{trans}) + RT) - TS \ \mathbf{(8)}$$

$$G = (((EF_e + ZPVE) + E_{vib} + E_{rot} + E_{trans}) + RT) - TS \textbf{ (9)}$$

Where G, H, T, and S are free energy, enthalpy, temperature, and entropy. Specifically, Gaussian models standard state conditions as it relies on a temperature of 298 K and a pressure of 1 atmosphere. Enthalpy is defined as the sum of Internal Energy, E, and RT (the universal gas constant R=8.314 J/mol*K). E is broken into E_0, E_{vib}, E_{rot}, and E_{trans} which are electronic, vibrational, rotational, and translational components of energy. Electronic energies are specifically calculated at the higher basis set as stated. Therefore, EF_e, the electronic energy specifically calculated from the frequency calculation must be replaced by the higher level energy calculations (EE_e) as shown in Equation 10.

$$G_{corrected} = G - EF_e + EE_e \textbf{ (10)}$$

$G_{corrected}$ is the calculated free energy that takes into account the high level energy calculations, which substitutes the lower level energy calculation. These manipulations offer the free energy of PCM solvated structures.

3.3. Results

Computational models were specifically used to add to open questions unanswered by kinetic analysis. Two major questions exist. First, how do metal ions bind to the phosphodiester bond in order to encourage catalysis? This question involves differentiating between inner sphere and outer sphere catalysis, as well as monodentate and bidentate binding. Second, why do thio-substitutions cause defects? This involves an investigation of metal ion bound phosphodiester thio-analog structure, energy, and electronics.

Analysis of Ligand Substitution Reactions

In order to make conclusions about binding, and the energetics of that particular step, it is critical to compare the energies of all complexes to the free metal ion with a full primary hydration shell as well a free phosphodiester compound. In order to identify the most stable binding modes we compared the energies of complexes that involve the loss of two water molecules to form bidentate inner sphere interactions (1), the loss of one water molecules to form a monodentate inner sphere interaction (2), and the loss of no water molecules to participate in purely outer sphere interactions (3). The ΔG of the ligand substitution to form each complex (Figure 29) is calculated in all three cases for both Mg^{2+} and Ca^{2+} using Equations 11-13, showing the reactions for a generic metal M. The magnesium metal ion has been previously characterized to have a primary hydration sphere of six waters (Mayaan et al., 2004), while the calcium metal ion has been found to have a sphere of seven waters (Carroll, 2008; Katz et al., 1996). Therefore, the monodentate interaction involves six waters for Ca^{2+} and five waters for Mg^{2+}. The bidentate interaction involves five waters for Ca^{2+} and four waters for Mg^{2+}. Energetic analysis of each possibility suggest in both cases that the inner sphere bidentate complex is favored (Figure 30, 31). Thio-substituted reactant structures exhibit the same trend, with all possibilities favoring inner sphere bidentate interactions. After identifying the binding mode it is then necessary to assess the affects of thio-substitutions on these modes.

$$M(H_2O)_x^{2+} + \text{Et-2-O-Et}^{2-} \rightarrow M(H_2O)_{x-2}^{2+}*\text{Et-2-O-Et}^{2-} + 2\ H_2O \quad (\mathbf{11})$$

$$M(H_2O)_x^{2+} + \text{Et-2-O-Et}^{2-} \rightarrow M(H_2O)_{x-1}^{2+}*\text{Et-2-O-Et}^{2-} + 1\ H_2O \quad (\mathbf{12})$$

$$M(H_2O)_x^{2+} + \text{Et-2-O-Et}^{2-} \rightarrow M(H_2O)_x^{2+}*\text{Et-2-O-Et}^{2-} \quad (\mathbf{13})$$

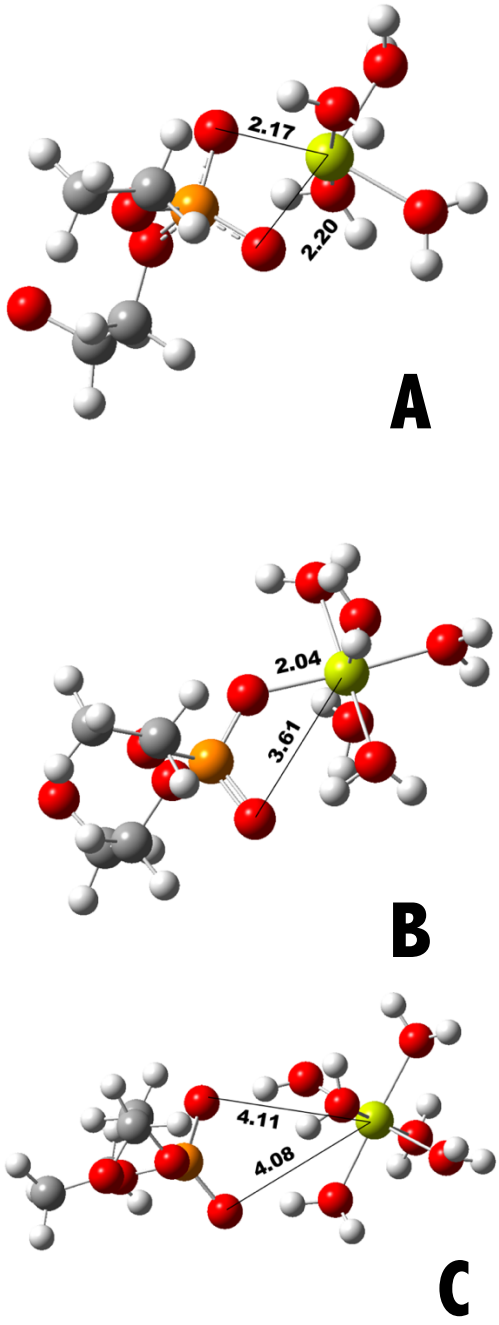

Figure 29. Optimized structures of Mg^{2+} interactions including bidentate, monodentate, and outer sphere interactions. 6-311G++ (d,p) structure optimizations of bidendate (A), monodentate (B), and outer sphere (C) interactions. The Ca^{2+} structures were similar and involve 5, 6, and 7 waters respectively.

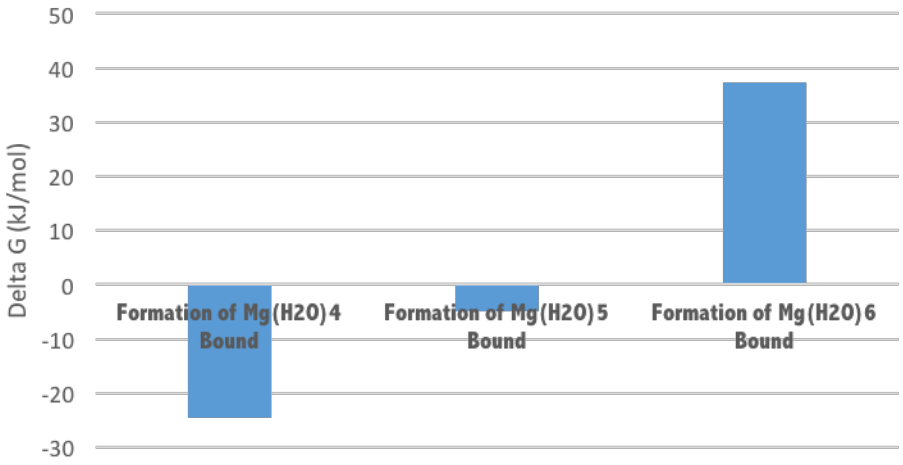

Figure 30. Energy for ligand substitution to gauge energy of Mg^{2+}-phosphodiester complex. Based on the ligand substitution reactions describe in Equations 11-13 above the ΔG for each binding reaction is calculated at using the TPSSTPSS functional using the 6-311G++(d,p) basis, with electronic energy calculated with 6-311G++(3df,2pd).

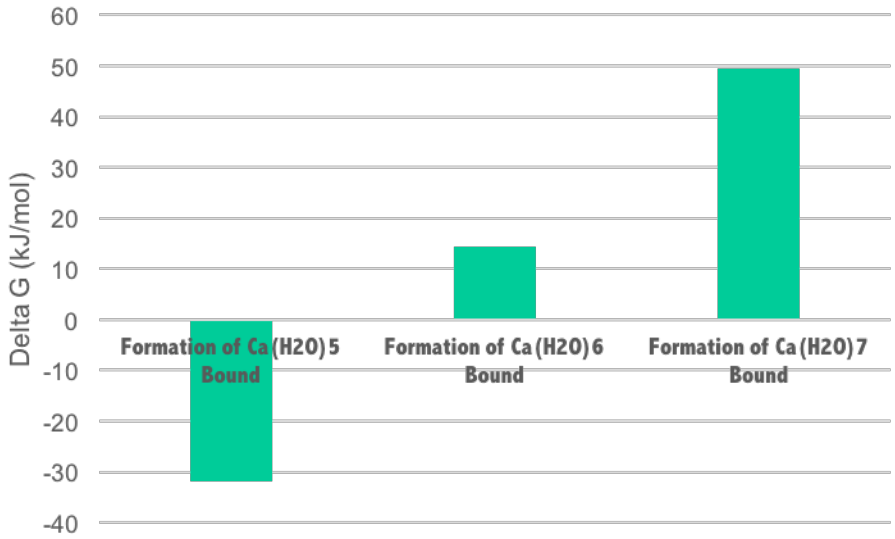

Figure 31. Energy for ligand substitution to gauge energy of Ca^{2+}-phosphodiester complex. Based on the ligand substitution reactions describe in Equations 11-13 above the ΔG for each binding reaction is calculated at using the TPSSTPSS functional using the 6-311G++(d,p) basis, with electronic energy calculated with 6-311G++(3df,2pd).

Structural Effects of Monothioate Substitutions

Monothioate substitutions seem to be minimally detrimental to catalysis in experimental studies, but have shown to shift the mode of metal ion binding (Dhaouadi et al., 2009). Therefore, we hypothesize that monothioate models will exhibit stronger interactions with the oxygen atom in a monodentate like fashion. In our system of Mg^{2+} and Ca^{2+} bindentate coordination, the metal distance from the non-bridging positions in reactant species were measured for the diester and compared to those of the R_p and S_p monothioate. Bond distances suggest that sulfur atoms have larger distances between Mg^{2+} and the non-bridging positions, with 0.4 Å increase (Table 5). The change is more dramatic in the case of Ca^{2+} with a 0.5 Å (Table 6). However, distances between the metal and the non-bridging oxygen atom remain consistent across the diester and both monothioates at approximately 1.6 Å. The slight increase is likely attributed to the steric bulk of sulfur, with an atomic radius 0.4 Å higher than oxygen due to its larger 3p valence shell (Bondi, 1964). Therefore, it is likely not suggesting anything major about coordination.

Table 5: Mg (II) Bound Reactant Structures for Diester, Monothioate Rp, and Monothioate Sp Models				
Model	**Optimized Structure**	**Bond**	**Distance (Å)**	**Wiberg Bond Order**
Diester	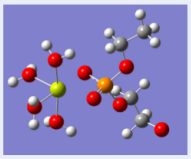	**Mg-O(S_P)**	**1.54**	**0.17**
		Mg-O(R_P)	**1.54**	**0.16**
Monothioate (Sp)	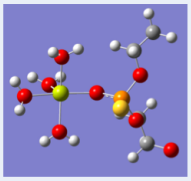	**Mg-S(S_P)**	**1.99**	**0.001**
		Mg-O(R_P)	**1.55**	**0.18**
Monothioate (Rp)	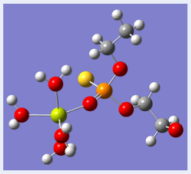	**Mg-O(S_P)**	**1.54**	**0.19**
		Mg-S(R_P)	**1.99**	**0.003**

Table 6: Ca (II) Bound Reactant Structures for Diester, Monothioate Rp, and Monothioate Sp Models				
Model	**Optimized Structure**	**Bond**	**Distance (Å)**	**Wiberg Bond Order**
Diester	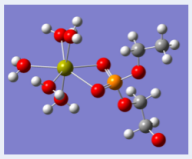	**Ca-O(S_P)**	**1.53**	**0.20**
		Ca-O(R_P)	**1.54**	**0.20**
Monothioate (Sp)	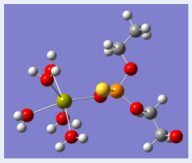	**Ca-S(S_P)**	**2.00**	**0.23**
		Ca-O(R_P)	**1.54**	**0.22**
Monothioate (Rp)	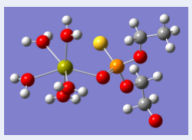	**Ca-O(S_P)**	**1.54**	**0.22**
		Ca-S(R_P)	**2.01**	**0.21**

Curiously in analyzing the reactant structures, despite the minimal difference in distance from the phosphoryl moiety, there is a dramatic structural shift upon a sulfur substitution. The Mg^{2+} shows a clear shift away from the sulfur substituted atoms (Figure 32), whereas Ca^{2+} shows a similar while less dramatic shift (Figure 33).

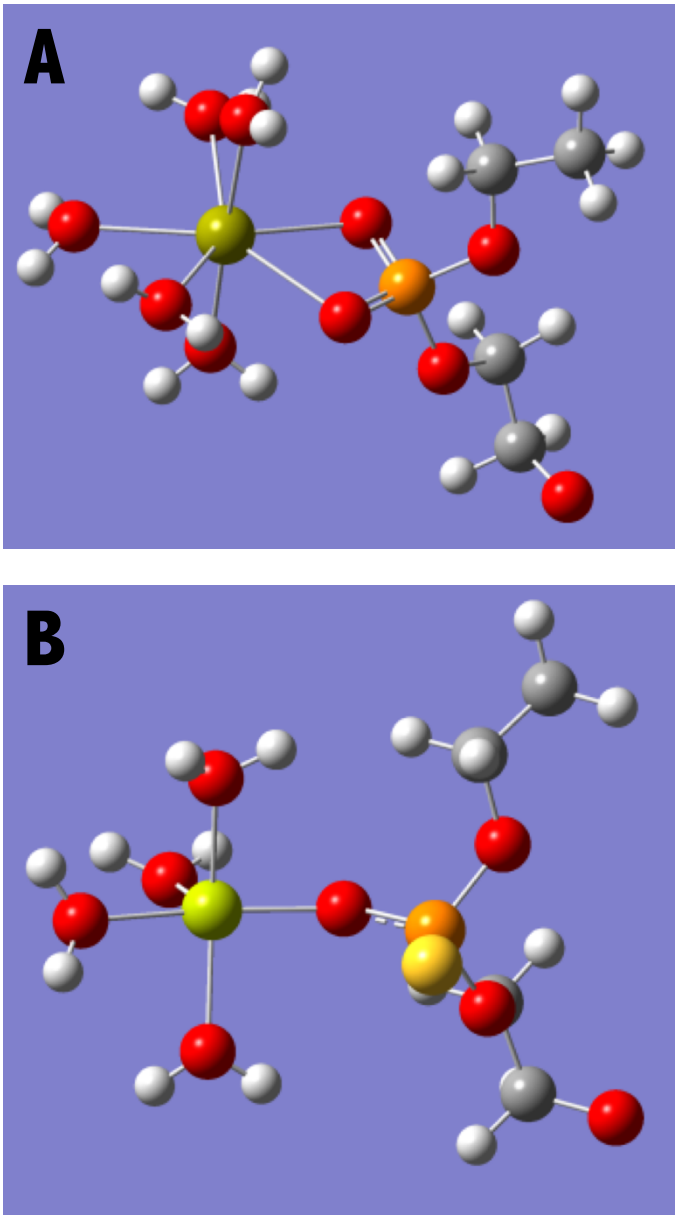

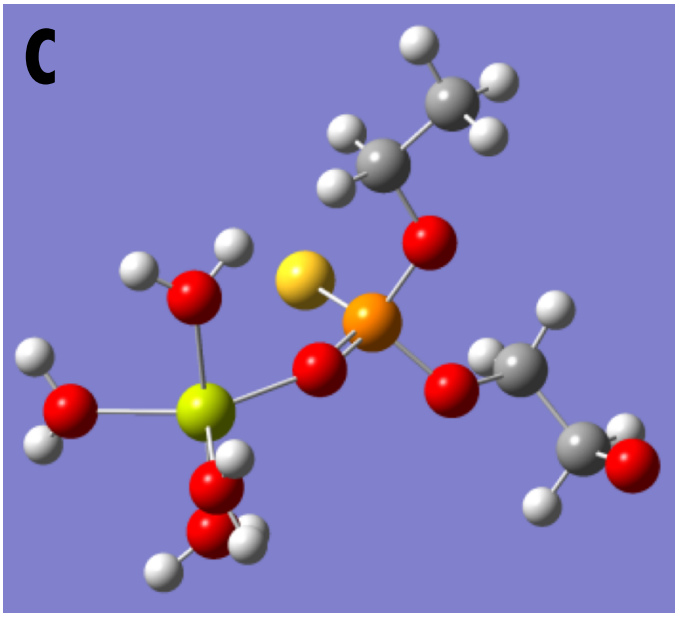

Figure 32. TPSSTPSS 6-311G++(d,p) optimized $Mg(H_2O)_4$ bound reactant structure for diester and monothioate, models. The structures the diester (A), monothioate Sp (B), and monothioate Rp (C) highlight Mg^{2+} preference for oxygen. Bond orders and distances are quantified in Table 7.

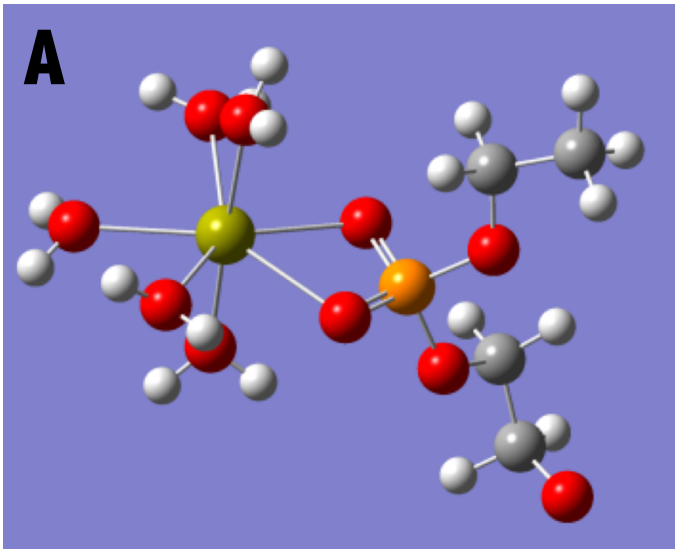

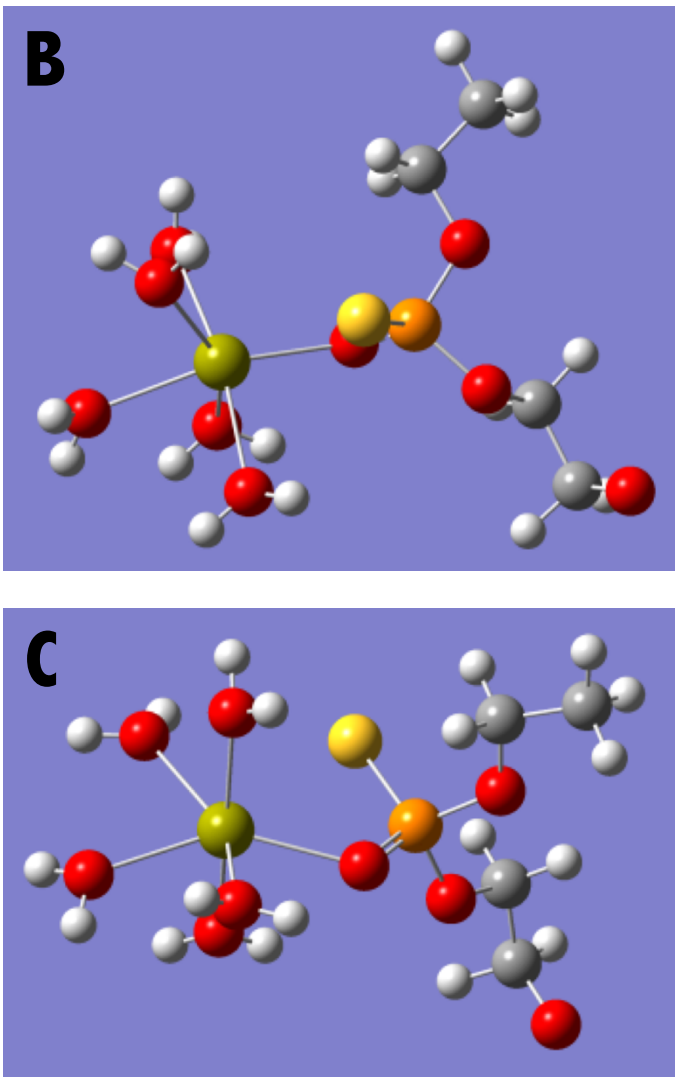

Figure 33. TPSSTPSS 6-311G++(d,p) optimized $Ca(H_2O)_5$ bound reactant structure for diester and monothioate, models. The structures the diester (A), monothioate Sp (B), and monothioate Rp (C) highlight Ca^{2+} preference for oxygen, which is significantly less dramatic than Mg^{2+}. Bond orders and distances are quantified in Table 8.

This shift can be quantified by investigating the bond angle between the magnesium atom, a non-bridging atom, and the phosphorus center atom (Figure 34). The Mg^{2+} atom bisects the non-bridging moieties with a measured angle of 90.4°; however, the thiosubstitution leads to a shift away from the center toward the oxygen atom with angles of 52.2° and 141.1° (Table 7). A similar, but less dramatic trend is seen with Ca^{2+} (Table

7), as it is farther from the phosphoryl moiety, with a distance of 3.02 Å from the phosphorus as opposed to 2.70 Å for Mg^{2+}. In any case, the metal ion shows a preference toward oxygen atoms, which highlights the need to investigate changes in electronics to investigate effects on coordination.

Table 7: Mg^{2+} and Ca^{2+} Bond Angles with respect to Rp non-bridging position and phosphorus to assess shift due to thio-substitution		
Model	**Mg-(Rp)-P**	**Ca-(Rp)-P**
Phosphodiester	**90.4**	**94.1**
Monothioate (R)	**52.2**	**71.7**
Monothioate (S)	**141.1**	**113.4**

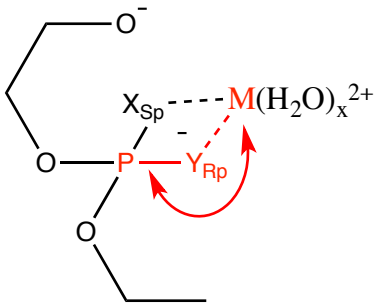

Figure 34. Metal-Non-Bridging Atom-Phosphorus Angle measured for analysis of shift is metal ion binding. Angle indicated in red conduct analysis on the Rp moiety for diester and monothioate structures.

Effects of Thio-substitutions on Electronic Interactions

While distances between the metal ion and sulfur substituted moieties were not as dramatic as anticipated the clear preference for oxygen atoms suggest potential effects on coordination. One way to make this analysis is through analysis of overlap between calculated atomic orbitals to assess the strength of the interaction between two atoms (Mayer, 1983), known as the Wiberg Bond Order. Sulfur atoms cause the Mg^{2+} bond order with that non-bridging position to drop to close to zero, suggesting a minimal interaction (Table 5). Ca^{2+} is mainly unaffected; however, the larger number of electrons may complicate the analysis of those bond orders, or the relative softness may allow for greater interactions (Table 6). Therefore, to more clearly investigate coordination it is necessary to analyze the charge of the respective atoms with and without coordination.

Natural Bond Order charge analysis allows for halving of bonding electrons and then allows us to quantify the occupancy of molecular orbitals on a particular atom (Mayer, 1983). The charge on the Sp and Rp non-bridging atoms were found to be severely effected by thio-substitutions (Figure 35). Sulfur charges are generally lower than that of oxygen atoms, being 0.35 charge units less negative even in the uncoordinated structure. This is likely because of the lower electronegativity of sulfur with its larger orbitals. However, this effects becomes more dramatic in the presence of metal ions with values 0.07 charge units less negative. Overall, the charge analysis suggest that the substitution of sulfur would exhibit worse electrostatic interactions, specifically impeding in proper coordination, which could explain slight kinetic defects.

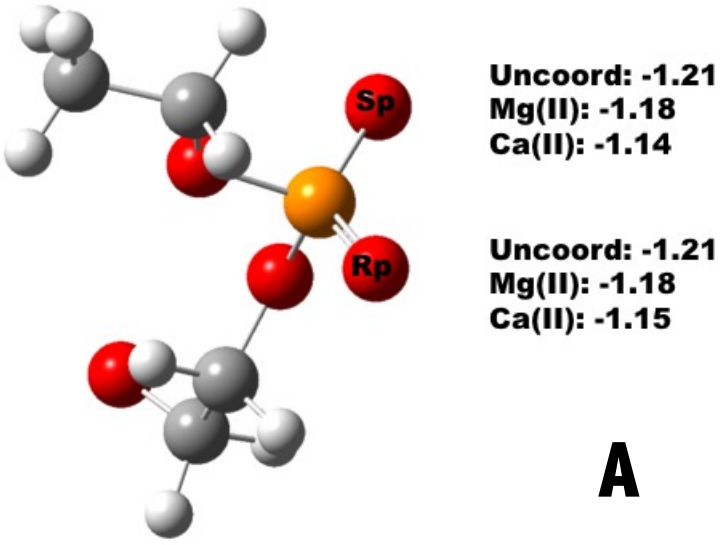

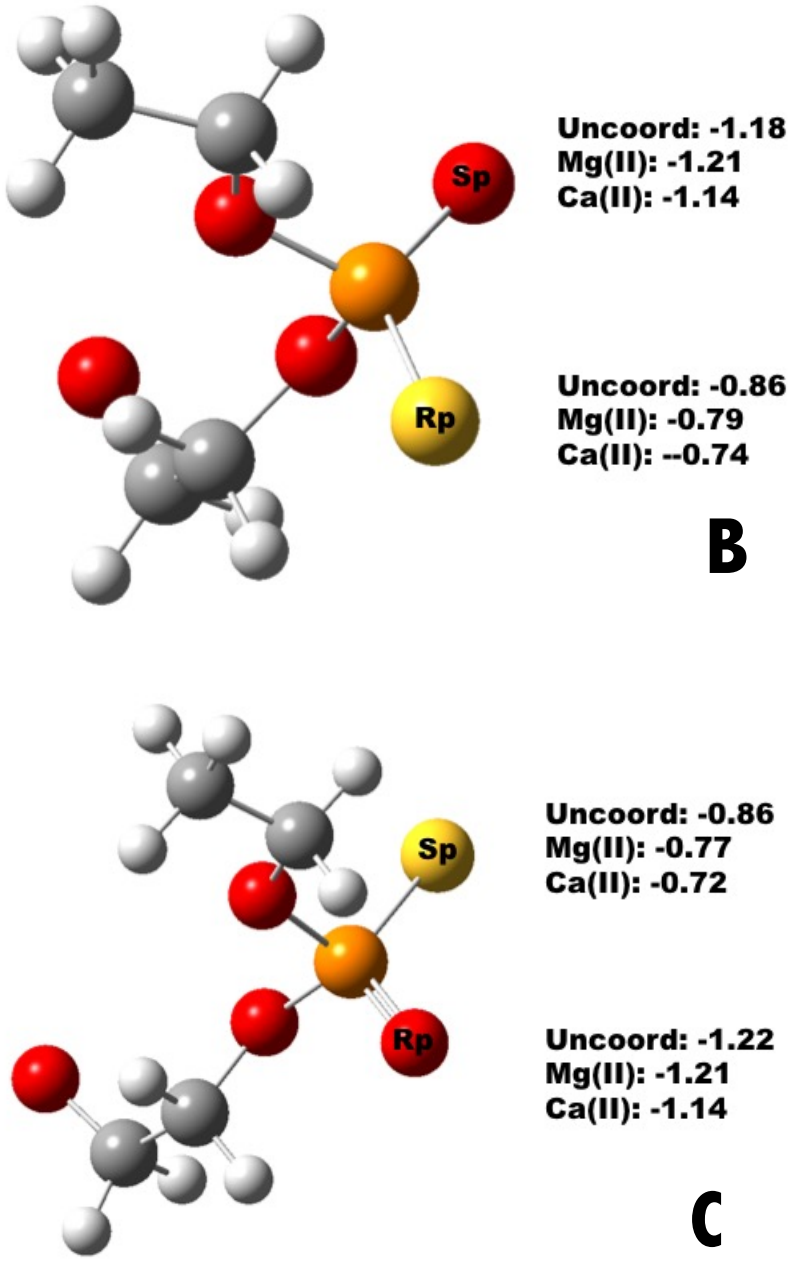

Figure 35. NBO Charge Analysis of non-bridging atoms for diester and monothioate structures. Charge for atoms with no coordination, Mg coordination, and Ca coordination are shown for the diester (A), monothioate Rp (B), and monothioate Sp (C). General trend shows a decrease in negative charge upon thio-substitutions which can impede on coordination.

Defects upon dithio-substitution

Analysis of monothioate substitutions provide evidence that highlight possible reasons for catalytic defects upon thio-substitutions. However, in our kinetic analysis major defects were only seen upon dithio-substitutions. Therefore, analysis of dithioate structures are necessary. Minimal changes in structure are seen upon a dithioate substitution in the reactant (Figure 36). In both Mg^{2+} and Ca^{2+} systems the metal ion continues to bisect the non-bridging atoms. Measured metal-non-bridging atom-phosphorus angles were 83.6^{o} and 88.3^{o} for Mg^{2+} and Ca^{2+} respectively, which suggest similar structures to that of the diester. The major difference in structure was simply an increase distanced between the metal ion and the non-bridging positions (Table 8, 9), which may be explained by sulfur's steric bulk.

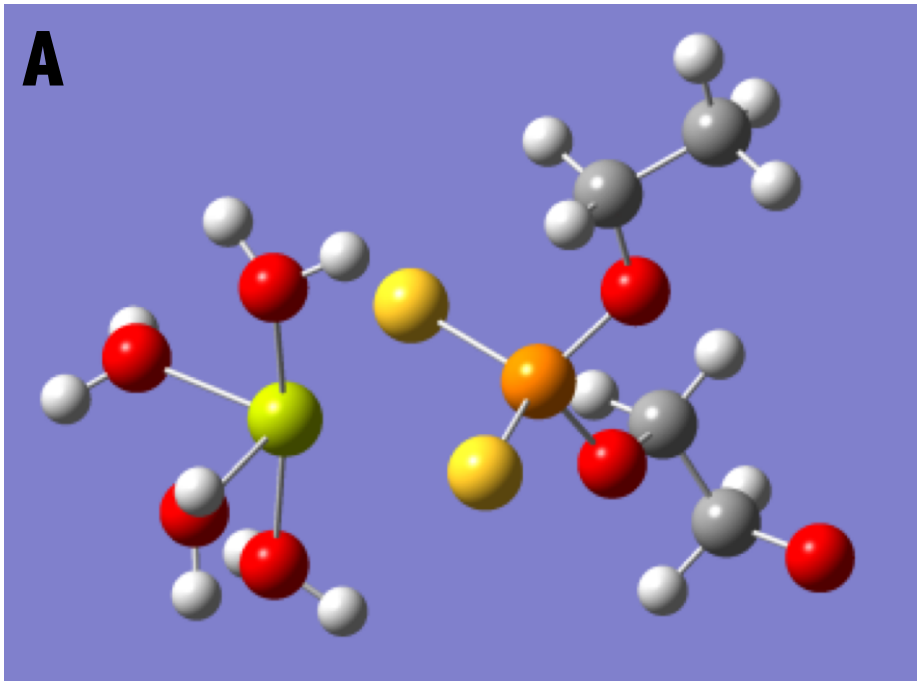

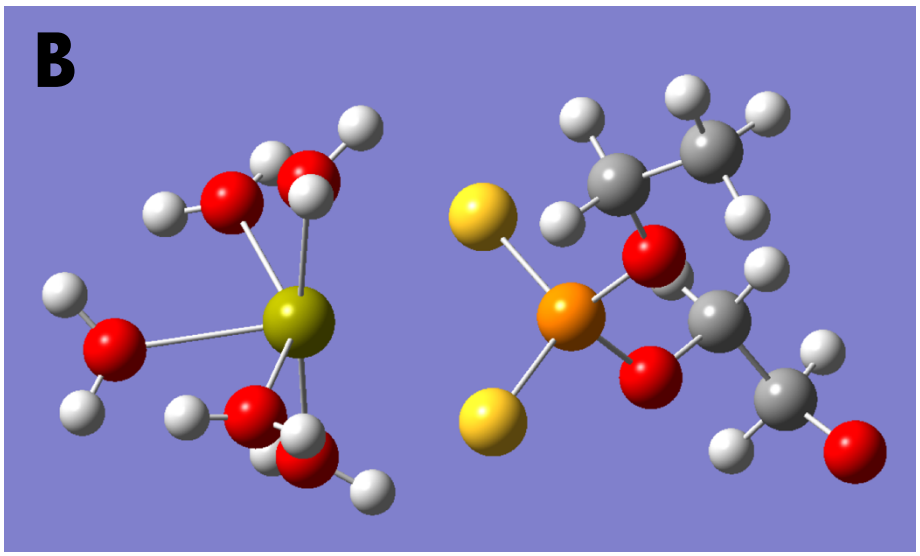

Figure 36. Optimized dithioate structures for Mg^{2+} and Ca^{2+} coordinated reactants. Mg^{2+} (A) and Ca^{2+} (B) show no shifts when two sulfurs are substituted unlike monothioate substitutions.

Table 8: Mg (II) Bound Reactant Structures for Diester, Monothioate Rp, Monothioate Sp, and Dithioate Models

Model	Optimized Structure	Bond	Distance (Å)	Wiberg Bond Order
Diester	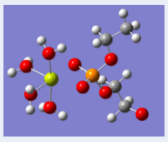	Mg-O(S_p)	1.54	0.17
		Mg-O(R_p)	1.54	0.16
Monothioate (Sp)	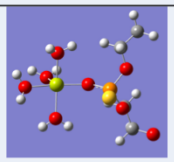	Mg-S(S_p)	1.99	0.001
		Mg-O(R_p)	1.55	0.18
Monothioate (Rp)	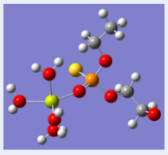	Mg-O(S_p)	1.54	0.19
		Mg-S(R_p)	1.99	0.003
Dithioate	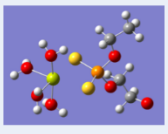	Mg-S(S_p)	2.02	0.33
		Mg-S(R_p)	2.03	0.31

Table 9: Ca (II) Bound Reactant Structures for Diester, Monothioate Rp, Monothioate Sp, and Dithioate Models				
Model	**Optimized Structure**	**Bond**	**Distance (Å)**	**Wiberg Bond Order**
Diester	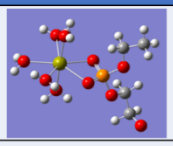	**Ca-O(S_p)**	**1.53**	**0.20**
		Ca-O(R_p)	**1.54**	**0.20**
Monothioate (Sp)	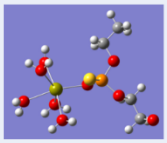	**Ca-S(S_p)**	**2.00**	**0.23**
		Ca-O(R_p)	**1.54**	**0.22**
Monothioate (Rp)	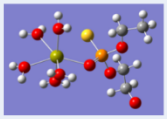	**Ca-O(S_p)**	**1.54**	**0.22**
		Ca-S(R_p)	**2.01**	**0.21**
Dithioate	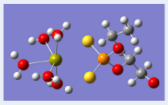	**Ca-S(S_p)**	**2.01**	**0.37**
		Ca-S(R_p)	**2.02**	**0.35**

While limited structural defects are found for the dithioate substitution, there is significantly less charge on both sulfur atoms, which decreases the ionic interaction for both Mg^{2+} and Ca^{2+} (Figure 37). In adding metal ion coordination, the charge of the non-bridging positions dropped to half the uncoordinated value which highlights a diminished electronic interaction. Furthermore, the charge on each metal ion atom was found to diminish specifically after a dithio-substitution. With diester and monothioate models the Mg had a charge of approximately 1.4 and Ca had a charge of 1.2, which subsequently dropped to 1.2 and 1.0 respectively. The loss in charge is likely associated with some covalent bond formation, limiting the ionic character of coordination, which could decrease stabilization. This would be the case because a strong ionic interaction is being replaced for a covalent bond with sulfur, which is weaker due to the increase in atomic radius of the non-bridging position. In the case of magnesium, the gas phase Mg-S

covelent bond is weaker at a bond energy of 234 kJ/mol in comparison to Mg-O with a bond energy of 363 kJ/mol (2017). In the case of diester compounds, less charge transfer is present so covalent bond formation is limited, while the dithioate exhibits advanced charge transfer, but maintains a weaker covalent bond. Therefore, it is likely that these electronic effects upon this particular substitution can be correlated to energetic defects.

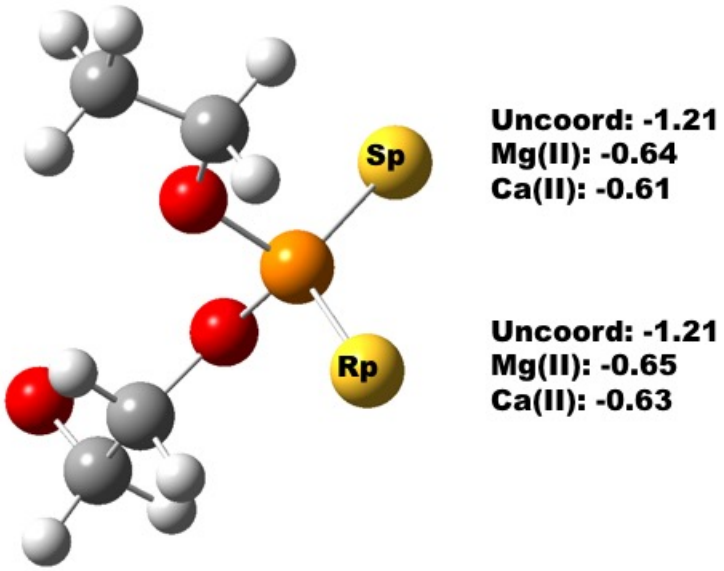

Figure 37. NBO Charge Analysis of non-bridging atoms for dithioate structures. General trend shows a decrease in negative charge upon thio-substitutions which can impede on coordination.

In order to investigate the thermochemical parameters of dithioate defect, it was necessary to calculate the energy of each reactant, phosphorane, and product structure with and without coordination. Each optimized structure's energy, after taking into account the production of two water molecules after the formation of a bidentate interaction, was compared to the aquo bound metal ion and unbound reactant for each

thio-model. This analysis was conducted through using the reaction presented in Equation 14, which was adapted for analysis of reactant, phosphorane, and product structures on the product side of the reaction.

$$\text{Et-2-O-Et}^{2-} + \text{M(H}_2\text{O)}_n^{2+} \rightarrow \text{M*Et-2-O-Et(H}_2\text{O)}_{n-2} + 2\ \text{H}_2\text{O} \quad \textbf{(14)}$$

In analyzing differences from unbound reactant it was clear that that metal ion exhibits severe energetic defects upon the dithio-substitutions for reactant, phosphorane, and product structures in the case of Ca^{2+} and Mg^{2+} (Figure 38, 39). This defect is most especially evident in the case of the reactant structures; whose energetic values represent the binding process involving the loss of two water molecules. While the diester and the monothioates are all stabilized upon binding for Mg^{2+} and Ca^{2+}, the dithioate exhibits a positive free energy change upon the dithio-substitution. Equation 15 was used calculate the dissociation constant in each case. The K_d increase slightly for monothioate, but dramatically in the case of dithioate, which suggests a dramatic decrease in affinity (Table 10).

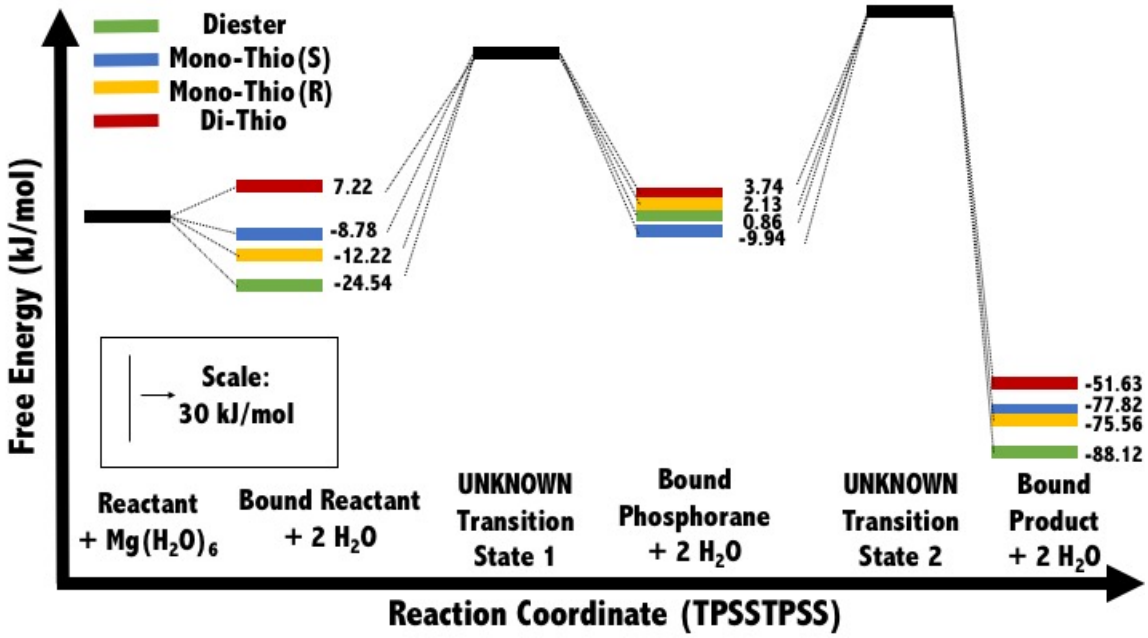

Figure 38. Magnesium (II) Binding Alterations of Reaction Coordinate Species Free Energy. TPSSTPSS 6-311G++(3df,2pd) energy calculations. Values presented are calculated differences in free energy (ΔG_{zero}) from an initial model with hydrated calcium unbound as the initial zero point. Bound reactants for Et-2-O-Et, Et-2-O-Et(S_s), Et-2-O-Et(S_R) were all stabilized while Et-2-O-Et(S_2) was destabilized. Similarly, in bound phosphorane and product structures, the energy was highest for Et-2-O-Et(S_2).

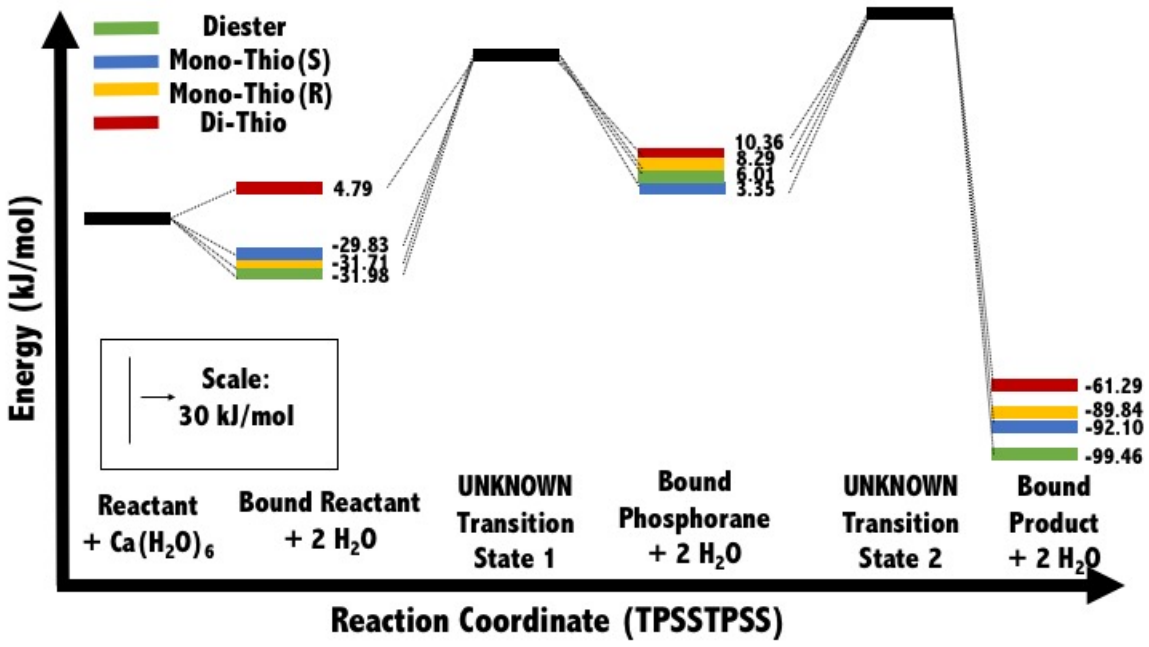

Figure 39. Calcium (II) Binding Alterations of Reaction Coordinate Species Free Energy. TPSSTPSS 6-311G++(3df,2pd) energy calculations. Values presented are calculated differences in free energy (ΔG_{zero}) from an initial model with hydrated calcium unbound as the initial zero point. Bound reactants for Et-2-O-Et, Et-2-O-Et(S_S), Et-2-O-Et(S_R) were all stabilized while Et-2-O-Et(S_2) was destabilized. Similarly, in bound phosphorane and product structures, the energy was highest for Et-2-O-Et(S_2).

$$\Delta G = -RTln(K) \textbf{ (15)}$$

Table 10: Thio-Effects for Calculated Dissociation Constant of Metal Ion Reactant Binding

Thio Model	Mg	Ca
Monothioate (R)	2.06E+02	1.12E+00
Monothioate (S)	9.11E+02	2.53E+00
Dithioate	9.23E+05	8.04E+06

The dramatic change in affinity was correlated to a change in 30 kJ/mol in going from the diester to the dithioate for both metal ions. In addition to a change of energy the

addition of sulfur increase the distance between the metal ion and phosphoryl center, which could mean the defect is primarily due to the weaker electrostatic interaction. For Mg^{2+} the Mg—P distance was increased from 2.70 Å to 3.15 Å upon the dithioate substitution. For Ca^{2+} the Ca—P distance was increased from 3.02 Å to 3.58 Å upon the dithioate substitutions. In using Equation 5, considering the process in a dielectric of water and assuming charges to be +2 and -1, the distance changes were correlated to a change of 1.87 kJ/mol and 1.82 kJ/mol for Mg^{2+} and Ca^{2+} respectively. Therefore, the effect must be correlated with destabilized electronics and slight deviations in structure to completely account for the destabilization.

The dithioate substitution, while extremely detrimental to bidentate binding, was found to be less energetically costly in the case of the outer sphere interaction described previously. In order to quantify this trend, the energy of the ligand substitution of the phosphate for two waters was calculated (Equation 16). In both the case of Mg^{2+} and Ca^{2+} the free energy of the inner sphere to outer sphere transition was lower for the dithioate model than the diester (Figure 40). This suggests the potential that the equilibrium for dithioate model may favor outer sphere interactions relative to the other model system. Overall, dithio-substitutions are found to dramatically hinder binding and stabilization, which is likely than to correlated with decreases in catalysis.

$$M^{*}Et\text{-}2\text{-}O\text{-}Et(H_2O)_{n-2} + 2\ H_2O \rightarrow M^{*}Et\text{-}2\text{-}O\text{-}Et(H_2O)_n \quad \textbf{(16)}$$

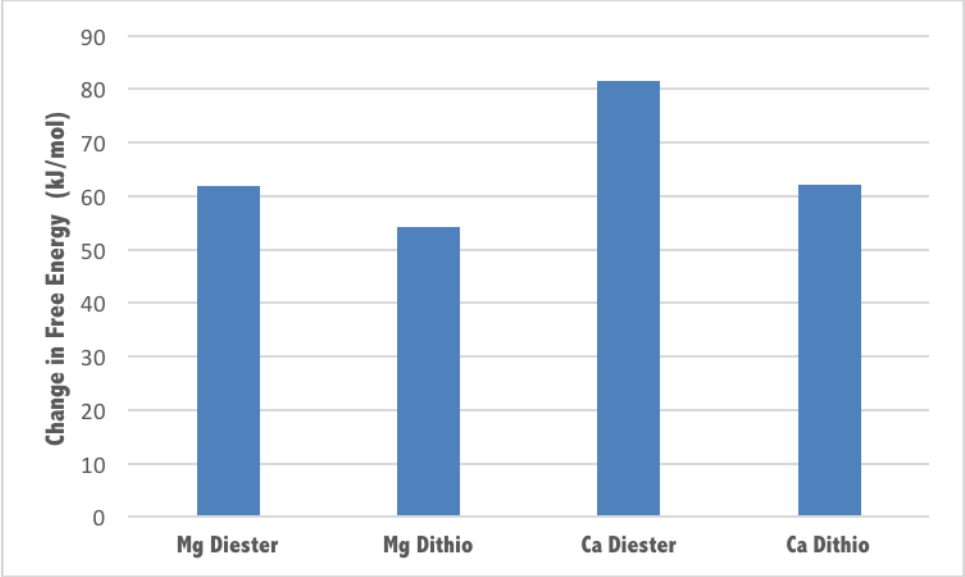

Figure 40. Comparison of Mg^{2+} and Ca^{2+} inner to outer sphere transition for diester and dithioate species. The dithioate substitution is found to be more favorable to undergo the transition in the cases of both metal ions. Calculations of free energy (kJ/mol) were based upon Equation 16.

Dithioate Substitutions Hinder Catalytic Stabilization

Thermodynamic data highlight the detrimental impact that dithio-substitutions have on coordination. However, much of this data suggest defects in binding and may not correlate directly to catalysis. Unfortunately, no metal ion coordinated transition state structure has been optimized despite countless attempted. The high energy phosphorane intermediate species can instead be analyzed as its structure likely mimics that of either transition state, so any stabilizing interaction may be relevant to overall catalysis (Figure 41). The dithio-substition is found to destabilize the phosphorane, specifically the symmetric vibration of the complex shows a higher frequency vibration for the diesters. For Ca^{2+} the diester has a vibration with a wavenumber of 169.96 cm^{-1} as compared to the dithioate's vibration at 149.17 cm^{-1}, which suggests the diester is a more energetically

stabilized complex. This is correlated with thermochemical data described above, which would suggest hindered catalysis in the case of the dithioate.

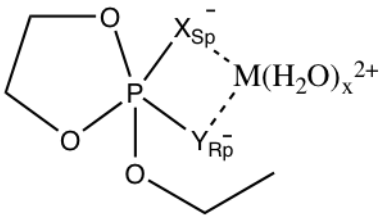

Figure 41. Phosphorane Structure, which can be used to analyzed potential interactions within transition state species.

The less stabilized system can involve the loss of several interactions, but the most clearly visible alteration upon dithioate substitution is a loss in hydrogen bonding. In the case of Mg^{2+} and Ca^{2+} hydrogen bonding with the primary hydration sphere, while not within the reactant, was present for the phosphorane. Thio-substitutions seems to cause a shift in electron density in such a way that hydrogen bonding with phosphorane moieties decreases, which are corroborated by the Wiberg bond orders of relevant hydrogen atoms (Figure 42, 43).

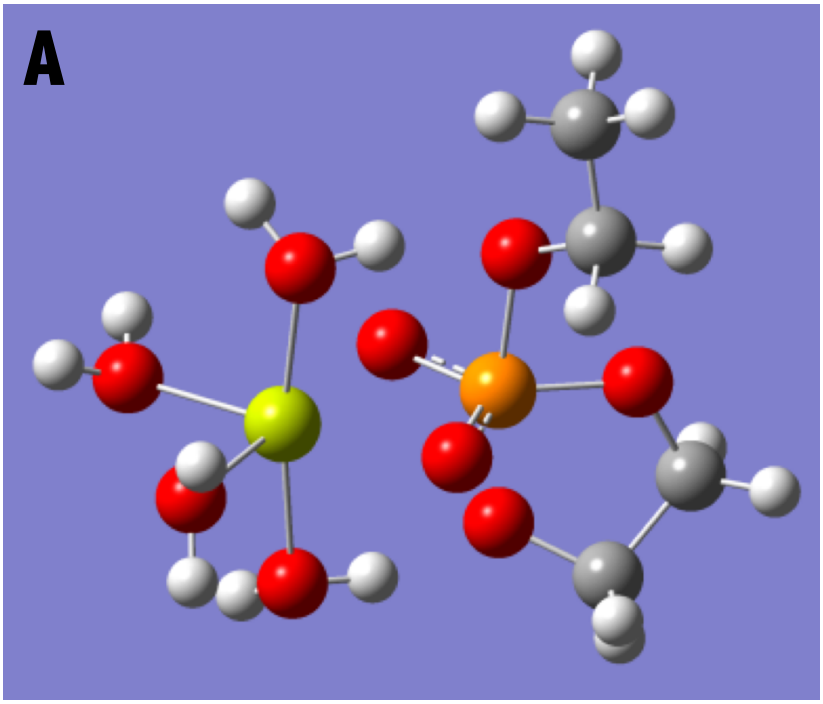
A

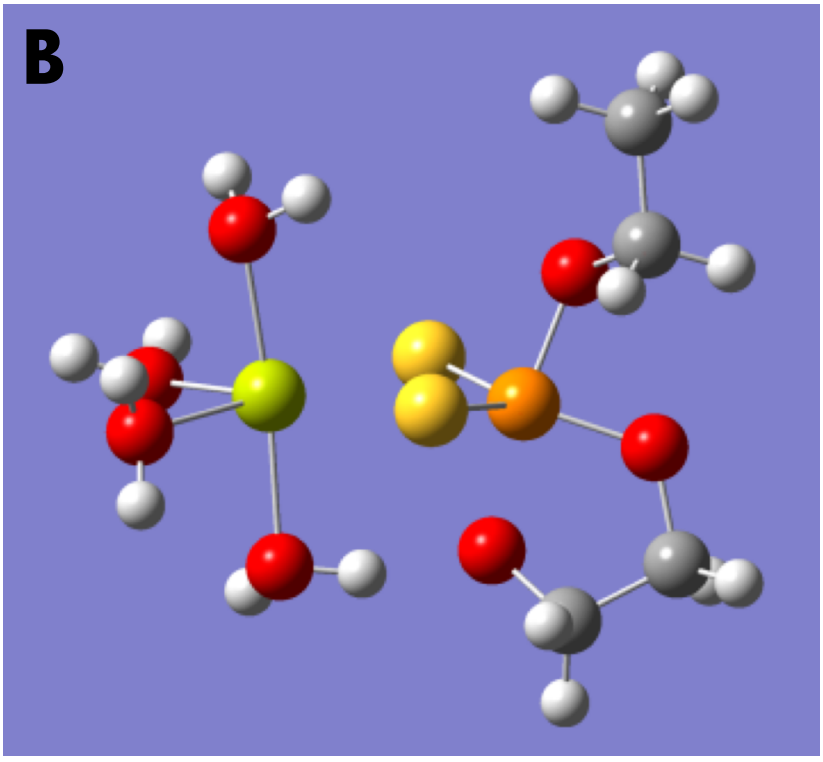
B

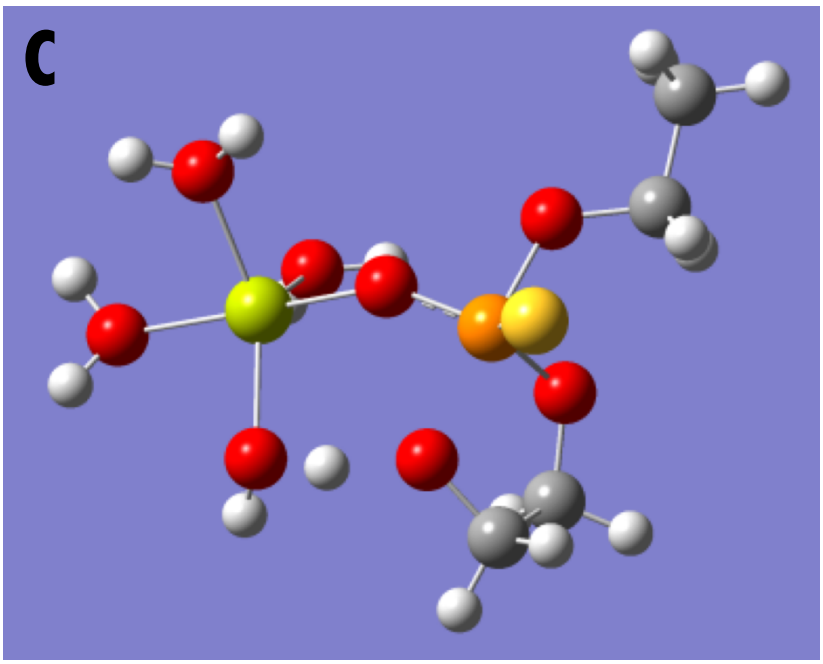
C

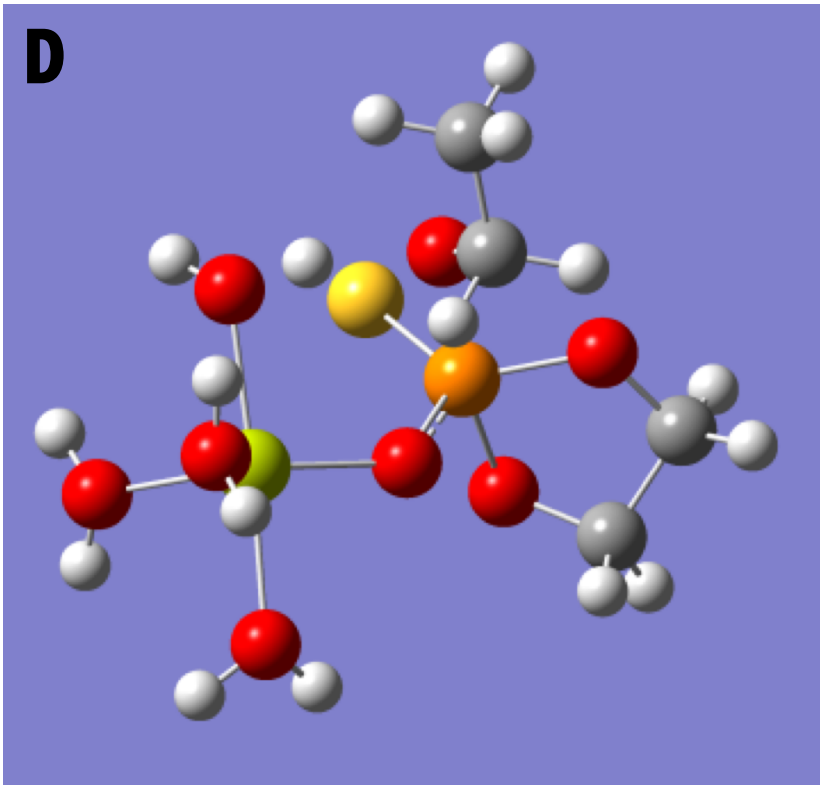
D

E Model	Optimized Structure	Number of Hydrogen Bonds	Oxygen H-Bond Donor Type	Wiberg Bond Orders
Diester	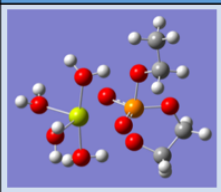	2	Leaving Group	0.08
			Nucleophile	0.09
Monothioate (Sp)	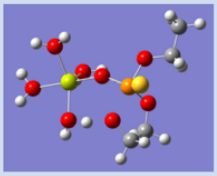	1	Leaving Group	0.0001
			Nucleophile	0.15
Monothioate (Rp)	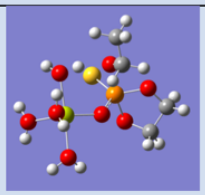	1	Leaving Group	0.12
			Nucleophile	0.00
Dithioate	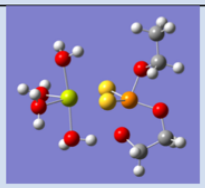	1	Leaving Group	0.0003
			Nucleophile	0.10

Figure 42. TPSSTPSS 6-311G++(d,p) optimized $Mg(H_2O)_4$ bound phosphorane structures for diester, monothioate, and dithioate models. A) Diester ,(B) Dithioate, (C) Thio (S), (D) Thio (R), (E) Changes in hydrogen bonding are counted and quantified using Wiberg bond orders.

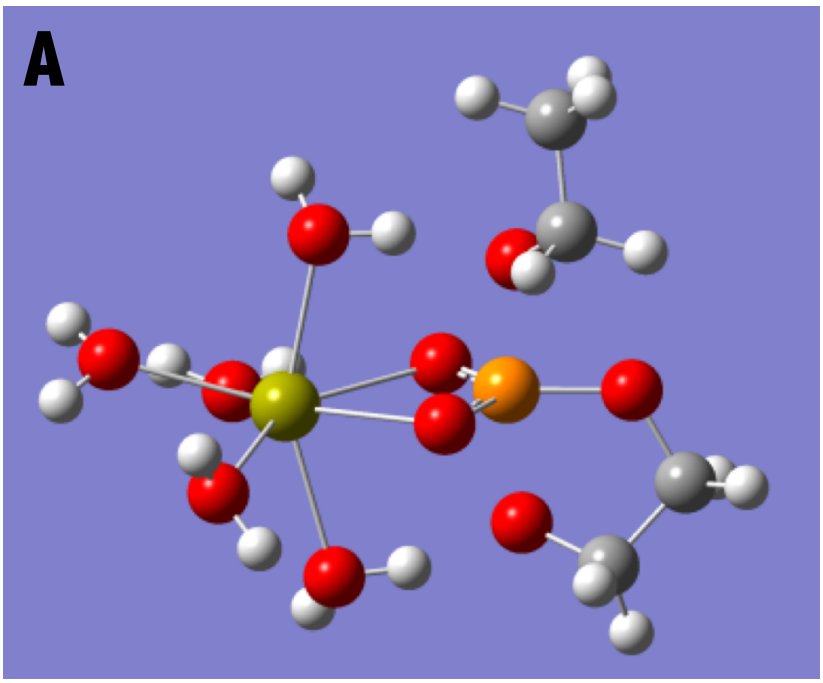
A

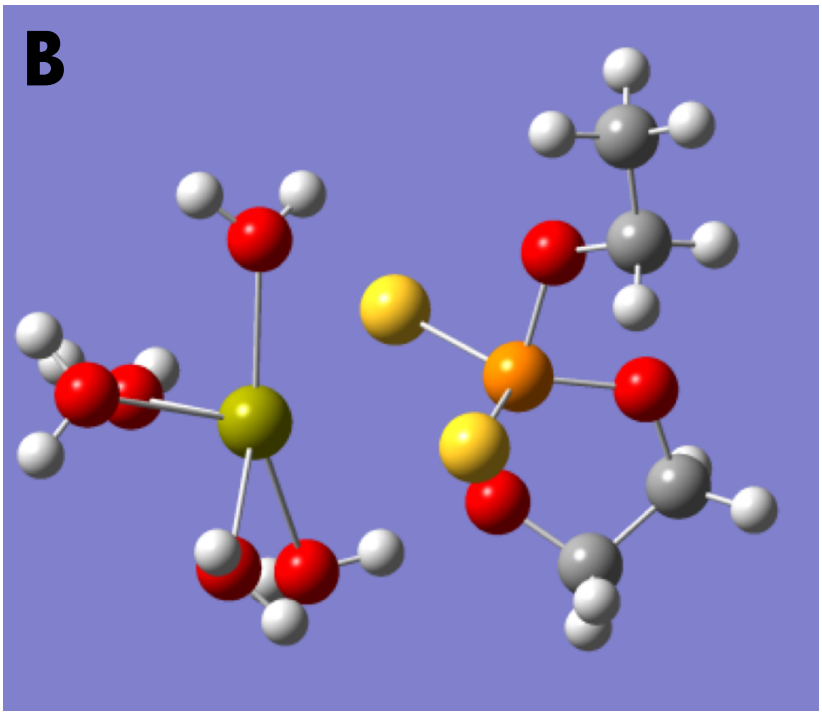
B

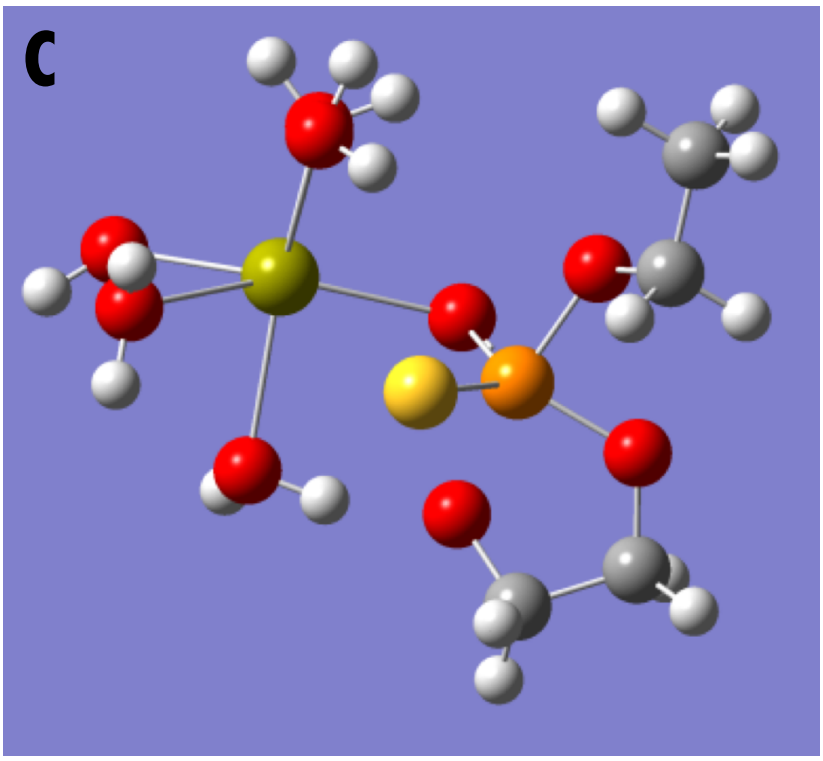
C

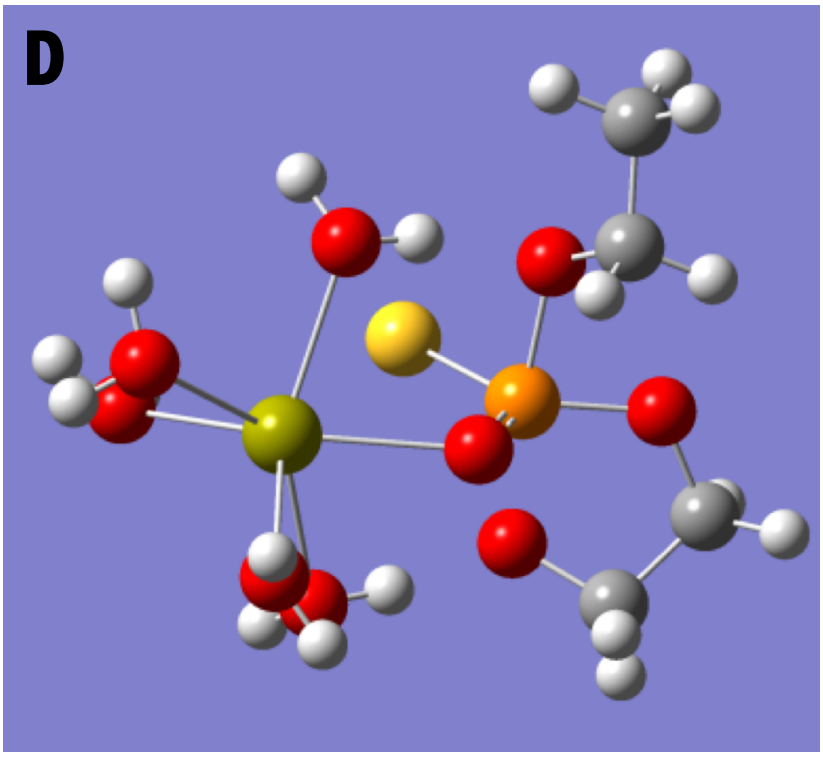
D

E Model	Optimized Structure	Number of Hydrogen Bonds	Oxygen H-Bond Donor Type	Wiberg Bond Orders
Diester	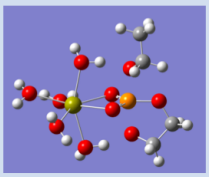	2	Leaving Group	0.08
			Nucleophile	0.09
Monothioate (Sp)	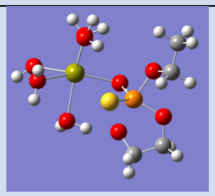	1	Leaving Group	0.0004
			Nucleophile	0.09
Monothioate (Rp)	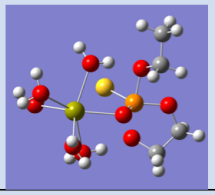	2	Leaving Group	0.07
			Nucleophile	0.09
Dithioate	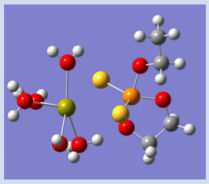	1	Leaving Group	0.0003
			Nucleophile	0.09

Figure 43. TPSSTPSS 6-311G++(d,p) optimized $Ca(H_2O)_5$ bound phosphorane structures for diester, monothioate, and dithioate models. A) Diester ,(B) Dithioate, (C) Thio (S), (D) Thio (R), (E) Changes in hydrogen bonding are counted and quantified using Wiberg bond orders.

Overall, phosphorane structures highlight interactions that are lost due to thio-substitutions, which may be catalytically important. Therefore, highlight the role of the solvent shell in catalysis, a role not considered in our inner sphere model previously.

3.4. Discussion

Bidentate Inner Sphere Binding Mode is the most favored thermochemically

Our kinetic studies suggest that catalysis is likely through inner sphere interactions that may involve the either bidendate, the displacement of two waters, or

monodentate, the displacement of one water, binding. Kinetic methods cannot unambiguously differentiate between these possibilities; however, our computational methods can highlight which conformation is more stable. Previous studies have shown that the ligands surrounding a particularly metal are critical in determining its structure and the number of solvent molecules coordinated in that geometry. For example, a B3LYP computation study showed that while ammonia and water ligands allowed Mg^{2+} to maintain an octahedral geometry, a single hydroxide caused a shift toward a trigonal bipyramidal geometry (Kluge & Weston, 2005). Two hydroxides lead to a preference toward a tetrahedral geometry. Therefore, the phosphate ligand in our system is expect to cause major geometric effects to the coordination sphere of Ca^{2+} and Mg^{2+}.

Previous models have actually used phosphate ligands, specifically dimethyl phosphate, to compare the coordination spheres of Ca^{2+} and Mg^{2+}. The study suggested that inner sphere coordination is favored by Ca^{2+}, while Mg^{2+} actually favors an outer sphere conformation (Petrov et al., 2005). This is in contrast to our model which favored the inner sphere bidentate conformation in the case of both metal ions, which is corroborated by Mayaan et al. 2004 and Dhaouadi et al. (2009). Our model system involves a nucleophilic alkoxide, which dramatically alters the electronics of the model, which can explain the difference. However, our model does suggest that Mg^{2+} does have a more stable outer sphere complex compared to Ca^{2+}, and a less stable inner sphere complex compared to Ca^{2+} (Figure 30, 31). Additionally, studies with Mg^{2+} complexes have suggested monodentate interactions with a single non-bridging oxygen (Mayaan et al., 2004), which have also been shown spectroscopically in an ribozyme active site

(Cunningham et al., 1998). However, these studies involved metal ions with more complex binding systems such as the di-bridge system in the case of Mayaan et al. (2004). Therefore, it is likely that the ligand surrounding the metal ion likely plays a large role in it binding mode. Overall, from our analysis it is suggested that both Mg^{2+} and Ca^{2+} promote catalysis through inner sphere bidentate coordination under optimal conditions within aqueous free metal ion model systems.

Monothioate Substitutions offer limited structural effects

Thio-substitutions have been shown to have limited impacts in uncoordinated kinetic and computational models (Liu et al., 2006; Liu et al., 2005a; Liu et al., 2005b; Oivanen et al., 1998; Oivanen et al., 1995). Furthermore, out kinetic results have suggested extremely minimal thio-defects in the case of all metal ions for both the Rp and the Sp. Therefore, it is unsurprising that the structural alterations due to monothioate substitutions were minimal. Sulfur substitutions have been found to cause limited changes in bond lengths and angles (Liu et al., 2006). Therefore, any defects that exist a more likely involved in other structures such as the phosphorane or involved electronic interactions.

Thiosubstitutions Impede in Electrostatic Interactions

Sulfur substitutions have been found to effect charge distribution in the progression of RNA transesterification, as the development of transition states involve the movement from a monoanionic state to a dianionic state (Liu et al., 2006). In transition state structure the sulfur atoms have been found to carry larger amounts of charge due to their polarizable nature. When a metal ion is present, as in the case of our

system, the charge distribution in these non-bridging position decreases. It is likely that this decrease is associated with an increase in covalent interaction. Therefore, it is likely that catalysis relies on ionic interactions rather than the formation of distinct bonds.

More importantly, the charge transfer highlights a preference metal ions have oxygen, which are correlated with increase bond orders. Previous studies with dimethyl phosphate corroborate this trend with Na^{+}, Mg^{2+}, K^{+} bisecting the non-bridging oxygen atoms, while deviating from the center in the presence of the sulfur (Dhaouadi et al., 2009). The dithioate is found to bisect the plane once again as corroborated with our study. However, there is a large decrease in charge compared to the uncoordinated species, which highlights worse coordination. This particular trend has not be cited in the literature previously, and highlights the electronic detriments thio-substitutions may cause.

Dithio-substitutions have synergistic energetic defects in binding

Our kinetic analysis and our analysis of charge transfer suggests that in the presence of a single oxygen there exists the possibility of compensatory interactions. In the absence of any oxygen atoms in the non-bridging positions, there is a significant decrease in the possible interaction that may exist. This destabilizes the interactions dramatically. First, the dithio substitution increases the metal ion-phosphorus distance for both Ca^{2+} and Mg^{2+}. However, this electrostatic interaction is found to be minimal as compared to the total energy defect that exists. Second, there is a decrease in ionic interaction upon dithio substitution. Overall, it is likely that the presence of the ionic interaction leads to the destabilization of the dithioate, which has not been found to be as

destabilized in uncoordinated settings (Liu et al., 2005a). The substitution of sulfur in uncoordinated setting reduces the benefit of solvent interactions, but allows for a great stabilization of charge in the larger sulfur atom (Liu et al., 2006). In our metal ion system, the metal ion interaction precludes the non-bridging positions from having any other interactions with the solvent. Therefore, the ion-ion interaction is more destabilized that the ion-dipole interaction. Overall, the dithioate substitution follows the synergistic pattern found in kinetic data and highlight the use of sulfur substitutions for studying metal ion interactions.

Thio-substitutions alter phosphorane structure to hinder catalysis

Major binding defects were found in the case of the dithioate model; however, these binding defects were also accompanied by the destabilization of catalysis. The phosphorane was destabilized, specifically losing hydrogen bonding interactions unique to that species, which are likely important to transition state stabilization. Mayaan et al. (2004) highlight the importance of these hydrogen bonding interactions in their dianionic phosphorane model, methyl(ethylene)phosphorane. The loss of these hydrogen bonds are the most significant structural change in the thio-complexes, which suggest that sulfur substitutions cause dramatic alterations to the electronic environment which cause kinks in the primary hydration shell of the metal ion. Therefore, these results inply that hydrogen bonding is critical to catalysis, which could potential shed light on to solvent deuterium isotope effects studies.

Hydrogen bonding has been found to exhibit isotope effects in different systems and have been found to be variable dependent on the system. Two key examples

highlight the fact that hydrogen bonding interactions could actually lead to inverse isotope effects. These results rely on the fact that O-H hydrogen bonds are stronger than O-D hydrogen bonds, because of the looser environment of O-H that allow for more appropriate hydrogen bond formation (Scheiner & Čuma, 1996; Van Hook, 1975). Vapor pressure isotope effects have been used to study this particular phenomenon, as several solvent rely on hydrogen bonding, so the effects of deuterium on boiling point should offer information about the link between hydrogen bonding and isotope effects. In the case of NH_3 versus ND_3 and CH_3COOH versus CH_3COOD, hydrogenated solvents show higher boiling points as opposed to their deuterated counterparts (Van Hook, 1975). Stronger hydrogen bonds yield stronger intermolecular forces, which decreases the vapor pressure. Therefore, pressure of the light isotope will be less than that of the heavy isotope, which give the inverse isotope effect (Van Hook, 1975). These isotope effects were also seen in work with proteins that use inverse isotope effects ranging between 0.3-0.8 that indicate the presence of hydrogen bonds (Krantz et al., 2002; Van Hook, 1975) . Therefore, it is likely that inverse solvent kinetic isotope effect is due to hydrogen bonding from inner sphere coordination that also agrees with our thio-effect results. Therefore, it is necessary to computationally model structures with hydrogens deuterated in specific positions, experimentally determining solvent kinetic isotope effects for thioate dinucleotides, and conduct fractionation studies to identify the number of exchangeable hydrogen in the system. Overall, these results highlight the importance of solvent interactions to catalysis, and suggest a mode of destabilization that thio-substitutions may cause their dramatic kinetic effects.

3.5. Conclusion

Overall, sulfur substitutions are found to cause alterations in metal ion coordination allowing for a series of conclusions:

1. Bidentate inner sphere interactions are the more favorable set of interactions for both metal ion systems with diesters.
2. Structural changes in the monothioate system are minimal, and would predict minimal catalytic effects.
3. All thio-substitutions cause a decrease in charge on sulfur atoms weakening ionic interactions, suggesting a preference toward interactions with oxygen,
4. Dithio-substitutions cause dramatic defects in binding, with destabilizing reaction coordinate species. This likely due to the absence of any compensatory interactions that exist in monothioate models.
5. Dithio-substitution interfere wit phosphorane stabilization by the primary hydration sphere, highlight the role of solvent in catalysis.

Overall, computational studies highlight both catalytic and binding defects that are expected up sulfur substitutions.

CHAPTER 4: CONCLUSIONS

4.1. Summary of Kinetic Conclusions

Kinetic conclusions give several pieces of evidence that highlight the importance of coordination to non-bridging oxygen atoms on the phosphoryl to promote RNA phosphodiester cleavage. Calcium catalyzed reactions allow for an investigation of these reactions at alkaline conditions, which isolates the cleavage reaction. Reactions with thio-substituted compounds of UpG show catalytic defects due to non-bridging thio atoms, which suggest decreased coordination. Additionally, these results show that thio atoms do not disrupt binding; therefore, suggesting that the metal ion-substrate complex is not destabilized, but that thio-substitutions weaken the interactions that would encourage catalysis. Comparisons to other metal ions further supported these conclusions as it seems that the outer sphere complex, cobalt hexamine (III), does not catalyze and the hard metal ion is found to be more sensitive to thio-substitutions. These reactions highlight the importance of direct coordination and electrophilic catalysis in Ca^{2+} catalyzed phosphodiester cleavage.

4.2. Summary of Computational Conclusions

Computational studies highlight energetic defects due to thio-substitutions, which are extremely detrimental in the dithioate model. The metal ion sulfur interaction is found to be weaker and more covalent compared to interactions with the diester model. Thio-substitutions are also found to destabilize the phosphorane, through interrupting hydrogen bonds, which would potentially lead to a kinetic isotope effect. These results would imply

energetic, binding, and catalytic defects upon thio-substitution and highlight the charge transfer interaction between the metal ion and phosphoryl that is inherent to catalysis.

4.3. Mechanistic Conclusions

These studies highlight defects caused by thio-substitutions in the non-bridging positions of the phosphoryl, which highlight the importance of electrophilic catalysis to metal ion catalysis of phosphodiester cleavage. Kinetic studies suggest that catalytic defects can exist when electrophilic catalysis in hindered, while maintaining binding. Computational data supports the claim on catalytic defects as the phosphorane is less stabilized overall. However, computational data suggests that thio-substitutions should be detrimental to binding rather than inconsequential. Therefore, we postulate that binding and catalysis may occur through different mechanisms. Catalysis relies on loss of solvent interactions to allow for inner sphere coordination, while outer sphere interactions are the primary form of binding which would exhibit limited energetic defects due to thio-substitutions (Figure 44). The relative rates of catalysis is then dependent on the stability of the inner sphere complex binding mode (Figure 45). This hypothesis is a possibility; however, current results with the outer sphere complex suggest that $Co(NH_3)_6^{3+}$ does not bind, with not saturation. This would argue against the outer sphere mechanism being the mode of binding. However, it is a possibility that the primary hydration sphere of $Co(NH_3)_6^{3+}$ interferes with the formation of a complex with limited compensation of energy from the ion-diester complex. Greater investigation of outer sphere complexes and solvation are necessary to isolate the mechanistic scheme. In addition, the limitation of computations must be modeled for or overcome to make more experimentally relevant

conclusions. Overall, due to the derived binding modes and mechanistic analysis from this study it becomes critical to utilize thioate models, specifically dithioate, in the future in order to better evaluate the roles of free ligands in binding to get optimal conclusions.

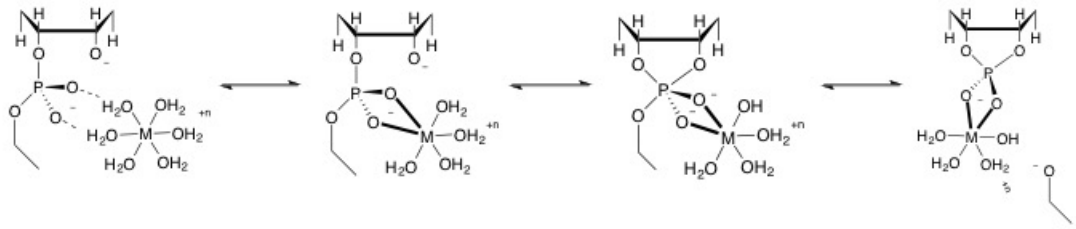

Figure 44. Proposed mechanism of interactions to lead to catalysis of cleavage. We propose that metal ion binding mainly occurs through outer sphere coordination, and eventually must overcome the energetic barrier of breaking solvent interactions to form the inner sphere complex. This inner sphere complex is catalytically active to form cleaved products.

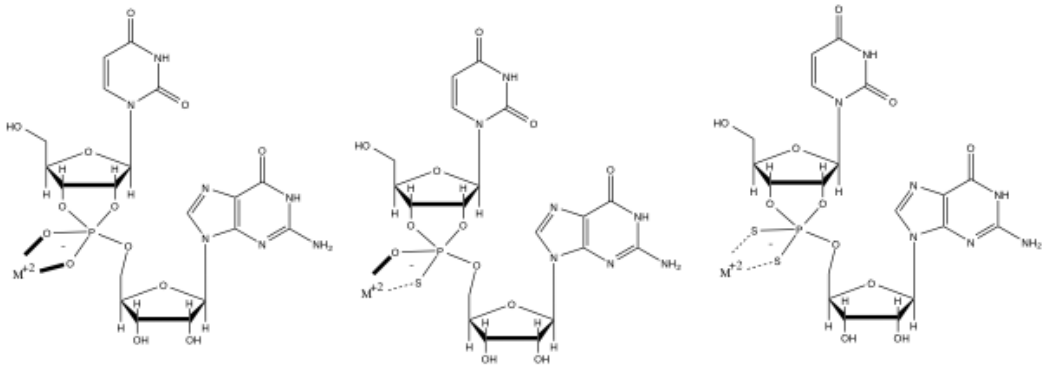

Figure 45. Modes of Catalysis with Thio Models. Results suggest catalysis stabilizing the phosphorane intermediate involving inner-sphere coordination. Disrupting the interaction with one non-bridging oxygen atom can be compensated by the remaining non-bridging oxygen atom. Phosphorodithioate substitution yields a synergistic catalytic defect relative to the S_P and R_P phosphoromonothioates.

4.4. Future Directions

In order to better explain results suggested by computational and experimental results, several future experiments can be run.

A primary concern is to further develop the computational model to overcome its current limitations. First, there needs to be a more efficient model to take the solvent into consideration. In future experiments it will be necessary to take into account solvent interactions of the diester models, which would impact enthalpic and entropic contributions. In addition, the use of more explicit solvent, may better model how the solvent effects catalysis. It has been found that an increase use of explicit solvent leads to more experimentally relevant vibrations, which may make the model wholly experimentally relevant (Dhaouadi et al., 2009). Second, while benchmarking studies have been done for DMP hydrolysis, the differences between Mg^{2+} and Ca^{2+} suggest the needs for benchmarking with metal ion catalysis, because of their unique electronic effects (Liu et al., 2006; Ribeiro et al., 2010). Third, the use of a solely deprotonated nucleophile may imply false mechanistic results because even at experimental conditions of pH 11.5 the nucleophile is only deprotonated 3% of the time (Cassano, Unpublished Results). Therefore, a better original model may better the electronic environment that will be interacting with the catalytic metal ion. Fourth, to truly gauge catalysis computational it is necessary to obtain transition state structure, which may rely upon more sophisticated theories for modeling the solvent as hydrogen bonding is found to be important to the phosphorane. Improvements to the computational model will assist with experimental analyses.

A secondary concern is to improve the inaccuracies in our experimental determinations of binding through the use of more sophisticated methods such a

potentiometric pH titrations (Sigel et al., 1997) or NMR studies (Suzumura et al., 2002). This will confirm binding measurements for an overall more accurate analysis.

A third concern is to understand the role of hydrogen bonding through the use of kinetics isotope effects in both computational and experimental systems. The substitutions of hydrogens in the solvent for deuterium in the computational model would highlight the importance of those interactions to the solvent (Goldstein et al., 1996). Experimentally, the use of proton inventories can help elucidate the number of exchangeable protons involved in the measured kinetic isotope effect (Venkatasubban & Schowen, 1984). In addition, some sort of manipulations might allow for the use of multiple isotope effects to isolate the order with which inner sphere or potential general acid-base interactions occur with respect to each other (Hermes et al., 1982). These added techniques would give mechanistic insight into the relevant steps and orders of those steps in catalysis.

A fourth concern would be to better assess the role of the charge transfer complex between the metal ion and phosphoryl. Computational studies suggested defects in binding and catalysis due to a decrease ionic interaction. In order to probe this experimentally it may be useful to use organometallic synthesis to design a metal ion ligand that would preserve inner sphere coordination from one conformation, but allow for alterations in the charge residing on the atom. This could be useful to assess the effects on kinetics, as this type of ligand design has been useful in the past to highlight important interactions (Korhonen et al., 2013).

Overall, several experiments need to be run to isolate the mechanism of binding, to understand the role of the solvent, and to defining the catalytic mechanism. The dithioate model serves are a good model to assess electrophilic interaction, but it is critical to to isolate the various components of catalysis and binding to recognize their individual contributions to the remarkable catalysis seen in phosphodiester bond cleavage.

References

(2017). Magnesium: properties of compounds, vol. 2017, pp. https://www.webelements.com/magnesium/compound_properties.html. WebElements.

ALVES, R., CHALEIL, R. A. G. & STERNBERG, M. J. E. (2002). Evolution of Enzymes in Metabolism: A Network Perspective. Journal of Molecular Biology, 324(2), 751–770.

AMOVILLI, C., BARONE, V., CAMMI, R., CANCÈS, E., COSSI, M., MENNUCCI, B., POMELLI, C. S. & TOMASI, J. (1998). Recent advances in the description of solvent effects with the polarizable continuum model. Advances in Quantum Chemistry, 32, 227-261.

ANDERSON, V. E., RUSZCZYCKY, M. W. & HARRIS, M. E. (2006). Activation of oxygen nucleophiles in enzyme catalysis. Chemical reviews, 106(8), 3236-3251.

BAI, C., ZHAO, L., TSAI, M.-D. & BRUZIK, K. S. (2010). Unique catalytic mechanism of phosphatidylinositol-specific phospholipase C from Streptomyces antibioticus. Journal of the American Chemical Society, 132(4), 1210-1211.

BASOLO, F. & PEARSON, R. G. (1988). Mechanisms of Inorganic Reactions. New York: John Wiley & Sons.

BAUERNSCHMITT, R. & AHLRICHS, R. (1996). Treatment of electronic excitations within the adiabatic approximation of time dependent density functional theory. Chemical Physics Letters, 256(4), 454-464.

BECKE, A. D. (1993). Density-functional thermochemistry. III. The role of exact exchange. The Journal of chemical physics, 98(7), 5648-5652.

BEEBE, J. A., KURZ, J. C. & FIERKE, C. A. (1996). Magnesium ions are required by Bacillus subtilis ribonuclease P RNA for both binding and cleaving precursor tRNAAsp. Biochemistry, 35(32), 10493-10505.

BEESE, L. S. & STEITZ, T. A. (1991). Structural basis for the 3'-5'exonuclease activity of Escherichia coli DNA polymerase I: a two metal ion mechanism. The EMBO Journal, 10(1), 25.

BONDI, A. (1964). van der Waals volumes and radii. The Journal of physical chemistry, 68(3), 441-451.

BONFÁ, L., GATOS, M., MANCIN, F., TECILLA, P. & TONELLATO, U. (2003). The ligand effect on the hydrolytic reactivity of Zn (II) complexes toward phosphate diesters. Inorganic chemistry, 42(12), 3943-3949.

BRESLOW, R. (1982). Artificial enzymes. Science, 218(4572), 532-537.

BRESLOW, R. & HUANG, D.-L. (1991). Effects of metal ions, including Mg2+ and lanthanides, on the cleavage of ribonucleotides and RNA model compounds. Proceedings of the National Academy of Sciences, 88(10), 4080-4083.

BRIDGEMAN, A., MAELFAIT, J., DAVENNE, T., PARTRIDGE, T., PENG, Y., MAYER, A., DONG, T., KAEVER, V., BORROW, P. & REHWINKEL, J. (2015). Viruses transfer the antiviral second messenger cGAMP between cells. Science, 349(6253), 1228-1232.

BRONSTED, J. (1928). Acid and Basic Catalysis. Chemical Reviews, 5(3), 231-338.

BROWN, D. & TODD, A. (1955). Evidence on the nature of the chemical bonds in nucleic acids. The nucleic acids, 1, 409-445.

CARROLL, M. (2007). **A Computational Study of the Coordination of Mg^{2+} and Ca2+ with Water, Hydroxide, and Phospha**te, Drew University.

CASTRO, C., SMIDANSKY, E., MAKSIMCHUK, K. R., ARNOLD, J. J., KORNEEVA, V. S., GÖTTE, M., KONIGSBERG, W. & CAMERON, C. E. (2007). Two proton transfers in the transition state for nucleotidyl transfer catalyzed by RNA-and DNA-dependent RNA and DNA polymerases. Proceedings of the National Academy of Sciences, 104(11), 4267-4272.

CATE, J. H., HANNA, R. L. & DOUDNA, J. A. (1997). A magnesium ion core at the heart of a ribozyme domain. Nature structural biology, 4(7), 553-558.

CHEN, H., GIESE, T. J., HUANG, M., WONG, K. Y., HARRIS, M. E. & YORK, D. M. (2014). Mechanistic insights into RNA transphosphorylation from kinetic isotope effects and linear free energy relationships of model reactions. Chemistry–A European Journal, 20(44), 14336-14343.

CHEN, H., PICCIRILLI, J. A., HARRIS, M. E. & YORK, D. M. (2015). Effect of Zn 2+ binding and enzyme active site on the transition state for RNA 2′-O-transphosphorylation interpreted through kinetic isotope effects. Biochimica et Biophysica Acta (BBA)-Proteins and Proteomics, 1854(11), 1795-1800.

CHEN, J., GANGULY, A., MISWAN, Z., HAMMES-SCHIFFER, S., BEVILACQUA, P. C. & GOLDEN, B. L. (2013). Identification of the catalytic Mg2+ ion in the hepatitis delta virus ribozyme. Biochemistry, 52(3), 557-567.

CHRISTIAN, E. L., ANDERSON, V. E., CAREY, P. R. & HARRIS, M. E. (2010). A Quantitative Raman Spectroscopic Signal for Metal− Phosphodiester Interactions in Solution. Biochemistry, 49(13), 2869-2879.

CHRISTIAN, E. L., ANDERSON, V. E. & HARRIS, M. E. (2011). Deconvolution of Raman spectroscopic signals for electrostatic, H-bonding, and inner-sphere interactions between ions and dimethyl phosphate in solution. Journal of inorganic biochemistry, 105(4), 538-547.

COOPER, G. M. (2000). The Central Role of Enzymes as Biological Catalysts. Sunderland (MA): Sinauer Associates.

CORONA-MARTÍNEZ, D. O., GOMEZ-TAGLE, P. & YATSIMIRSKY, A. K. (2012). Electrophilic assistance to the cleavage of an RNA model phopshodiester via specific and general base-catalyzed mechanisms. The Journal of organic chemistry, 77(20), 9110-9119.

CUNNINGHAM, L. A., LI, J. & LU, Y. (1998). Spectroscopic evidence for inner-sphere coordination of metal ions to the active site of a hammerhead ribozyme. Journal of the American Chemical Society, 120(18), 4518-4519.

CURTISS, L. A., RAGHAVACHARI, K., TRUCKS, G. W. & POPLE, J. A. (1991). Gaussian-2 theory for molecular energies of first-and second-row compounds. The Journal of chemical physics, 94(11), 7221-7230.

DAS, S. R. & PICCIRILLI, J. A. (2005). General acid catalysis by the hepatitis delta virus ribozyme. Nature chemical biology, 1(1), 45-52.

DAVIS, A. M., HALL, A. D. & WILLIAMS, A. (1988). Charge description of base-catalyzed alcoholysis of aryl phosphodiesters: a ribonuclease model. Journal of the American Chemical Society, 110(15), 5105-5108.

DENNINGTON, R., KEITH, T. A. & MILLAM, J. M. (2009). GaussView. Semichem Inc, Shawnee Mission, KS.

DHAOUADI, Z., NSANGOU, M., HERNÁNDEZ, B., PFLÜGER, F., LIQUIER, J. & GHOMI, M. (2009). Geometrical and vibrational features of phosphate, phosphorothioate and phosphorodithioate linkages interacting with hydrated cations: A DFT study. Spectrochimica Acta Part A: Molecular and Biomolecular Spectroscopy, 73(5), 805-814.

DOUDNA, J. A. & LORSCH, J. R. (2005). Ribozyme catalysis: not different, just worse. Nature structural & molecular biology, 12(5), 395-402.

ELLIOTT, S. G. & MCLAUGHLIN, C. S. (1978). Rate of macromolecular synthesis through the cell cycle of the yeast S*accharomyces cerevisiae*. Proc Natl Acad Sci USA, 75(9), 4384-4388.

EMILSSON, G. M., NAKAMURA, S., ROTH, A. & BREAKER, R. R. (2003). Ribozyme speed limits. Rna, 9(8), 907-918.

FAN, Y. & GAO, Y. Q. (2007). A DFT study on the mechanism of phosphodiester cleavage mediated by monozinc complexes. Journal of the American Chemical Society, 129(4), 905-913.

FENG, G., NATALE, D., PRABAHARAN, R., MAREQUE-RIVAS, J. C. & WILLIAMS, N. H. (2006). Efficient Phosphodiester Binding and Cleavage by a ZnII Complex Combining Hydrogen-Bonding Interactions and Double Lewis Acid Activation. Angewandte Chemie, 118(42), 7214-7217.

FLORIÁN, J., ÅQVIST, J. & WARSHEL, A. (1998). On the reactivity of phosphate monoester dianions in aqueous solution: Brønsted linear free-energy relationships do not have an unique mechanistic interpretation. Journal of the American Chemical Society, 120(44), 11524-11525.

FORESMAN, J. B. & FRISCH, Æ. (1996). Exploring chemistry with electronic structure methods: a guide to using Gaussian.

GALBURT, E. A. & STODDARD, B. L. (2002). Catalytic mechanisms of restriction and homing endonucleases. Biochemistry, 41(47), 13851-13860.

GAO, H., KE, Z., DEYONKER, N. J., WANG, J., XU, H., MAO, Z.-W., PHILLIPS, D. L. & ZHAO, C. (2011). Dinuclear Zn (II) complex catalyzed phosphodiester cleavage proceeds via a concerted mechanism: a density functional theory study. Journal of the American Chemical Society, 133(9), 2904-2915.

GARCIA-VILOCA, M., GAO, J., KARPLUS, M. & TRUHLAR, D. G. (2004). How enzymes work: analysis by modern rate theory and computer simulations. Science, 303(5655), 186-195.

GENTILI, M., KOWAL, J., TKACH, M., SATOH, T., LAHAYE, X., CONRAD, C., BOYRON, M., LOMBARD, B., DURAND, S. & KROEMER, G. (2015). Transmission of innate immune signaling by packaging of cGAMP in viral particles. Science, 349(6253), 1232-1236.

GOLDSTEIN, E., BENO, B. & HOUK, K. (1996). Density functional theory prediction of the relative energies and isotope effects for the concerted and stepwise mechanisms of the Diels− Alder reaction of butadiene and ethylene. Journal of the American Chemical Society, 118(25), 6036-6043.

GRIMME, S., ANTONY, J., SCHWABE, T. & MÜCK-LICHTENFELD, C. (2007). Density functional theory with dispersion corrections for supramolecular structures, aggregates, and complexes of (bio) organic molecules. Organic & Biomolecular Chemistry, 5(5), 741-758.

HARRIS, D. C. (2010). Quantitative Chemical Analysis. New York: W. H. Freeman and Company.

HARRIS, M. E. & CASSANO, A. G. (2008). Experimental analyses of the chemical dynamics of ribozyme catalysis. Curr Opin Chem Biol, 12, 626-639.

HARRIS, M. E., DAI, Q., GU, H., KELLERMAN, D. L., PICCIRILLI, J. A. & ANDERSON, V. E. (2010). Kinetic isotope effects for RNA cleavage by 2′-O-transphosphorylation: nucleophilic activation by specific base. Journal of the American Chemical Society, 132(33), 11613-11621.

HELGAKER, T., WATSON, M. & HANDY, N. C. (2000). Analytical calculation of nuclear magnetic resonance indirect spin–spin coupling constants at the generalized gradient approximation and hybrid levels of density-functional theory. The Journal of Chemical Physics, 113(21), 9402-9409.

HENGGE, A. C. (2002). Isotope effects in the study of phosphoryl and sulfuryl transfer reactions. Accounts of chemical research, 35(2), 105-112.

HENGGE, A. C., BRUZIK, K. S., TOBIN, A. E., CLELAND, W. & TSAI, M.-D. (2000). Kinetic isotope effects and stereochemical studies on a ribonuclease model: Hydrolysis reactions of uridine 3′-nitrophenyl phosphate. Bioorganic chemistry, 28(3), 119-133.

HERMES, J. D., ROESKE, C., O'LEARY, M. H. & CLELAND, W. (1982). Use of multiple isotope effects to determine enzyme mechanisms and intrinsic isotope effects. Malic enzyme and glucose 6-phosphate dehydrogenase. Biochemistry, 21(20), 5106-5114.

HERSCHLAG, D. & JENCKS, W. P. (1987). The effect of divalent metal ions on the rate and transition-state structure of phosphoryl-transfer reactions. Journal of the American Chemical Society, 109(15), 4665-4674.

HERSCHLAG, D., PICCIRILLI, J. A. & CECH, T. R. (1991). Ribozyme-catalyzed and nonenzymic reactions of phosphate diesters: rate effects upon substitution of sulfur for a nonbridging phosphoryl oxygen atom. Biochemistry, 30(20), 4844-4854.

HOUGLAND, J. L., KRAVCHUK, A. V., HERSCHLAG, D. & PICCIRILLI, J. A. (2005). Functional identification of catalytic metal ion binding sites within RNA. PLoS Biol, 3(9), e277.

HUAI, Q., COLICELLI, J. & KE, H. (2003). The crystal structure of AMP-bound PDE4 suggests a mechanism for phosphodiesterase catalysis. Biochemistry, 42(45), 13220-13226.

HUANG, M. & YORK, D. M. (2014). Linear free energy relationships in RNA transesterification: theoretical models to aid experimental interpretations. Physical Chemistry Chemical Physics, 16(30), 15846-15855.

HUMPHRY, T., IYER, S., IRANZO, O., MORROW, J. R., RICHARD, J. P., PANETH, P. & HENGGE, A. C. (2008). Altered transition state for the reaction of an RNA model catalyzed by a dinuclear zinc (II) catalyst. Journal of the American Chemical Society, 130(52), 17858-17866.

IKENAGA, H. & INOUE, Y. (1974). Metal (II) ion catalyzed transphosphorylation of four homodinucleotides and five pairs of dinucleotide sequence isomers. Biochemistry, 13(3), 577-582.

JARVINEN, P., OIVANEN, M. & LONNBERG, H. (1991). Interconversion and phosphoester hydrolysis of 2', 5'-and 3', 5'-dinucleoside monophosphates: kinetics and mechanisms. The Journal of Organic Chemistry, 56(18), 5396-5401.

JENCKS, D. A. & JENCKS, W. P. (1977). The characterization of transition states by structure-reactivity coefficients. Journal of the American Chemical Society, 99(24), 7948-7960.

JENCKS, W. P. (1969). Catalysis in Chemistry and Enzymology. Mineola, NY: Dover Publications.

JENSEN, F. (2016). Introduction to computational chemistry: John wiley & sons.

JONES, J. P., WEISS, P. M. & CLELAND, W. (1991). Secondary oxygen-18 isotope effects for hexokinase-catalyzed phosphoryl transfer from ATP. Biochemistry, 30(15), 3634-3639.

KAMERLIN, S. C., SHARMA, P. K., PRASAD, R. B. & WARSHEL, A. (2013). Why nature really chose phosphate. Q Rev Biophys, 46(1), 1-132.

KATZ, A. K., GLUSKER, J. P., BEEBE, S. A. & BOCK, C. W. (1996). Calcium ion coordination: a comparison with that of beryllium, magnesium, and zinc. Journal of the American Chemical Society, 118(24), 5752-5763.

KHAN, S. & KIRBY, A. (1970). The reactivity of phosphate esters. Multiple structure–reactivity correlations for the reactions of triesters with nucleophiles. Journal of the Chemical Society B: Physical Organic, 1172-1182.

KIRBY, A. & JENCKS, W. (1965). The Reactivity of Nucleophilic Reagents toward the p-Nitrophenyl Phosphate Dianion1. Journal of the American Chemical Society, 87(14), 3209-3216.

KIRBY, A. & VARVOGLIS, A. (1968). The reactivity of phosphate esters: reactions of monoesters with nucleophiles. Nucleophilicity independent of basicity in a bimolecular substitution reaction. Journal of the Chemical Society B: Physical Organic, 135-141.

KIRBY, A. & YOUNAS, M. (1970). The reactivity of phosphate esters. Reactions of diesters with nucleophiles. Journal of the Chemical Society B: Physical Organic, 1165-1172.

KIRK, B. A., CUSACK, C. L., LAAGER, E., ROCHLIS, E., THOMAS, T. & CASSANO, A. G. (2010). Mononuclear and dinuclear mechanisms for catalysis of phosphodiester cleavage by alkaline earth metal ions in aqueous solution. Journal of inorganic biochemistry, 104(2), 207-210.

KLEIN, D. J. & FERRÉ-D'AMARÉ, A. R. (2006). Structural basis of glmS ribozyme activation by glucosamine-6-phosphate. Science, 313(5794), 1752-1756.

KLUGE, S. & WESTON, J. (2005). Can a hydroxide ligand trigger a change in the coordination number of magnesium ions in biological systems? Biochemistry, 44(12), 4877-4885.

KNOBLOCH, B., NAWROT, B., OKRUSZEK, A. & SIGEL, R. K. (2008). Discrimination in Metal-Ion Binding to RNA Dinucleotides with a Non-Bridging Oxygen or Sulfur in the Phosphate Diester Link. Chemistry–A European Journal, 14(10), 3100-3109.

KOOL, E. T. & WATERS, M. L. (2007). The model student: what chemical model systems can teach us about biology. Nature Chemical Biology, 3(2), 70-73.

KORHONEN, H., KOIVUSALO, T., TOIVOLA, S. & MIKKOLA, S. (2013). There is no universal mechanism for the cleavage of RNA model compounds in the presence of metal ion catalysts. Organic & biomolecular chemistry, 11(48), 8324-8339.

KOSONEN, M., YOUSETI-SALAKDEH, E., STRÖMBERG, R. & LÖNNBERG, H. (1997). Mutual isomerization of uridine 2′-and 3′-alkylphosphates and cleavage to a 2′, 3′-cyclic phosphate: the effect of the alkyl group on the hydronium-and hydroxide-ion-catalyzed reactions. Journal of the Chemical Society, Perkin Transactions 2, (12), 2661-2666.

KRANTZ, B. A., SRIVASTAVA, A. K., NAULI, S., BAKER, D., SAUER, R. T. & SOSNICK, T. R. (2002). Understanding protein hydrogen bond formation with kinetic H/D amide isotope effects. Nature Structural & Molecular Biology, 9(6), 458-463.

KROEMER, G. & POUYSSEGUR, J. (2008). Tumor Cell Metabolism: Cancer's Achilles Heel. Cancer Cell, 13, 472-482.

KUUSELA, S., AZHAYEV, A., GUZAEV, A. & LÖNNBERG, H. (1995). The effect of the 3′-terminal monophosphate group on the metal-ion-promoted hydrolysis of the phosphodiester bonds of short oligonucleotides. Journal of the Chemical Society, Perkin Transactions 2, (6), 1197-1202.

LASSILA, J. K., ZALATAN, J. G. & HERSCHLAG, D. (2011). Biological phosphoryl-transfer reactions: understanding mechanism and catalysis. Annual review of biochemistry, 80, 669.

LEE, C., YANG, W. & PARR, R. G. (1988). Development of the Colle-Salvetti correlation-energy formula into a functional of the electron density. Physical review B, 37(2), 785.

LI, L., YIN, Q., KUSS, P., MALIGA, Z., MILLÁN, J. L., WU, H. & MITCHISON, T. J. (2014). Hydrolysis of 2′ 3′-cGAMP by ENPP1 and design of nonhydrolyzable analogs. Nature chemical biology, 10(12), 1043-1048.

LILLEY, D. M. (2004). The Varkud satellite ribozyme. Rna, 10(2), 151-158.

LIU, Y., GREGERSEN, B. A., HENGGE, A. & YORK, D. M. (2006). Transesterification thio effects of phosphate diesters: free energy barriers and kinetic and equilibrium isotope effects from density-functional theory. Biochemistry, 45(33), 10043-10053.

LIU, Y., GREGERSEN, B. A., LOPEZ, X. & YORK, D. M. (2005a). Density functional study of the in-line mechanism of methanolysis of cyclic phosphate and thiophosphate esters in solution: insight into thio effects in RNA transesterification. The Journal of Physical Chemistry B, 109(42), 19987-20003.

LIU, Y., LOPEZ, X. & YORK, D. M. (2005b). Kinetic isotope effects on thio-substituted biological phosphoryl transfer reactions from density-functional theory. Chemical communications, (31), 3909-3911.

LÖNNBERG, H. (2011). Cleavage of RNA phosphodiester bonds by small molecular entities: a mechanistic insight. Organic & biomolecular chemistry, 9(6), 1687-1703.

LÖNNBERG, H., STRÖMBERG, R. & WILLIAMS, A. (2004). Compelling evidence for a stepwise mechanism of the alkaline cyclisation of uridine 3′-phosphate esters. Organic & biomolecular chemistry, 2(15), 2165-2167.

LÖNNBERG, T., ORA, M., VIRTANEN, S. & LÖNNBERG, H. (2007). Thio Effects on the Departure of the 3′-Linked Ribonucleoside from Diribonucleoside 3′, 3′-Phosphorodithioate Diesters and Triribonucleoside 3′, 3′, 5′-Phosphoromonothioate Triesters: Implications for Ribozyme Catalysis. Chemistry–A European Journal, 13(16), 4614-4627.

M. J. FRISCH, G. W. T., H. B. SCHLEGEL, G. E. SCUSERIA, M. A. ROBB, J. R. CHEESEMAN, G. SCALMANI, V. BARONE, B. MENNUCCI, G. A. PETERSSON, H. NAKATSUJI, M. CARICATO, X. LI, H. P. HRATCHIAN, A. F. IZMAYLOV, J. BLOINO, G. ZHENG, J. L. SONNENBERG, M. HADA, M. EHARA, K. TOYOTA, R. FUKUDA, J. HASEGAWA, M. ISHIDA, T. NAKAJIMA, Y. HONDA, O. KITAO, H. NAKAI, T. VREVEN, J. A. MONTGOMERY, JR., J. E. PERALTA, F. OGLIARO, M. BEARPARK, J. J. HEYD, E. BROTHERS, K. N. KUDIN, V. N. STAROVEROV, R. KOBAYASHI, J. NORMAND, K. RAGHAVACHARI, A. RENDELL, J. C. BURANT, S. S. IYENGAR, J. TOMASI, M. COSSI, N. REGA, J. M. MILLAM, M. KLENE, J. E. KNOX, J. B. CROSS, V. BAKKEN, C. ADAMO, J. JARAMILLO, R. GOMPERTS, R. E. STRATMANN, O. YAZYEV, A. J. AUSTIN, R. CAMMI, C. POMELLI, J. W. OCHTERSKI, R. L. MARTIN, K. MOROKUMA, V. G. ZAKRZEWSKI, G. A. VOTH, P. SALVADOR, J. J. DANNENBERG, S. DAPPRICH, A. D. DANIELS, Ö. FARKAS, J. B. FORESMAN, J. V. ORTIZ, J. CIOSLOWSKI, AND D. J. FOX. (2009). *Gaussian 09*. Gaussian Inc., Wallington, CT.

MA, X., HORTELAO, A. C., PATINO, T. & SANCHEZ, S. (2016). Enzyme Catalysis to Power Mico/Nanomachines. ACS Nano, 10, 9111-9122.

MANNINO, S. J., JENKINS, C. L. & RAINES, R. T. (1999). Chemical mechanism of DNA cleavage by the homing endonuclease I-Ppo I. Biochemistry, 38(49), 16178-16186.

MARTIN, R. B. (1986). Bioinorganic chemistry of metal ion toxicity. Metal ions in biological systems, 20, 21-65.

MAYAAN, E., RANGE, K. & YORK, D. M. (2004). Structure and binding of Mg (II) ions and di-metal bridge complexes with biological phosphates and phosphoranes. JBIC Journal of Biological Inorganic Chemistry, 9(7), 807-817.

MAYER, I. (1983). Charge, bond order and valence in the ab initio SCF theory. Chemical Physics Letters, 97(3), 270-274.

MESSINA, K. (2013). **Investigation of the Mechanism of Ca 2+ Catalyzed RNA Phosphodiester Hydrolysis** Drew University.

MICHAL, G. & SCHOMBURG, D. (2012). Biochemical Pathway: An Atlas of Biochemistry and Molecular Biology, 2nd edition. Hoboken, New Jersey: John Wiley& Sons, Inc.

MIKKOLA, S., STENMAN, E., NURMI, K., YOUSEFI-SALAKDEH, E., STRÖMBERG, R. & LÖNNBERG, H. (1999). The mechanism of the metal ion promoted cleavage of RNA phosphodiester bonds involves a general acid catalysis by the metal aquo ion on the departure of the leaving group. Journal of the Chemical Society, Perkin Transactions 2, (8), 1619-1626.

MORTISON, J. D. & SHERMAN, D. H. (2010). Frontiers and Opportunities in Chemoenzymatic Synthesis. J Org Chem, 75(21), 7041-7051.

MURTOLA, M. & STRÖMBERG, R. (2008). PNA based artificial nucleases displaying catalysis with turnover in the cleavage of a leukemia related RNA model. Organic & biomolecular chemistry, 6(20), 3837-3842.

NAKANO, S.-I., CHADALAVADA, D. M. & BEVILACQUA, P. C. (2000). General acid-base catalysis in the mechanism of a hepatitis delta virus ribozyme. Science, 287(5457), 1493-1497.

NARLIKAR, G. J. & HERSCHLAG, D. (1997). Mechanistic aspects of enzymatic catalysis: lessons from comparison of RNA and protein enzymes 0. Annual review of biochemistry, 66(1), 19-59.

OIVANEN, M., KUUSELA, S. & LÖNNBERG, H. (1998). Kinetics and mechanisms for the cleavage and isomerization of the phosphodiester bonds of RNA by Brønsted acids and bases. Chemical reviews, 98(3), 961-990.

OIVANEN, M., ORA, M., ALMER, H., STROMBERG, R. & LONNBERG, H. (1995). Hydrolytic reactions of the diastereomeric phosphoromonothioate analogs of uridylyl (3', 5') uridine: Kinetics and mechanisms for desulfurization, phosphoester hydrolysis, and transesterification to the 2', 5'-isomers. The Journal of Organic Chemistry, 60(17), 5620-5627.

ORA, M. & HANSKI, A. (2011). Stepwise Mechanism of Hydroxide Ion Catalyzed Cyclization of Uridine 3′-Thiophosphates. Helvetica Chimica Acta, 94(9), 1563-1574.

ORA, M., PELTOMÄKI, M., OIVANEN, M. & LÖNNBERG, H. (1998). Metal-Ion-Promoted Cleavage, Isomerization, and Desulfurization of the Diastereomeric Phosphoromonothioate Analogues of Uridylyl (3', 5') uridine. The Journal of Organic Chemistry, 63(9), 2939-2947.

PAULING, L. (1946). Molecular Architecture and Biological Reactions. Chem Eng News, 24, 1375-1377.

PAULING, L. (1948). Nature of Forces Between Large Molecules of Biological Interest. Nature, 161, 707-709.

PETROV, A. S., FUNSETH-SMOTZER, J. & PACK, G. R. (2005). Computational study of dimethyl phosphate anion and its complexes with water, magnesium, and calcium. International journal of quantum chemistry, 102(5), 645-655.

PICCIRILLI, J. A., VYLE, J. S., CARUTHERS, M. H. & CECH, T. R. (1993). Metal ion catalysis in the Tetrahymena ribozyme reaction.

PINJARI, R. V., KAPTAN, S. S. & GEJJI, S. P. (2009). Alkali metals (Li, Na, and K) in methyl phosphodiester hydrolysis. Physical Chemistry Chemical Physics, 11(26), 5253-5262.

PLEY, H. W., FLAHERTY, K. M. & MCKAY, D. B. (1994). hammerhead ribozyme. Nature, 372, 3.

PUDNEY, C. R., HAY, S., PANG, J., COSTELLO, C., LEYS, D., SUTCLIFFE, M. J. & SCRUTTON, N. S. (2007). Mutagenesis of morphinone reductase induces multiple reactive configurations and identifies potential ambiguity in kinetic analysis of enzyme tunneling mechanisms. Journal of the American Chemical Society, 129(45), 13949-13956.

QUINN, D. M. & SUTTON, L. D. (1991). Theoretical basis and mechanistic utility of solvent isotope effects. Enzyme mechanism from isotope effects, 73-126.

RADZICKA, A. & WOLFENDEN, R. (1995). A PROFICIENT ENZYME. Science, 267(5194), 90-93.

RAINES, R. T. (1998). Ribonuclease a. Chemical reviews, 98(3), 1045-1066.

RAWLINGS, J., CLELAND, W. W. & HENGGE, A. C. (2006). Metal-catalyzed phosphodiester cleavage: secondary 18O isotope effects as an indicator of mechanism. Journal of the American Chemical Society, 128(51), 17120-17125.

RIBEIRO, A. J., RAMOS, M. J. & FERNANDES, P. A. (2010). Benchmarking of DFT functionals for the hydrolysis of phosphodiester bonds. Journal of chemical theory and computation, 6(8), 2281-2292.

ROSTA, E., KAMERLIN, S. C. & WARSHEL, A. (2008). On the Interpretation of the Observed Linear Free Energy Relationship in Phosphate Hydrolysis: A Thorough Computational Study of Phosphate Diester Hydrolysis in Solution†. Biochemistry, 47(12), 3725-3735.

RUPERT, P. B. & FERRÉ-D'AMARÉ, A. R. (2001). Crystal structure of a hairpin ribozyme–inhibitor complex with implications for catalysis. Nature, 410(6830), 780-786.

SCHEINER, S. & ČUMA, M. (1996). Relative stability of hydrogen and deuterium bonds. Journal of the American Chemical Society, 118(6), 1511-1521.

SCHOWEN, R. L. (1972). Mechanistic deductions from solvent isotope effects. Prog. Phys. Org. Chem, 9, 275-332.

SCHRAMM, V. L. (1998). Enzymatic Transition States and Transition State Analog Design. Annu Rev Biochem, 67, 693-720.

SCHRAMM, V. L. (2006). Introduction: Principles of Enzymatic Catalysis. Chemical Reviews, 106(8), 3029-3030.

SCHROEDER, G. K., LAD, C., WYMAN, P., WILLIAMS, N. H. & WOLFENDEN, R. (2006). The time required for water attack at the phosphorus atom of simple phosphodiesters and of DNA. Proceedings of the National Academy of Sciences of the United States of America, 103(11), 4052-4055.

SCOTT, W. G. (1999). Biophysical and biochemical investigations of RNA catalysis in the hammerhead ribozyme. Quarterly reviews of biophysics, 32(03), 241-284.

SEEGER, R. & POPLE, J. A. (1977). Self-consistent molecular orbital methods. XVIII. Constraints and stability in Hartree–Fock theory. The Journal of Chemical Physics, 66(7), 3045-3050.

SIGEL, R. K., SONG, B. & SIGEL, H. (1997). Stabilities and structures of metal ion complexes of adenosine 5'-O-thiomonophosphate (AMPS2-) in comparison with those of its parent nucleotide (AMP2-) in aqueous solution. Journal of the American Chemical Society, 119(4), 744-755.

SILVERMAN, R. B. (2000). The Organic Chemistry of Enzyme-Catalyzed Reactions. London: Academic Press.

SIVAK, A. (1972). Activation of cell membrane enzymes in the stimulation of cell division. Biochemical and biophysical research communication, 46(2), 605-609.

STAHLEY, M. R. & STROBEL, S. A. (2005). Structural evidence for a two-metal-ion mechanism of group I intron splicing. Science, 309(5740), 1587-1590.

STAROVEROV, V. N., SCUSERIA, G. E., TAO, J. & PERDEW, J. P. (2003). Comparative assessment of a new nonempirical density functional: Molecules and hydrogen-bonded complexes. The Journal of chemical physics, 119(23), 12129-12137.

SUGA, H., COWAN, J. A. & SZOSTAK, J. W. (1998). Unusual metal ion catalysis in an acyl-transferase ribozyme. Biochemistry, 37(28), 10118-10125.

SUN, H. & TONKS, N. K. (1994). The coordinated action of protein tyrosine phosphatases and kinases in cell signaling. Trends in Biochemical Sciences, 19(11), 480-485.

SUZUMURA, K.-I., YOSHINARI, K., TANAKA, Y., TAKAGI, Y., KASAI, Y., WARASHINA, M., KUWABARA, T., ORITA, M. & TAIRA, K. (2002). A reappraisal, based on 31P NMR, of the direct coordination of a metal ion with the phosphoryl oxygen at the cleavage site of a hammerhead ribozyme. Journal of the American Chemical Society, 124(28), 8230-8236.

TAKANO, Y. & HOUK, K. (2005). Benchmarking the conductor-like polarizable continuum model (CPCM) for aqueous solvation free energies of neutral and ionic organic molecules. Journal of Chemical Theory and Computation, 1(1), 70-77.

TAO, J., PERDEW, J. P., STAROVEROV, V. N. & SCUSERIA, G. E. (2003). Climbing the density functional ladder: Nonempirical meta–generalized gradient approximation designed for molecules and solids. Physical Review Letters, 91(14), 146401.

THOMPSON, J. E., KUTATELADZE, T. G., SCHUSTER, M. C., VENEGAS, F. D., MESSMORE, J. M. & RAINES, R. T. (1995). Limits to catalysis by ribonuclease A. Bioorganic chemistry, 23(4), 471.

TOPF, M., VÁRNAI, P. & RICHARDS, W. G. (2002). Ab initio QM/MM dynamics simulation of the tetrahedral intermediate of serine proteases: insights into the active site hydrogen-bonding network. Journal of the American Chemical Society, 124(49), 14780-14788.

TORRES, R. A., HIMO, F., BRUICE, T. C., NOODLEMAN, L. & LOVELL, T. (2003). Theoretical examination of Mg2+-mediated hydrolysis of a phosphodiester linkage as proposed for the hammerhead ribozyme. Journal of the American Chemical Society, 125(32), 9861-9867.

VAN HOOK, A. (1975). Condensed phase isotope effects, especially vapor pressure isotope effects: aqueous solutions: ACS Publications.

VENKATASUBBAN, K. & SCHOWEN, R. L. (1984). The Proton Inventory Techniqu. Critical Reviews in Biochemistry, 17(1), 1-44.

WANG, S. & KOOL, E. T. (1995). Origins of the large differences in stability of DNA and RNA helixes: C-5 methyl and 2'-hydroxyl effects. Biochemistry, 34(12), 4125-4132.

WARSHEL, A. (2003). Computer simulations of enzyme catalysis: methods, progress, and insights. Annual review of biophysics and biomolecular structure, 32(1), 425-443.

WESTHEIMER, F. H. (1968). Pseudo-rotation in the hydrolysis of phosphate esters. Accounts of Chemical Research, 1(3), 70-78.

WESTHEIMER, F. H. (1987). Why nature chose phosphates. Science, 235(4793), 1173-1178.

WILCOX, D. E. (1996). Binuclear metallohydrolases. Chemical Reviews, 96(7), 2435-2458.

WILFRED CHEN , F. B., RICHARD D RICHINS, ASHOK MULCHANDANI. (1999). Engineering of improved microbes and enzymes for bioremediation. Current Opinion in Biotechnology, 10(2), 137–141.

WILKINSON, A. J., FERSHT, A. R., BLOW, D. M. & WINTER, G. (1983). Site-directed mutagenesis as a probe of enzyme structure and catalysis: tyrosyl-tRNA synthetase cysteine-35 to glycine-35 mutation. Biochemistry, 22(15), 3581-3586.

YANG, M.-Y., IRANZO, O., RICHARD, J. P. & MORROW, J. R. (2005). Solvent deuterium isotope effects on phosphodiester cleavage catalyzed by an extraordinarily active Zn (II) complex. Journal of the American Chemical Society, 127(4), 1064-1065.

YASHIRO, M., HIGUCHI, M., WASHIZU, Y. & KOMIYAMA, M. (2002). Effect of Alkaline Earth Metal Ions on the Phosphodiester Hydrolysis of RNA. Bulletin of the Chemical Society of Japan, 75(8), 1843-1844.

YE, J. D., LI, N. S., DAI, Q. & PICCIRILLI, J. A. (2007). The mechanism of RNA strand scission: an experimental measure of the Brønsted coefficient, βnuc. Angewandte Chemie International Edition, 46(20), 3714-3717.

ZASTROW, M. L. & PECORARO, V. L. (2013). Designing functional metalloproteins: From structural to catalytic metal sites. Coordination chemistry reviews, 257(17), 2565-2588.

ZHANG, S., GU, H., CHEN, H., STRONG, E., OLLIE, E. W., KELLERMAN, D., LIANG, D., MIYAGI, M., ANDERSON, V. E. & PICCIRILLI, J. A. (2016). Isotope effect analyses provide evidence for an altered transition state for RNA 2′-O-transphosphorylation catalyzed by Zn 2+. Chemical Communications, 52(24), 4462-4465.

ZHOU, W., SARAN, R., HUANG, P. J. J., DING, J. & LIU, J. (2017). An Exceptionally Selective DNA Cooperatively Binding Two Ca2+ Ions. ChemBioChem, 18(6), 518-522.